University of Huddersfield Repository

Lapa, Raymond

Remote machine condition monitoring based on power supply measurements

Original Citation

Lapa, Raymond (2013) Remote machine condition monitoring based on power supply measurements. Masters thesis, University of Huddersfield.

This version is available at http://eprints.hud.ac.uk/19323/

The University Repository is a digital collection of the research output of the University, available on Open Access. Copyright and Moral Rights for the items on this site are retained by the individual author and/or other copyright owners. Users may access full items free of charge; copies of full text items generally can be reproduced, displayed or performed and given to third parties in any format or medium for personal research or study, educational or not-for-profit purposes without prior permission or charge, provided:

- The authors, title and full bibliographic details is credited in any copy;
- A hyperlink and/or URL is included for the original metadata page; and
- The content is not changed in any way.

For more information, including our policy and submission procedure, please contact the Repository Team at: E.mailbox@hud.ac.uk.

http://eprints.hud.ac.uk/

University of Huddersfield
School of Computing and Engineering

Remote machine condition monitoring based on power supply measurements

Master of Science by Research
School of Computing and Engineering

Student:	Raymond Koubou Lapa
Main Supervisor:	Professor Andrew Ball
Co-Supervisor:	Dr Fengshou Gu

August 2013

Table of Contents

List of symbols

AC	Alternating Current
DC	Direct Current
AFD	Adjustable Frequency Drive
ANN	Artificial Neural Network
CSI	Current Source Inverter
VSI	Voltage Source Inverter
CT	Current Transformer
DC	Direct Current
DOL	Direct On Line
DSP	Digital Signal Processor
DWT	Discrete Wavelet Transform
FFT	Fast Fourier Transform
FL	Fuzzy Logic
FLC	Full Load Current
FLT	Full Load Torque
HMI	Human Machine Interface
HVAC	Heating, Ventilation and Control (for building management)
IEEE	Institute of Electrical and Electronics Engineers
IGBT	Insulated Gate Bipolar Transistor
LAD	Ladder (PLC programming language)
LRT	Locked Rotor Torque
MCSA	Motor Current Signature Analysis
MOSFET	Metal Oxide Semiconductor Field Effect Transistor
MRAS	Model Reference Adaptive System
PC	Personal Computer
PI	Proportional Integral
PID	Proportional Integral Derivative
RMS	Root-Mean Squared
SCR	Semiconductor /Silicon Controlled Rectifier

STL	Structured Text Language (Siemens PLC programming language usually)
VFD	Variable Frequency Drive
VSD	Variable Speed Drive
FC	Frequency Converter
ASD	Adjustable Speed Drives
VVI	Variable Voltage Inverter
V/F	Variable Frequency
PWM	Pulse Width Modulation
GCT	Gate Commutated Thyristors
SGCT	Symmetrical Gate Commutated Thyristors
GTO	Gate Turn-Off Thyristor
AFE	Active Front End
MOSFET	Metal-Oxide-Semiconductor Field-Effect Transistor
IGBT	Insulated-Gate Bipolar Transistor
SCADA	Supervisory Control and Data Acquisition
FOC	Field Oriented Control
IP	Internet Protocol (IP address is a numerical label assigned to each device on a network)
CM	Condition Monitoring
VPN	Virtual Private Network
WEP	Wired Equivalent Privacy
WPA	WI-FI Protected Access

Figures List

Tables List

Acknowledgements

I wish to express my sincere gratitude to Dr Fengshou Gu for his support and guidance all through this research. I would also like to thank Professor Andrew Ball for his assistance in starting the project and his generous advice.

I am indebted to Presspart Manufacturing Limited, where I am currently employed, and a special thanks to Phil Wilkinson and Pete Wooldridge for their invaluable support.

In addition I am grateful to InduSoft for kindly offering Indusoft HMI SCADA Software development licenses for the purpose of this research.

I thank my family for their moral support and continuous encouragement. Finally, I express my sincere gratitude to all those people who helped me in their capacity to complete this project.

Abstract

The most widely used rotating machines in the industry are three phase alternative current (AC) induction machines. With the advances in variable speed drive (VSD) technology, they have become even more reliable than their direct current (DC) counterpart. However, inevitably these motors soon begin to fail with time due to mechanical, electrical or thermal stress hence the need for condition monitoring (CM). Condition monitoring systems help keep machines running productively by detecting potential equipment failures before it actually fails.

Many condition monitoring methods exist on the market including vibration monitoring; acoustic emission monitoring, thermal monitoring, chemical monitoring, current monitoring but most of these methods require additional sensors and expensive data acquisition system on top of a specialise software tool. This all increases the cost of ownership and maintenance.

For more efficient monitoring of induction motor drive systems, this research investigates an innovative remote monitoring system using existing data available in AC drives based on AC motor operating process. This research uses standard automation components already present in most automated control systems. A remote data communication platform is developed, allowing access to the control data remotely over a wireless network and internet using PLC and SCADA system. Remote machine condition monitoring is not a new idea but its application to machine monitoring based on power supply parameters indirectly measured by an inverter is new.

To evaluate the basic performance of the platform, the monitoring of shaft misalignment, a typical fault in mechanical system is investigated using an in-house gearbox test rig. It has resulted in a model based detection method based on different speed and load settings against the motor current feedback read by the inverter. The results have demonstrated that the platform is reliable and effective. In addition the monitoring method can be employed to detect and diagnose different degrees of misalignment in real time.

This dissertation has major contributions to knowledge which includes:

- Understanding of real life machine condition monitoring problems for this application, including use of wireless sensor, communication over Industrial Ethernet and network security.
- The use of standard automation components (PLC and SCADA) in machine condition monitoring.

- An improved gearbox test rig platform which has the capability of remote control, acquiring and transferring data for monitoring induction machine drive system.

The presented work shows that any machine using automated components such as PLC and SCADA and incorporating motor drive systems and other actuators has the potential to use the automated components for control, condition monitoring and reporting but this will require more tests to be done using the proposed platform.

Chapter 1 Introduction

1.1 Overview

The aims of this study is to research techniques of gathering data relating to the gearbox test rig control loops and transfer this data remotely to a computer for diagnosis and analysis of fault over different conditions. The data collected is the motor electrical supply parameters measure by the inverter controlling the motor. Therefore rather than using additional sensors, data acquisition equipment and software, the parameters measured by the drive, to control the motor, are also used to monitor the condition of the motor. An induction motor can be modelled most simply (and controlled) using two currents rather than the familiar three phase currents actually applied to the motor. These two currents called direct current (Id) and quadrature current (Iq) are responsible for producing flux and torque respectively in the motor. These parameters with others will read from the drive and transferred to a device using a wireless network for the motor condition monitoring.

1.2 Research Objectives

The main objectives of this research is to investigate the operation of an inverter driven induction motor with a view of determining whether it is possible to extract power supply parameters from the inverter that could be used for diagnosis and analysis of fault on the rig over different conditions. This involves using an existing inverter on an existing gearbox test rig and selecting a standard fieldbus communication for data extraction so that the results of the research are relevant to any motor control system.

The research objectives are addressed in five phase of research work:

- Investigate remote condition monitoring techniques with the view of establishing whether any existing research has been conducted in the field of remote condition monitoring of induction motors using power supply measurements from the inverter controlling the motor.
- Analyse the test rig's control system and identify the maximum number of parameters that can be monitored because in its current state it is likely that the system may have hardware and/or software limitation, which can restrict the amount of data that can be read from the Variable Speed Drive.
- Optimise the rig control system by upgrading the control system to a PLC that supports a fieldbus communication system or using an additional PLC just for condition monitoring. Look at means of reading data from the drive directly using this fieldbus system either by adding a field bus communication card to the existing drive or upgrading the drive to one that has a build in field bus communication card.
- Design and develop a prototype control system based on this research to demonstrate remote condition monitoring, reading control loops signals from the inverter controlling the test rig induction motor and transferring these signals wirelessly to a computer for analysis.
- Finally experimentally investigate a mechanical fault on the gearbox test rig to ensure that the data collected from the prototype are reliable and can be used for condition monitoring.

1.3 Thesis Organisation

The research work is presented in eight chapters of this thesis as follows:

Chapter 1 presents an overview on remote condition monitoring on induction motors and objectives of work along with the organisation of the thesis.

Chapter 2 deals with the detailed literature survey and review of previous on induction motor condition monitoring, the purpose of condition monitoring and remote communication and remote condition monitoring.

Chapter 3 talks about induction motor fundamentals. A study of the construction and operation of induction motor, induction motor model, mathematical description of induction motor and the need for variable speed drive for speed control. This chapter also looks at an induction motor current response to a fault condition.

Chapter 4 deals with Variable Speed Drive Technology and control platform while looking in details at sensorless vector control platform as it is the one used on the test rig.

Chapter 5 contains details of the test rig specification, the motor and gearboxes used on the rig, the type of inverter, PLC, HMI and the control philosophy.

Chapter 6 presents in details the proposed condition monitoring platform, the communication between the drive and the remote condition monitoring PLC, the communication between the PLC and the site computer running the SCADA software performing the data logging and trending and how these devices are configured and programmed.

Chapter 7, in this chapter the tests carried out on the actual test rig with no shaft misalignment and with a misaligned shaft will be presented and the experimental data will be analysed.

Chapter 8 contains the conclusions, contributions from the research performed and suggestions for future work.

Chapter 2 Literature Review

2.1 Introduction

Condition monitoring has been used over the years for continuous monitoring, protection of expensive equipment from catastrophic failure, predictive maintenance and reduction of downtime and asset management. This has been used on different types of machinery including turbines, feed pumps, fans, pumps, gearboxes, compressors etc. With machine condition motoring maintenance is not done periodically as is usually the case, it is rather performed depending on the accurate information gathered and analysed by the condition monitoring system or procedure in place. Figure 2-1 below illustrates condition based maintenance.

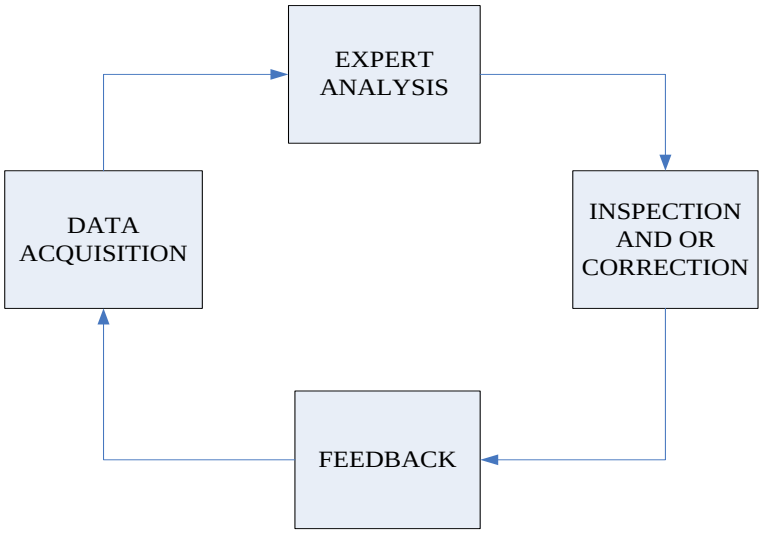

Figure 2-1: Condition Based Maintenance

Remote condition monitoring allows the collection and transmission of machine data remotely without disturbing the machine control system or putting someone at risk trying to get the data while the machine is running.

2.2 Purpose of condition monitoring

A lot of engineering organisations actually carry out condition monitoring on their machinery without realising it. Whether it is each shift producing a report on the operation of the machine during the shift, visual inspections, abnormal sound and smells or using data from their building management system to check the performance of the machine, these are all machine condition monitoring techniques.

AC machine condition monitoring is the process of monitoring parameters (thermal, torque, noise, speed, current, vibration etc.) of the machine, such that a significant change is indicative of a developing failure [1]. It is a most important element of preventive maintenance. The use of conditional monitoring allows maintenance to be scheduled, or other actions to be taken to avoid the consequences of machine failure.

Faults develop within machinery regardless of even the most thorough and comprehensive scheduled maintenance with often-undetected faults leading to unexpected failures before the next scheduled maintenance break.

Condition monitoring in whatever form have some advantages and disadvantages [2].

2.2.1 Advantage of machine condition monitoring

Monitoring the condition of a machine present a lot advantages to the company:

- Increased machine availability and reliability
- Improved operating efficiency
- Improved risk management (less downtime)
- Reduced maintenance costs (better planning)
- Reduced spare parts inventories
- Improved safety
- Improved knowledge of the machine condition (safe short-term overloading of machine possible)
- Extended operational life of the machine
- Improved customer relations (less planned/unplanned downtime)
- Elimination of chronic failures (root cause analysis and redesign)
- Reduction of post overhaul failures due to improperly performed maintenance or reassembly.
- Provides an efficient way to diagnose the faults occurring in the induction motor.
- Uses certain signal processing techniques to detect the faults related to different parameters which provides a detail analysis of the problem.

2.2.2 Disadvantage of machine condition monitoring

Although machine condition monitoring has a wealth of advantages, it also has some disadvantages that need to be taken into account:

- Operational costs (running the program).
- Strong management commitment needed.
- Reduced costs are usually harder to sell to management in general and financial team in particular as benefits when compared with increased profits.
- The sensors used for condition monitoring and the intelligent devices used for data acquisition are quite expensive. Not to mention the software for data processing and decision making, e.g. the sensors used in the rotor diagnosis are vibration pickups, accelerometers, piezoelectric transducers which are more expensive compared to other transducers.
- The set up required to diagnose the fault is very complex and requires well trained engineers.

2.3 Existing condition monitoring techniques

Fault diagnosis is the determination of a specific fault present in a machine. Figure 2-2 illustrates different diagnosis techniques for induction motors.

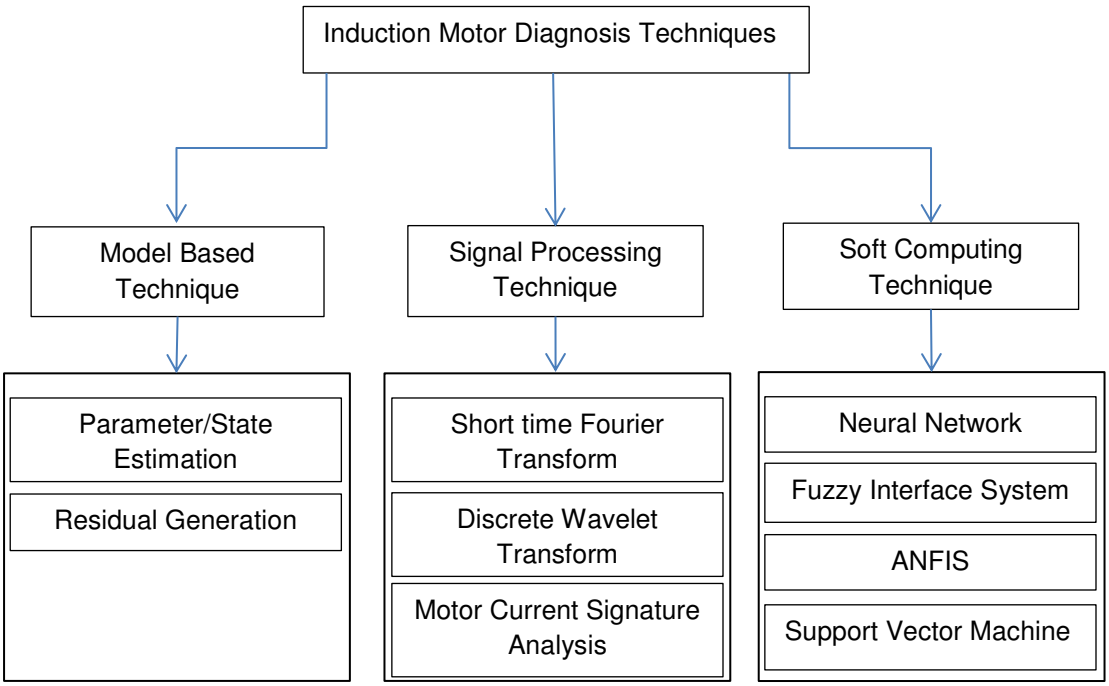

Figure 2-2: Different Fault Diagnosis Techniques

There are several condition monitoring methods in the market but the most prominent are motor current signature analysis, wavelet analysis, park's current vector, vibration monitoring, thermal monitoring, noise monitoring and torque monitoring.

2.3.1 Motor current signature analysis (MCSA)

Motor current signature analysis (MCSA) is the most common type of condition monitoring used in the industry as it is simple to implement with no additional hardware required and can detect failures like bearings collapsed, load issues and damaged rotor bars. The current of the motor can be monitored remotely in the motor control centre (MCC) by using a current transformer (CT) on one of the phases of the motor. [3, 4]
MCSA uses the current spectrum of the motor to locate characteristic fault frequencies; when a machine develops a fault, the frequency spectrum of the line current differs from the frequency spectrum of a healthy motor [4]. MCSA techniques can be used in conjunction with vibration and thermal analysis to confirm key machinery diagnostic decisions [4].

R. R. Schoen et al. [5] addresses the application of motor current spectral analysis for the detection of rolling-element bearing damage in induction machines. Vibration monitoring of mechanical bearing frequencies is currently used to detect the presence of a fault condition. Investigation of the efficacy of current monitoring for bearing fault detection by correlating the relationship between vibration and current frequencies caused by incipient bearing failures is done in this study. The bearing failure modes are reviewed and the characteristic bearing frequencies associated with the physical construction of the bearings are defined. The effects on the stator current spectrum are described and the related frequencies determined. Experimental results which show the vibration and current spectra of an induction machine with different bearing faults are used to verify the relationship between the vibrational and current frequencies. The test results clearly prove that the stator current signature can be used to identify the presence of a bearing fault.

2.2.2 Wavelet analysis

Wavelet transforms [6] are mathematical ways to perform signal analysis when signal frequency varies over time. For certain classes of signals and images, wavelet analysis provides more precise information about signal data than other signal analysis techniques. Common applications of wavelet transforms include speech and audio processing, image and video processing, biomedical imaging, and 1-D and 2-D applications in communications, geophysics and also induction machine condition monitoring. Wavelet detection methods show good sensitivity, short detection [4].
Hocine Bendjama et al [7] produced a paper on rotating machinery condition monitoring and fault diagnostic using wavelet transforms. The proposed method have some advantages over the spectral analysis based on Fourier transform as the latter have some limitations on non-stationary signals. This paper presents a fault diagnosis method based on the Discrete Wavelet Transform and Continuous Wavelet Transform, tested on real measurement signals collected from a vibration system containing mass unbalance and gear fault. The results on this paper conclude that wavelet transform can diagnose abnormal change in the measure data.

2.2.3 Park's Current Vector

Park's Current Vector is another electrical monitoring technique. Usually there is no consideration of neutral when it comes to connecting three phase induction motors to the mains which means current signals are measured between phase to phase rather than phase to neutral. Therefore the measured current has no homo-polar component. In pursuit of simplicity with regards of the study of electrical machines R.H. Park developed a two dimensional representation that can be used to represent three phase induction motor [8] by transforming the motor equations into a two phased orthogonal reference frame. The transformation of the three-phased system to the two-phased orthogonal one can be performed upon [9]:

$$\begin{bmatrix} f_d \\ f_q \\ f_0 \end{bmatrix} = [P_{dq0}]. \begin{bmatrix} f_a \\ f_b \\ f_c \end{bmatrix} \qquad \textbf{Equation 2-1}$$

Where *f* is the function to be transformed (it can be the current, voltage or magnetic flux). The Park transformation matrix is:

$$|P_{dq0}| = \sqrt{\frac{2}{3}} \begin{bmatrix} \cos(\theta) & \cos(\theta - \frac{2\pi}{3}) & \cos(\theta - \frac{4\pi}{3}) \\ -\sin(\theta) & -\sin(\theta - \frac{2\pi}{3}) & -\sin(\theta - \frac{4\pi}{3}) \\ \frac{1}{\sqrt{2}} & \frac{1}{\sqrt{2}} & \frac{1}{\sqrt{2}} \end{bmatrix} \qquad \textbf{Equation 2-2}$$

Where $\theta = wt$ is the angular displacement.
By using the above transformation the orthogonal components of the Park's current vector can be computed from the symmetrical three-phased current system, having the components: *ia*, *ib* and *ic*:

$$i_d = \sqrt{\frac{2}{3}} \left[i_a cos\theta + i_b \cos\left(\theta - \frac{2\pi}{3}\right) + i_c \cos\left(\theta + \frac{2\pi}{3}\right) \right]$$

$$i_q = \sqrt{\frac{2}{3}} \left[i_a sin\theta + i_b \sin\left(\theta - \frac{2\pi}{3}\right) + i_c \sin\left(\theta + \frac{2\pi}{3}\right) \right] \qquad \textbf{Equation 2-3}$$

If $\theta = 0$, meaning that the reference is fixed, the equation above becomes:

$$i_d = i_a - \frac{i_b}{2} - \frac{i_c}{2}$$

$$i_q = \frac{\sqrt{3}}{2}(i_b - i_c) \qquad \textbf{Equation 2-4}$$

When the induction machine if healthy its three-phased stator current system is perfectly symmetric:

$$\begin{aligned} i_a &= \sqrt{2}Isin(w_s t) \\ i_b &= \sqrt{2}Isin\left(w_s t + \frac{2\pi}{3}\right) \\ i_c &= \sqrt{2}Isin\left(w_s t + \frac{4\pi}{3}\right) \end{aligned}$$ **Equation 2-5**

Where I is the maximum value of the supply phase current, ω_s is the supply frequency and t is the time variable.

Izzet Yilmaz Önel and Mohamed El Hachemi Benbouzid [10] produced a study that deals with the problem of bearing failure detection and diagnosis in induction motors. The proposed approach is a sensor-based technique using the mains current and the rotor speed measurement from a tachometer. The proposed approach is based on the stator current Park patterns. They also compared results from Park transform approach and the Concordia transform detection and diagnosis techniques. Experimental tests were carried out on a 0.75 kW two-pole induction motor with artificial bearing damage. The results indicate that the Park transform approach has better diagnostic capabilities than the Concordia transform.

2.2.4 Vibration monitoring

Vibration is a machine response to an internal or external stimulus causing it to oscillate. Vibration has three important parameters which can be measured [11]:

- **Frequency** – How many times does the machine or structure vibrate per minute or per second?
- **Amplitude** – How much vibration in microns, millimetres/sec?
- **Phase** – How is the member vibrating in relation to a reference point?

Different machines have different toleration to vibration and monitoring vibration is one of the oldest techniques used in the field of machine condition monitoring and it is usually used to detect mechanical faults like bearings faults, mechanical load imbalance etc. [1].

Suratsavadee K. Korkua, Wei-Jen Lee and Chiman Kwan [12] proposed a method to monitor and analyse the vibration of an induction machine due to rotor imbalance. A novel health monitoring system of electric machine based on wireless sensor network (ZigBee™) is developed in this paper. The communication protocol and software design for both wireless sensor network node and base station are also presented in detail. Moreover, the positioning scheme in ZigBee wireless network is also investigated. Based on the receiving strength signal indicator (RSSI), they can determine the distance of the sensed node by applying the distance-based positioning method. By observing the RSSI value and applying the distance-based positioning method, they can estimate the distance of the data collector node where the fault happened.

2.2.5 Thermal monitoring

When electrical energy is being converted into mechanical energy by an induction machine, the stator and rotor heat up and the temperature rises inside the motor and can cause damage; to prevent it the motor stator and rotor temperature is continuously monitored and shut down when the temperature exceeds an acceptable limit. The heat produced by the motor is called motor head dissipation or motor power losses which are made up of the following [13]:

- Motor current dependent losses: Stator I^2R losses, Rotor I^2R losses and No-load losses
- Losses independent to current: Core loss and Friction and Windage loss

Table 2-1 below shows a breakdown of where losses are present and their percentage.

LOSSES	2 POLE AVERAGE	4 POLE AVERAGE
CORE LOSSES	19%	21%
FRICTION & WINDAGE	25%	10%
STATOR I2R	26%	34%
ROTOR I2R	19%	21%
STRAY LOAD LOSSES	11%	14%

Table 2-1: Motor heat losses table and percentage [14]

Most modern drives have the facility to shut down the motor when temperature rises, provided that the motor thermistor signal is connected to the drive. In control systems where there is no thermistor input on the drive, a thermistor relay is used and stops the motor when it gets hot. However temperature varies depending on whether the motor is on starting stage or running stage therefore a good temperature estimation technique needs to be able to distinguish the two stages and can detect variations. Two temperature estimation techniques exist: the thermal model-based temperature estimation technique and the parameter-based temperature estimation technique.

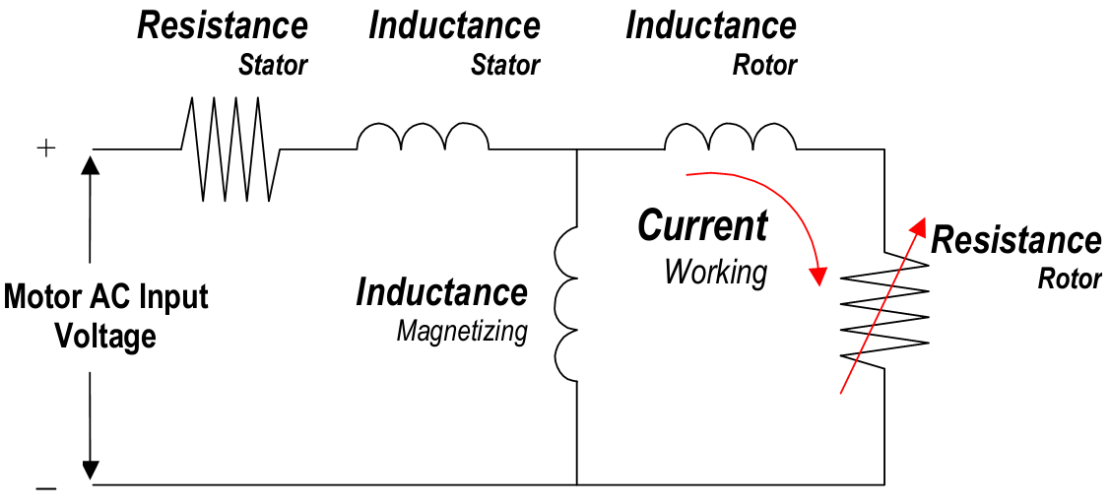

Figure 2-3: Equivalent Circuit Diagram of an AC Induction motor with temperature dependent rotor resistance [15]

The circuit above shows that the Rotor resistance will vary with temperature and affects torque production hence the importance of rotor temperature monitoring.

Drive designs with motor temperature compensation techniques are typically classified as field-oriented control drives discussed in section 4.3.4. These drives use voltage feedback circuits to calculate changes in motor resistance through voltage drop. These drives adjust the field flux based upon motor operating temperature, providing more accurate operation from a cold condition to normal operating temperature. Speed regulation is more stable too. Depending on the design and setup, these systems may cost more and be more complex to set up.

J. Niyompongwirat, N. Wararatkul and T. Suesut their work referred to the temperature measurement and monitoring system for industrial induction motors. The aim of temperature monitoring systems was to analyse and detect abnormalities on the motor and prevent the damage in case of unbalanced voltage. The experimental setup consists of a temperature measurement circuit using TEXAS INSTRUMENTS LM 35DZ IC with analogue transformer used as a temperature sensor and transducer and a PC with a data acquisition card from National Instrument PCI 6014 running LabView for analysing temperature data. The AC source was performed by adjusting voltage unbalance of

10%, 20% to 50% for each phase to monitor the temperature changes. The experiment results shows that unbalanced voltage on induction motors can be detected using temperature monitoring.

Milanfar and Lang [16] developed a thermal model of electric machine for condition monitoring. This thermal model is used to estimate the temperature of the motor and identify faults. Thermal monitoring can, in general, be used as an indirect method to detect some stator faults (turn-to-turn faults) and bearing faults. In a turn-to-turn fault, the temperature rises in the region of the fault, but this might be too slow to detect the incipient fault before it progresses into a more severe phase-to-phase or phase-to-neutral fault. In the case of detecting bearing faults, the increased bearing wear increases the friction and the temperature in that region of the machine. This increase in temperature of the motor can be detected by thermal monitoring.

2.2.6 Torque monitoring

Research by John S. Hsu [17] suggests a method of fault detection on an induction motor rotor bar and stator by calculating the air-gap torque whilst the motor is running with no additional down time required. Air-gap torque is the torque created by the flux linkages and the currents in both the stator and the rotor of the entire motor. These torque values are periodically kept for comparison with the motor estimated torque; the difference between these two values indicates the existence of a broken rotor bar. Since more data than just a line current are taken, this method offers other potential possibilities that cannot be handled by examining only a line current.
The air-gap torque equation can be expressed by the following equation:

$$Torque[Nm] = \frac{P}{2\sqrt{3}} \begin{Bmatrix} (i_a - i_b) \int [V_{CA} - R(i_c - i_a)]dt \\ -(i_c - i_a) \int [V_{AB} - R(i_a - i_b]dt \end{Bmatrix} \qquad \textbf{Equation 2-6}$$

Equation 2-6 is valid for either *star*- or delta-connected motors, where *P* = number of poles. i_a, i_b and i_c = lines currents, and *R* = half of the line-to-line resistance value.

Since the time increment between data points is small, a simple Euler method is used for numerical evaluation in this study.

2.2.7 Noise monitoring

A great number of mechanical failures on machines can be detected using acoustic noise from air gap eccentricity in induction motors; this is done by measuring and analysing the acoustic noise spectrum [18].
The typical mechanical failures detected on induction motors are the following:

- Bearing wear and failure. As a result of bearing wear, air gap eccentricity can increase, and this can generate serious stator core damage and even destroy the winding of the stator;
- High mechanical unbalance in the rotor increases centrifugal forces on the rotor;
- Looseness or decreased stiffness in the bearing pedestals can increase the forces on the rotor;
- Critical speed shaft resonance increases force and vibration on the rotor core.

2.3 Remote communication and condition monitoring

Remote condition monitoring configurations in general, complement data collectors and other monitoring methods, by expanding coverage into areas where traditional methods would be cost prohibitive or hazardous.
The advances in mobile phone technologies (smartphones) and personal digital assistants (PDAs) have facilitated remote condition monitoring as these devices can easily connect to other remote devices via wireless network (WI-FI, Bluetooth, ZigBee, etc.) or over the internet and quickly get machine data for analysis.
A typical remote condition monitoring system consists of data acquisition (information collecting i.e. collect analogue data of the machine status and convert into digital data), data processing and/or diagnostic recognition (information handling and/or fault diagnostic i.e. convert digital data to real quantities of the machine's working conditions and detect when a fault occurs and triggers an alarm

and recommend how the issue can be resolved efficiently), and remote communication (transmission of machine's status via a remote communication system e.g. WI-FI, Bluetooth, VPN etc.). Data acquisition utilises sensory technology to extract the information about the machine's health and transfers physical quantities such as vibration, acoustic emission, torque and speed to analogue voltage (0-10V DC) or analogue current (0-20mA or 4-20mA), which are then digitised. 4-20mA is a robust sensor signalling standard widely used for condition monitoring as it is inherently insensitive to electrical noise and it is possible to detect wire breaks and tell if the sensor is defective.

The data acquisition in some applications can be achieved using a wireless network were a sensor is connected to a wireless transmitter capable of transmitting the machine status to a receiver. This receiver can be an intelligent device like a PC that logs and analyses the data. It can also be a standalone wireless data logger.

2.3.2 Benefits of remote condition monitoring

As the predictive maintenance industry changes, plant management will embrace the new communication technologies that can make their facilities more efficient. Remote condition monitoring has the following benefits [19]:

- **More time is spent analysing data and less time collecting it.**
  Reductions in personnel have put a strain on the predictive maintenance departments of most companies. Remote monitoring enables analysts to be more efficient, and helps departments do more with less staff.
- **Collect data from previously inaccessible machines.**
  Vital equipment that is difficult to access or located in hazardous or restricted areas can be monitored because collection is automated.
- **Increase safety.**
  Large cranes, conveyors, drag lines, open drive shafts, huge wind turbines and open gear sets all pose dangers to personnel collecting data via traditional walk-around methods.
- **Automated round the clock data collection.**
  Data can be obtained day, night, weekends, and holidays. Sick days, vacation days, and staff turnover will not impact collection.
- **Collect additional metrics.**
  Perform better analysis by having additional types of data collected, such as speed, pressure, temperature, flow rate etc.
- **Consistent data collection.**
  When manual routes are run, inevitably some machines will not be in operation. Automated collection can be scheduled for when machines are running.
- **Increase collection rate for problematic machines.**
  The more data that can be collected on the problematic machine the more accurate the diagnosis. Automated data collection removes the difficulties associated with manual data collection, such as taking multiple readings in a day especially evenings, weekends, and holidays.
- **View plant-wide data.**
  A database tracks data from all machines at all plants. Multiple analyses and/or manufacturers can view the same data at the same time.
- **Setting of accurate alarms.**
  Automated, consistent data collection can provide hundreds of data points, enough to establish statistically accurate alarms.
- **Ability to monitor supervisory panels mounted on vital machines.**
  There is a higher likelihood that a remote system will catch increased vibration prior to trip than a walk-around program.

2.3.3 Remote condition monitoring methods

Remote condition monitoring varies from simple to complex as illustrated on Table 2-2 below.

Methods	Techniques	Results
Simple remote monitoring	• Convert output from the sensor (a vibration transducer, tachometer, encoder or current transformer etc.) to a 4-20mA or 0-10V DC • Collect these outputs directly to the plant data logging system • View data remotely using remote desktop or similar tools	Little information is gained other than whether vibration, machine speed, machine torque or output current is high or low. The cause of the variation high or low depending on the sensor cannot be determined without additional information.
Complex remote monitoring	Collect output from real time analysis that interfaces with a site computer using Industrial Ethernet and/or wireless networks. The site computer has internet capabilities and information can be accessed remotely via a wireless network or a VPN (Virtual Private Network) connection.	Typically provides spectra, waveform overall, DC gaps, and orbits. Some systems can track transient conditions, such as start-ups, ramp-ups and coast downs. Some are also equipped with statistical process control (SPC) information on request. Some can perform advanced functions like run out subtraction.

Table 2-2: Remote Condition monitoring methods

A company decision on whether to opt for a complex or simple remote monitoring system usually depend on the competencies of the personnel reviewing and analysing the data, because a complex system with more information and advanced data sampled will only provide more value if a qualified person is there to interpret the information. With the use of remote condition monitoring and technology like industrial Ethernet a multinational company with plants around the world can have all their machines monitored from one central location; this will make the complex monitoring method expensive to setup in each plant but will save money over time as the same personnel can be used for interpreting information from various plants.

2.3.4 Industrial Ethernet

Some complex remote condition systems use Industrial Ethernet for communication with sensor, actuator or servers. Industrial Ethernet is a term specifically used to describe Ethernet switches and media converters that are designed for industrial rather than home use. Most applications that use Ethernet use TCP/IP which happens to be the underlying protocols of the internet. For this reason, it is possible to connect industrial networks to each other allowing data sharing and remote control and condition monitoring even if the organisation's sites are on opposite sides of the world. If the data being shared between sites is of a sensitive nature, point to point VPN (Virtual Private Network) tunnels can be established to keep data secure across the public (internet) parts of the link. Many Industrial routers are now available with firewall and VPN capabilities built in.
Industrial Ethernet enables a more flexible, responsive system that encompasses both real time data from the machine. This end to end networking architecture provides connectivity, collaboration, and integration from the device level to enterprise business systems. The use of industrial Ethernet has some advantages over traditional serial communication counterpart:

- Increased speed, typically speed of up to 9.6 kbit/s can be achieved with RS-232 while it is possible to get 1 Gbit/s with Gigabit Ethernet over Cat5e/Cat6 cables or optical fibre

- Increased distance
- Ability to use standard network devices like those use in domestic homes (access points, routers, switches, hubs, network cables)
- Ability to have more than two node on the network which was possible using RS-485 but not RS-232
- Security
- Ability to add innovative technologies such as voice, video and collaboration

Industrial Ethernet technology is rapidly being embraced by multiple organisations and vendors, including the Industrial Ethernet Association (IEA), the Open DeviceNet Vendor Association (ODVA), Modbus.org, Fieldbus Foundation, and PROFINET and PROFIBUS international (PI).
PROFINET ("Process Field Network"), the automation standard of PROFIBUS&PROFINET International (PI) is the innovative open standard for Industrial Ethernet and satisfies all requirements of automation technology. It enables solutions to be developed for factory automation, process automation, safety applications, and the entire range of drive technology up to and including isochronous motion control applications.
PROFINET is based on standard Ethernet and TCP/IP and is predominantly used in Europe. The protocol's main area of application is factory automation without a need for hard real time performance with typical cycle time of 5-50ms.

PROFINET [20] is differentiated into different performance classes to address various timing requirements: PROFINET RT for soft real-time, or no real-time requirements at all, and PROFINET IRT for hard real-time performance. The technology was developed by Siemens and the member companies of the PROFIBUS user organization, PNO. The Ethernet-based successor to PROFIBUS DP, PROFINET I/O specifies all data transfer between I/O controllers as well as the parameterisation, diagnostics, and layout of a network.
In order to cover the different performance classes [20], PROFINET makes free use of the producer/consumer principle and resorts to various protocols and services. High-priority payload data sent directly via the Ethernet protocol travels in Ethernet frames with VLAN prioritisation, whereas diagnostics and configuration data, for instance, is sent using UDP/IP. That enables the system to achieve cycle times of around 10 ms for I/O applications.
With PROFINET, the following minimum data communication requirements are automatically established:

- 100 Mbps data communication with copper or fibre optic transmission (100 Base TX and 100 Base FX)
- Full duplex transmission
- Switched Ethernet
- Auto negotiation (negotiating of transmission parameters)
- Auto crossover (sending and receiving lines are crossed in the switch)
- Wireless communication (IWLAN(Industrial Wireless LAN) and Bluetooth)

IWLAN is a technology that means WLAN is applied to industrial environment. It is used in these situations, where difficult to realise wired connections between devices in some environments, as well as not to allow or expect wired connection in the view of technology. [21]
IWLAN wireless interface modules enable distributed input/output system to communicate wirelessly. The technology could find applications in driverless transport systems, warehouse logistics, electrical trolley conveyors and remote condition monitoring applications. The main advantage of wireless communication solutions is easy and flexible access to plant equipment's status and control. Figure 2-4 shows an IWLAN system configuration.

Figure 2-4: IWLAN system configuration

On the figure above, the S7-300 PLC can control actuators while at the same gathering data about the status of the actuators remotely via IWAN through PROFINET. The collected data can therefore be used for condition monitoring by an operator using a WI-FI enabled laptop.
When a large machine control systems has PROFINET communication interface, it makes sense to also use the technology for condition monitoring.

2.3.5 Wireless Networking Protocols

There is various wireless networking protocols that can enable machine's data to be transmitted within a plant environment. The most common are 802.11a/b/g, ZigBee (IEEE 802.15.4), and Bluetooth, each has its benefits and drawbacks. For example, ZigBee uses much less power than the others, but are not as fast. The 802.11 protocol uses more power, but makes integrating different applications and commercial devices easy because it is the same technology used on laptops and wireless office LAN. The IEEE 802.11a/b/g has also found increased use in industrial applications for monitoring and certain specific automation functions and is able to meet the technical needs of condition monitoring (e.g., high bandwidth) and, as an infrastructure choice, offers several advantages in network security, standard implementation well understood by IT departments, multi-use and cost-effectiveness.
The 802.11 b has a data rate 11Mb/s - 2.4 GHz with maximum distance in factory 100 metres and can be stopped by walls. The 802.11 a has a data rate 54 Mb/s – 5.2Ghz with a maximum distance in factory 30 metres and will be stopped by walls – even more so than "g". While The 802.11 b has a data rate 54Mb/s - 2.4 GHz with maximum distance in factory 30 metres and will be stopped by walls.

The IEEE 802.15.4 standard is a robust wireless personal area network (PAN) that is specifically targeted toward the low-power, low-bandwidth networks commonly used in industrial monitoring and control. IEEE 802.15.4 transceiver integrated with an industrial switch or sensor communicates to a monitoring receiver that can handle multiple switches in a star-configuration network. Every network, and each wireless device in the network, has a unique identification number that allows the device

and its associated monitor to encode their signals. This ensures that the communication link between them is private and virtually immune to crosstalk from other switches or networks.

The ZigBee Alliance is a group of companies that develop and maintain the ZigBee standard. ZigBee is a specification for a suite of high level communication protocols built over IEEE 802.15.4 [22]. These 802.15.4 radios provide reliable connectivity in large indoor open spaces and/or outdoor installations with a relatively open line-of-sight between device and monitor. A 35-dB link margin ensures that minor obstacles or even heavy precipitation will not compromise communications. In some installations and depending on materials, the signal can penetrate intervening walls. This also prevents temporary outages when a truck or other mobile piece of equipment is moved between the sensors and the receiver. The allowable operating range of an IEEE 802.15.4 radio is greater than 1000 ft (304 m). In extreme conditions such as heavy precipitation, the signal could be reduced by approximately 75 ft (23 m).
As 802.15.4 devices draw so little power, they can be operated by industry-standard batteries, for reliable operation and varied installation options. They also eliminate the need for situation-dependent, unreliable, and expensive energy scavenging. A wireless sensor or switch may operate for several years without a battery replacement or re-charging, depending on the design.
Typically, the monitor/receiver unit in a wireless network can support either one device or multiple devices. For example, one receiver can support up to 14 remote battery-powered wireless devices. The controller can monitor sensor and switch status, signal strength, and battery levels for each device on its network. If a battery starts to die, or a switch gets blocked, the operator will know instantly and can take corrective measures.

Suratsavadee K. Korkua et al [12] presented in their study a method to monitor and analyse the vibration of induction machines due to the rotor imbalance. A novel health monitoring system of electric machines based on ZigBee wireless sensor network is developed in this paper as illustrated on Figure 2-5 below.

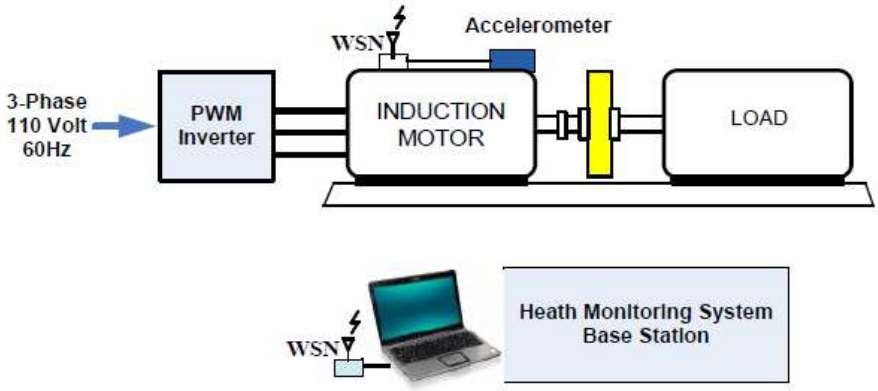

Figure 2-5: Schematic diagram of the wireless machine health monitoring system [12]

In this proposed wireless sensor system above, vibration signals from a three-axis accelerometer are recorded and stored at the base station. Signal analysis is used to extract detailed information for induction machine health diagnostic.

2.3.6 Wireless Network security

Wireless communication have revolutionised condition motoring, reducing high cost of installation in inaccessible and hazardous areas and temporary installation for troubleshooting and remote monitoring. With all these advantages for choosing a wireless network for condition monitoring, the system becomes more vulnerable to unauthorised access and sabotage as someone can access the system without necessarily being in the plant. It is crucial to ensure that the network is secured to prevent unauthorised access or damage to the network devices.
The most common types of wireless security for 802.11 networks are Wired Equivalent Privacy (WEP) and WI-FI Protected Access (WPA).

WEP is the less secured of the two as it is designed to provide the same level of security as that of a wired LAN. LANs are protected by the physicality of their structure, as they have some or part of the network in a building that can be protected from unauthorised access; they are naturally more secure than WLANs. WLANs which are over radio waves do not have the same physical structure and therefore are more vulnerable to tampering. WEP security is achieved by encrypting data over radio waves so that it is protected as it is transmitted from one end point to another. However, it has been found that WEP is not as secure as once believed. WEP is used at the two lowest layers of the OSI model - the data link and physical layers; it therefore does not offer end-to-end security. WEP is more suitable for home/small office applications with 64 or 128 bit key available.

Wi-Fi Protected Access (WPA) [23] was introduced as an interim security enhancement over WEP while the 802.11i wireless security standard was being developed. Most current WPA implementations use a pre-shared key (PSK), commonly referred to as WPA Personal, and the Temporal Key Integrity Protocol (TKIP) for encryption. WPA Enterprise uses an authentication server to generate keys or certificates.

Wi-Fi Protected Access version 2 (WPA2) [23] is based on the 802.11i wireless security standard, which was finalised in 2004. The most significant enhancement to WPA2 over WPA is the use of the Advanced Encryption Standard (AES) for encryption. The security provided by AES is sufficient (and approved) for use by the U.S. government to encrypt information classified as top secret, this will be good enough for industry too.

According to Brad Bowers from CISCO [24] ZigBee wireless attacks and security has attracted a lot of interest by government and industry security professionals as well as the hacker community. Each is looking at the security capabilities of the 802.15.4 protocol as well as how manufacturers are implementing the ZigBee radios into products and equipment. Often it is the "implementations" part of the equation that is causing most of the security risks. This is clearly evident in the types of attacks used against the devices. Although ZigBee and 802.15.4 protocol were designed with security in mind, we have learned with past experience that security is only as effective as its implementation. While there are numerous types of attacks that have been successfully levered against ZigBee devices, they generally fall into three categories: physical attacks, key attacks, and replay and injection attacks [24].

Pedram Radmand et al [25] carried out research on Zigbee security and produced a paper presenting two different ways for grabbing the cryptographic key in ZigBee: remote attack and physical attack. It also surveys and categorises some additional attacks which can be performed on ZigBee networks: eavesdropping, spoofing, replay and DoS attacks at different layers. In this paper a survey of existing vulnerability in the security services available in ZigBee is presented. It also presents evidence that ZigBee is still vulnerable to some attacks especially those related to capturing its cryptographic keys.

Chapter 3 Induction motors fundamentals

After the introduction of the DC electrical distribution system by Edison in the United States [26], a gradual transition to the more economical AC system commenced. Lighting worked as well on AC as on DC. Transmission of electrical energy covered longer distances at lower loss with alternating current. However, motors were a problem with alternating current. Initially, AC motors were constructed like DC motors. Problems were encountered due to varying magnetic fields, as compared to the static fields in DC motor field coils. The magnetic field in AC motors has a sinusoidal variation, just as the current in the coil varies.
The most used motors in industrial motion control machinery are AC induction motors, as well as in mains powered home appliances such as washing machines, tumble dryers, blenders etc. They are called induction motors because voltage is induced in the rotor therefore there is no need for brushes. For voltage to be induced in the rotor, the rotor must rotate at a lower speed than the magnetic field to allow for the existence of an induced voltage. If the rotor was to rotate at the same speed as the rotating field, the flux lines of the starter could not cut the rotor bars which means no voltage will be induced into the rotor. The slip is the difference between the rotor speed and the synchronous speed.
Various types of AC induction motors exist in the market and are designed to suit different applications. The three phase AC induction motor is the only type where the rotating magnetic field is created naturally in the stator because of the nature of the supply. Three-phase AC induction motors are widely used in industrial and commercial applications. They are classified either as squirrel cage or wound-rotor motors. They are self-starting and use no capacitor, start winding, centrifugal switch or other starting device. They produce medium to high degree of starting torque. The power capabilities and efficiency in these motors range from medium to high compared to their single-phase counterparts. Popular applications include grinders, lathes, drill presses, pumps, compressors, conveyors, printing equipment, farm equipment, power presses, electronic cooling and other mechanical duty applications. An AC motor speed is determined by the following equation:

$$Speed = \frac{120 * F}{N} \qquad \textbf{Equation 3-1}$$

Where: F is the frequency and the only variable to affect a motor speed and N is the number of poles.
The magnetic field produced in the rotor because of the induced voltage is alternating in nature.
To reduce the relative speed, with respect to the stator, the rotor starts running in the same direction as that of the stator flux and tries to catch up with the rotating flux.
However, in practice, the rotor never succeeds in “catching up” to the stator field. The rotor runs slower than the speed of the stator field. This speed is called the Base Speed (N_b).
The difference between N_s and N_b is called the slip. The slip varies with the load. An increase in load will cause the rotor to slow down or increase slip. A decrease in load will cause the rotor to speed up or decrease slip. The slip is expressed as a percentage and can be determined with the following formula:

$$\%\ slip = \frac{N_s - N_b}{N_b} \qquad \textbf{Equation 3-2}$$

Where N_s is the synchronous speed in RPM and N_b is the base speed also in RPM

3.1 AC induction motor construction and operation

Induction motors generally consist of two basic assemblies: The stator, or stationary part, and the rotor, or rotating part. They have two sets of windings: armature windings, to which the power is applied, and field windings, which produce a magnetic field that interacts with the magnetic field from the armature windings to produce torque on the rotor. This torque causes the rotor to rotate.
Like most motors, an AC induction motor has a fixed outer portion, called the stator and a rotor that spins inside with a carefully engineered air gap between the two.
The stator consists of several thin laminations of aluminium or cast iron. They are punched and clamped together to form a hollow cylinder (stator core) with slots (as shown Figure 3-1 below component 16) with coils of insulated wires inserted into these slots. Each grouping of coils, together with the core it surrounds, forms an electromagnet (a pair of poles) on the application of AC supply. The number of poles of an AC induction motor depends on the internal connection of the stator windings. The stator windings are connected directly to the power source. Internally they are connected in such a way, that on applying AC supply, a rotating magnetic field is created.

The rotor has several thin steel laminations with evenly spaced bars, which are made up of aluminium or copper, along the periphery. In squirrel cage rotor, these bars are connected at ends mechanically and electrically by the use of rings. Almost 90% of induction motors have squirrel cage rotors. This is because the squirrel cage rotor has a simple and rugged construction. The rotor consists of a cylindrical laminated core with axially placed parallel slots for carrying the conductors. Each slot carries a copper, aluminium, or alloy bar. These rotor bars are permanently short-circuited at both ends by means of the end rings (as shown in figure below component 1). This total assembly resembles the look of a squirrel cage, which gives the rotor its name. The rotor slots are not exactly parallel to the shaft. Instead, they are given a skew for two main reasons.
The first reason is to make the motor run quietly by reducing magnetic hum and to decrease slot harmonics.
The second reason is to help reduce the locking tendency of the rotor. The rotor teeth tend to remain locked under the stator teeth due to direct magnetic attraction between the two. This happens when the numbers of stator teeth are equal to the number of rotor teeth. The rotor is mounted on the shaft using bearings on each end; one end of the shaft is normally kept longer than the other for driving the load. Some motors may have an accessory shaft on the non-driving end for mounting encoder, tachometer or position sensing devices. Between the stator and the rotor, there is an air gap, through which due to induction, the energy is transferred from the stator to the rotor. The generated torque forces the rotor to rotate and therefore rotating the load as it is attached to the rotor. The principle employed for rotation remains the same regardless of the type of rotor used.
Figure 3-1 below is intended to illustrate the general structure of an AC motor. It is only to show what components exist (see Table 3-1) on a generic motor; there will be discrepancies depending on the motor size and manufacturer version.

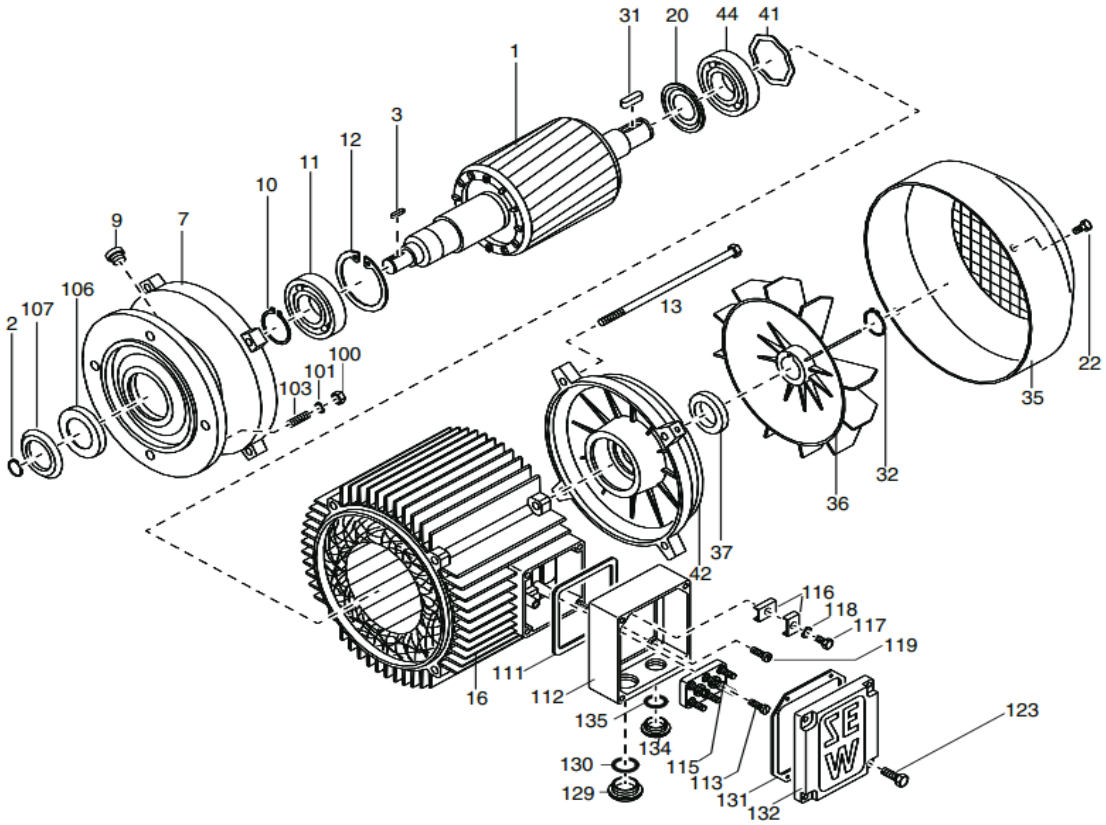

Figure 3-1: Basic structure of AC motors [27]

	Description		Description
1	Rotor	100	Hex nut
2	Circlip	101	Lock Washer
3	Key	103	Stud
7	Flange end Key	106	Oil seal
9	Screw plug	107	Oil-flinger ring
10	Circlip	111	Gasket
11	Grooved ball bearing	112	Terminal box lower part
12	Circlip	113	Machine screw
13	Hex head screw (tie rod)	115	Terminal board
16	Stator	116	Terminal yoke
20	Nilos ring	117	Hex head bolt
20	Hex head bolt	118	Lock washer
31	Key	119	Machine screw
32	Circlip	123	Hex head bolt
35	Fan Guard	129	Screw plug
36	Fan	130	Sealing washer
37	V-Ring	131	Sealing washer
41	Equalising Ring	132	Terminal box cover
42	Non drive-end bearing shield	134	Screw plug
44	Grooved ball bearing	135	Sealing washer

Table 3-1: Induction Motor Parts

Surveys carried out on induction machine failure have found the most common failure mechanisms in induction machines as follows: 13% stator, 10% rotor, 40% bearings and 12% others faults [28]

3.2 Direct On Line (DOL) Operation

Direct on Line (DOL) starting or sometimes called across the Line starting connects the motor windings/terminals directly to the circuit voltage “across the line” for a “full voltage start”. This is the simplest way to start a motor and usually the least expensive and motors connected in DOL are capable of drawing the full in-rush current and develop the maximum starting torque to accelerate the load to full speed in the shortest time possible. There are two different types of common DOL starters: Manual motor starters and magnetic motor starters.

3.2.1 Manual Motor Starters

A manual motor starter is a motor starting system consisting of a switch rated to suit the motor kW rating with one set of contacts for each phase and corresponding thermal overload devices for motor overload protection to ensure maximum operating life. The main advantage of a manual motor starter is lower cost than a magnetic motor starter with equivalent motor protection but less motor control capability. These types of motor starters are often used for smaller motors. Since the switch contacts remain closed if power is removed from the circuit without operating the switch, the motor restarts when power is reapplied which can be a safety concern. Figure 3-2 illustrates a manual DOL starter.

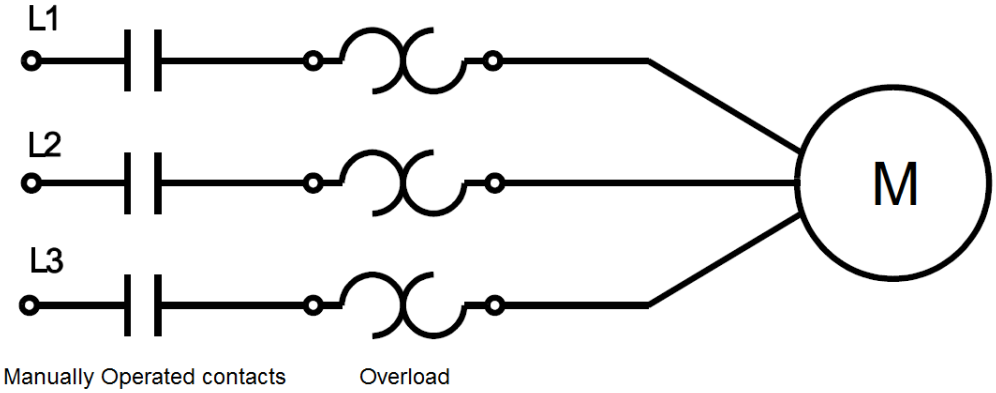

Figure 3-2: Manual DOL Starter

3.2.2 Magnetic Motor Starters

Magnetic DOL starter consist of a Moulded Case Circuit Breakers (MCCB) or Circuit Breaker, Contactor and an overload relay for protection. The electromagnetic contactor can be opened by the thermal overload relay under fault conditions. Typically, the contactor will be controlled by separate start and stop buttons, and an auxiliary contact on the contactor is used, across the start button, as a hold in contact which latches the contactor closed electrically while the motor is operating. Figure 3-3 illustrates a magnetic DOL Starter.

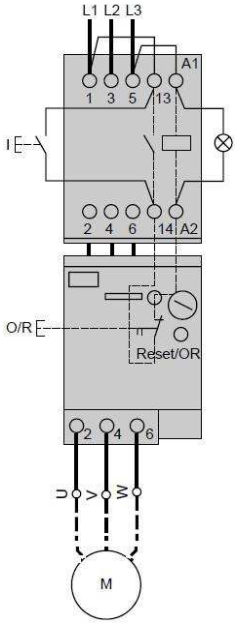

Figure 3-3: Magnetic DOL Starter

By pressing the Start button on Figure 3-3 the contactor coil will be energised. The contact on the contactor seals in the coil circuit. The contactor de-energises if the control circuit is interrupted, the Stop button is operated, or if power is lost. The overload contact is arranged so an overload trip on any phase will cause the contactor to open and de-energise all phases.

When the contactor is energised, all the contacts to the phases will close applying full line voltage to the motor terminals/windings. The motor will draw a very high inrush current for a very short time and then the current will be limited to the Locked Rotor Current of the motor. The motor will develop Locked Rotor Torque and begin to accelerate towards full speed. The current will begin to drop when the motor accelerates but will not drop significantly until the motor is at a high speed, typically about 85% of synchronous speed [29]. The actual starting current curve is a function of the motor design, and the terminal voltage, and is totally independent of the motor load. The actual starting current curve is a function of the motor design, and the terminal voltage, and is totally independent of the motor load. The motor load will affect the time taken for the motor to accelerate to full speed and therefore the duration of the high starting current, but not the magnitude of the starting current. DOL starting have a maximum start current and maximum start torque. This may cause an electrical problem with the supply, or it may cause a mechanical problem with the driven load. So this will be inconvenient for the users of the supply line, always experience a voltage drop when starting a motor. But if this motor is not of a high kW rating it does not affect much.

3.3 Torque production

A motor load system can be described by a fundamental torque equation [30].

$$T - T_l = J\frac{dw_m}{dt} + w_m\frac{dJ}{dt} \qquad \textbf{Equation 3-3}$$

Where:
T is the instantaneous value of the developed motor torque in N-m or lb.-inch
T_l is the instantaneous value of the load torque in N-m or lb.-inch
w_m is the instantaneous velocity of the motor shaft in rad/sec
And J is the moment of inertia of the motor load system express in $kg - m^2$ or $lb - inch^2$
For drives with constant inertia, $(\mathrm{dJ/dt})$ = 0. Therefore, the equation would be:

$$T = J\frac{dw_m}{dt} + T_l \qquad \textbf{Equation 3-4}$$

This shows that the torque developed by the motor is counter balanced by a load torque, T_l and a dynamic torque, *J*(*dωm*/*dt*). The torque component, *J*(*dω*/*dt*), is called the dynamic torque because it is present only during the transient operations. The drive accelerates or decelerates depending on whether T is greater or less than T_l. During acceleration, the motor should supply not only the load torque, but an additional torque component, (*dωm*/*dt*), in order to overcome the drive inertia. In drives with large inertia, such as electric trains, the motor torque must exceed the load torque by a large amount in order to get adequate acceleration. In drives requiring fast transient response, the motor torque should be maintained at the highest value and the motor load system should be designed with the lowest possible inertia. The energy associated with the dynamic torque, *J*(*dωm*/*dt*), is stored in the form of kinetic energy (KE) given by, *J*(ω2*m*/*2*). During deceleration, the dynamic torque, *J*(*dωm*/*dt*), has a negative sign. Therefore, it assists the motor developed torque *T* and maintains the drive motion by extracting energy from the stored kinetic energy. To summarise, in order to get steady state rotation of the motor, the torque developed by the motor (T) should always be equal to the torque requirement of the load (T_l). The torque-speed curve of the typical three-phase induction motor is shown in Figure 3-4 below.

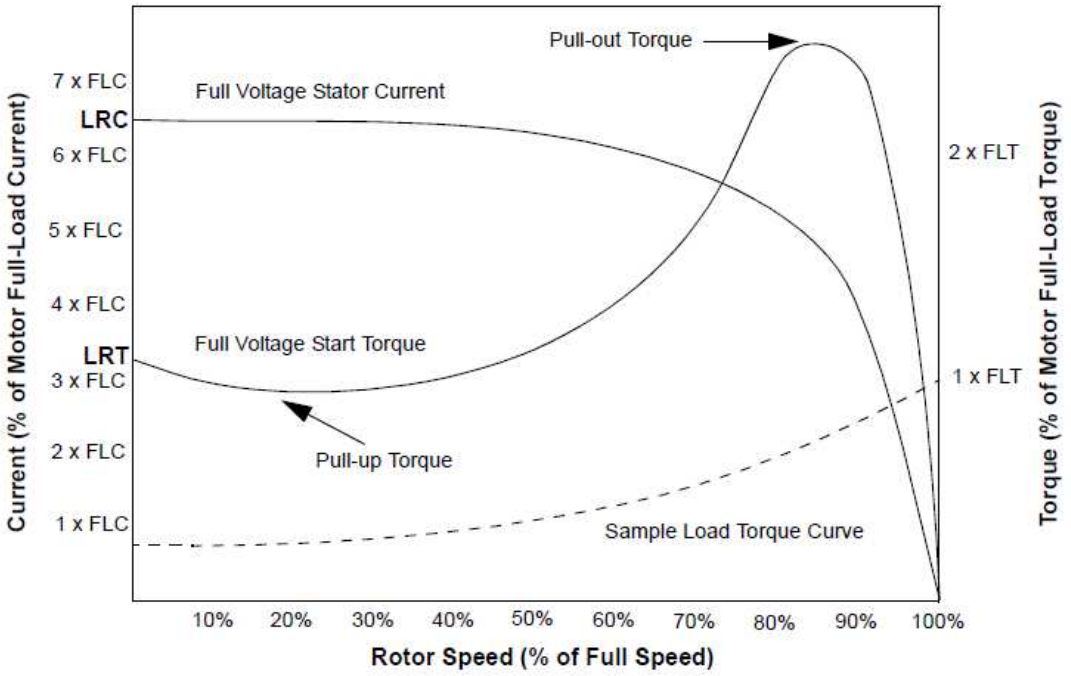

Figure 3-4: Typical induction motor speed-torque characteristic [30]

3.4 AC induction motor model

The Induction Motor block represents the electrical and torque characteristics of an induction motor powered by an ideal AC supply. The following figure shows the equivalent circuit model of the Induction Motor block.

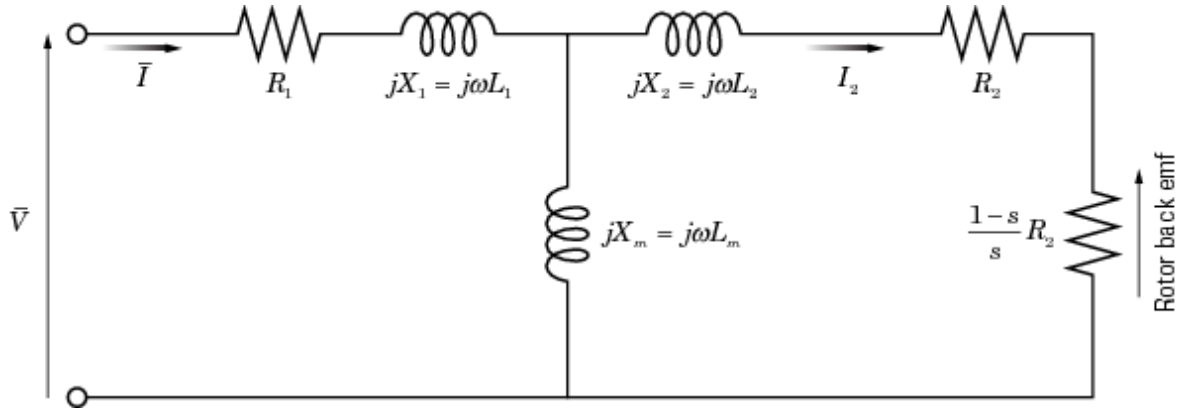

Figure 3-5: AC induction motor Model [31]

In the figure:

- R_1 is the stator resistance.
- R_2 is the rotor resistance with respect to the stator.
- L_1 is the stator inductance.
- L_2 is the rotor inductance with respect to the stator.
- L_m is magnetising inductance.
- s is the rotor slip.
- $\overline{V}$ and $\overline{I}$ are the sinusoidal supply voltage and current phasors.

[31] Rotor slip s is defined in terms of the mechanical rotational speed ω_m, the number of pole pairs p, and the electrical supply frequency ω by $s = 1 - \frac{pw_m}{w}$ and the torque speed relationship is given by:

$$T = \frac{npR_2}{s\omega} \frac{{V_{rms}}^2}{\left(R_1 + R_2 + \frac{1-s}{s}R_2\right)^2 + (X_1 + X_2)^2}$$ **Equation 3-5**

Where:

- V_{rms} is the line to neutral supply voltage for a star-configuration induction motor, and the line to line voltage for a delta-configuration induction motor.
- *n* is the number of phases.

A generalised dynamic model of induction motor consists of an electrical sub-model to implement the 3 phase to two phase axis transformation of stator voltage and current calculation, a torque sub-model to calculate the developed electromagnetic torque and a mechanical sub-model to yield the rotor speed [32].
The electromagnetic torque is obtained from the stationary frame rotor and stator currents as given by the following equation:

$$T_e = \frac{3}{2} * \frac{P}{2} * L_m\left(i_{s\beta} i_{r\alpha} - i_{r\beta} i_{s\alpha}\right)$$ **Equation 3-6**

The mechanical rotor speed is obtained from the electromagnetic torque as given by:

$$\omega_r = \int \frac{(T_e - T_l)}{J} dt$$ **Equation 3-7**

Where P is the number of poles of the machine and J is the moment of inertia.

3.5 Mathematical Description of AC Induction Motors

Since we are trying to use electrical supply parameters of an induction motor for condition monitoring, bearing in mind that the parameters are measured by a vector drive, it is important to understand space vector theory. The 3-phase motor quantities (such as voltages, currents, magnetic flux, etc.) are expressed in terms of complex space vectors. Such a model is valid for any instantaneous variation of voltage and current and adequately describes the performance of the machine under both steady-state and transient operation [33].
Assume that i_{sa} , i_{sb} and i_{sc} are the instantaneous balanced 3-phase stator currents:

$$i_{sa} + i_{sb} + i_{sc} = 0$$ **Equation 3-8**

The stator current space vector can then be defined as follows:

$$\overline{i_s} = k(i_{sa} + a i_{sb} + a^2 i_{sc})$$ **Equation 3-9**

Where
$a \; and \; a^2$ are the spatial operators,$a = e^{j2\pi/3}$, $a^2 = e^{j4\pi/3}$
k = The transformation constant and is chosen $k = 2/3$

The figure below illustrates the stator current space vector projection.

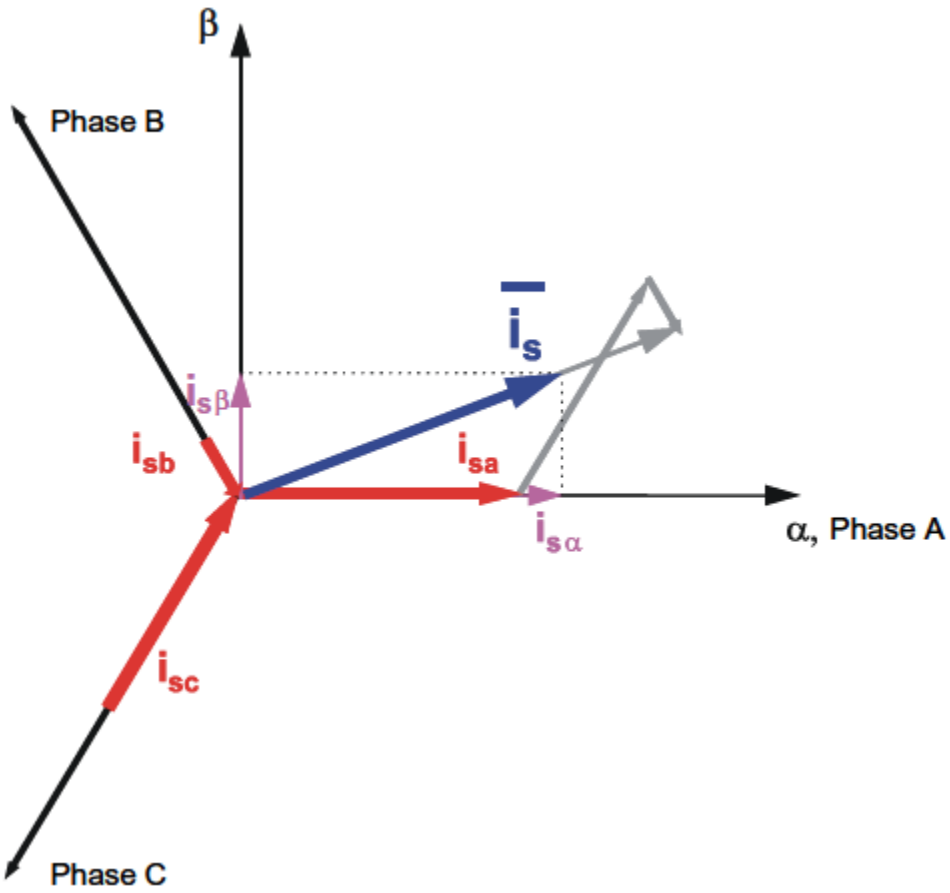

Figure 3-6: Stator Current Space Vector and Its Projection [33]

The space vector above can be expressed utilising the two-axis theory. The real part of the space vector is equal to the instantaneous value of the direct-axis stator current component,$i_{s\alpha}$ and whose imaginary part is equal to the quadrature-axis stator current component $i_{s\beta}$. Thus, the stator current space vector in the stationary reference frame attached to the stator can be expressed as:

$$\overline{i_s} = i_{s\alpha} + j i_{s\beta}$$ **Equation 3-10**

In symmetrical 3-phase machines, the direct and quadrature axis stator currents i_{sa}, i_{sb} are fictitious quadrature-phase (2-phase) current components, which are related to the actual 3 phase stator currents as per the following equations:

$$i_{s\alpha} = k\left(i_{sa} - \frac{1}{2}i_{sb} - \frac{1}{2}i_{sc}\right)$$

$$i_{s\beta} = k\frac{\sqrt{3}}{2}(i_{sb} - i_{sc})$$ **Equation 3-11**

Where:
k *=2/3* is a transformation constant
The space vectors of other motor quantities (voltages, currents, magnetic fluxes, etc.) can be defined in the same way as the stator current space vector.

3.6 Motor current response to fault

In order to fully appreciate induction motors for condition monitoring purposes, it is essential to understand motor current behaviour when healthy and when a fault occurs.

3.6.1 Motor current response with no fault

According to [34, 35], motor current signals in a healthy status can be described by an equation. To simplify the analysis process, the ideal electromagnetic relationships are examined in phase A, one of the three phases of power supply, and the higher harmonics in the phase is not considered. Referring to supply voltage, the current signal in phase A for a healthy motor drive can be expressed by the following equation:

$$i_A = \sqrt{2} I \cos(2\pi f_s t - \alpha_I) \qquad \textbf{Equation 3-12}$$

The equivalent magnetic flux in the motor stator is expressed by the following equation:

$$\phi_A = \phi\sqrt{2} \cos(2\pi f_s t - \alpha_\phi) \qquad \textbf{Equation 3-13}$$

The produced electrical torque by the interaction between the current and the flux can be express as follows:

$$T = 3P\phi I \sin(\alpha_I - \alpha_\phi) \qquad \textbf{Equation 3-14}$$

In the above equations *I* and ϕ are the root mean squared (RMS) amplitudes of the supply current and linkage flux respectively, α_I and α_ϕ are the phases of the current and flux referring to supply voltage. f_s is the fundamental frequency of electrical supply and *P* is the number of pole pairs.

3.6.2 Motor current response with active fault

When a fault occurs on a motor drive system, for example broken rotor bar, damaged gear or misaligned shaft, an additional mechanical torque component will be induced by the fault. In order to turn the load a corresponding electric torque will be generated by the motor. Supposing that the additional torque is a sinusoidal wave with a frequency f_F and an associated current wave with an amplitude I_F and phase α_F , the oscillatory torque can be expressed by the following equation:

$$\Delta T = 3P\phi I_F \sin[2\pi f_F t - (\alpha_I - \alpha_\phi) - \alpha_F] \qquad \textbf{Equation 3-15}$$

This will cause a corresponding angular oscillation expressed by the following equation:

$$\Delta\alpha_F = \int \Delta\omega dt = \frac{3P^2\phi I_F}{4\pi^2 f_F^2 J} \sin[2\pi f_F t - (\alpha_\phi - \alpha_F)] \qquad \textbf{Equation 3-16}$$

J is the inertia of the rotor system of motor. This angular oscillation modulates the phases of linkage flux in Equation 3-13. This leads to additional motor current signals in conjunction with associated phases to be approximated as [36]:

$$\begin{aligned} i^F{}_A \approx{}& \sqrt{2} I \cos(2\pi f_s t - \alpha_I) \\ &+ \sqrt{2} I_l \cos[2\pi(f_s - f_F)t - \alpha_I - \alpha_F - \varphi] \\ &- \sqrt{2} I_r \cos[2\pi(f_s + f_F)t - 2\alpha_\phi + \alpha_I - \alpha_F - \varphi] \end{aligned} \qquad \textbf{Equation 3-17}$$

where φ is the angular displacement of the motor equivalent circuit impedance at the supply frequency, I_l and I_r are the RMS values of the lower sideband component and the upper sideband component, respectively, which are the currents induced by the back-EMF voltages produced by the flux variations at frequencies of $f_s - f_F$ and $f_s + f_F$. Using the above equation a lot downstream mechanical fault can be diagnosed with good accuracy.

3.7 Need for variable speed drive

When an induction motor starts, it will draw very high inrush current due to the absence of the back EMF at start. This results in higher power loss in the transmission line and also in the rotor, which will eventually heat up and may fail due to insulation failure. The high inrush current may cause the voltage to dip in the supply line if the motor is of a reasonable size, which may affect the performance of other utility equipment connected on the same supply line.
While operating the motor, it might be necessary to stop/start the motor, ramp up to speed or ramp down depending on the application. In applications like cranes, the torque of the drive motor may have to be controlled so that the load does not have any undesirable acceleration or in applications like web transport the torque may have to be controlled to maintain the same web tension. The speed and accuracy of stopping or reversing operations improves the productivity of the system and the quality of the product which will not be possible with DOL starter.
In the past, variable speed drives were developed mainly for process control purposes; however, energy conservation has fast become an equally important advantage. A variable speed drive uses less energy than an alternative fixed speed DOL mode of operation because it will adjust the speed of the electric motor to match the actual demand of the application thereby reducing motor energy consumption by typically 20 to 50%. The energy saving potential in industries and utilities using variable speed drive is enormous. Nearly 70% of all electrical energy consumed by industry is used by the millions of electrical motors installed worldwide [37]. Every year, several more million motors are added. These motors are the workhorses of industry, driving machines, compressors, fans, pumps, power presses, conveyors and processes in virtually all industrial sectors.
With all the above problems both the consumers and the industry strongly supported the need for variable speed for induction motors.

Chapter 4 Induction motors speed control using AC drive

4.1 Introduction to AC drive systems

AC drives are electrical devices used to control the speed of electrical motors either induction motors or synchronous motors by varying the voltage and frequency supplied to the motor. AC drives are made up of active/passive power electronic devices like insulated-gate bipolar transistor (IGBT), metal-oxide-semiconductor field-effect transistor (MOSFET), TRIAC, etc., a high speed central controlling unit and optional sensing devices depending upon the application requirement. They are also known by various other names such as adjustable speed drives (ASD) or adjustable frequency drives (AFD) or variable frequency drives (VFD) or variable speed drives (VSD) or frequency converters (FC) or simply inverters, drives or converters. All medium voltage industrial AFDs consist of a converter section, a DC link, and an inverter section as illustrated on the figure bellow.
In power electronics the word 'inverter' refers a class of power conversion (or power conditioning) circuits that operates from a DC voltage source or a DC current source and converts it into AC voltage or current. The inverter does the opposite of what AC-to-DC 'converter' does. Even though input to an inverter circuit is a DC source except for a few special cases of very high power applications where cycloconverters are used, it is not uncommon to have this DC derived from an AC source such as utility AC supply. Thus, for example, the primary source of input power may be utility AC voltage supply that is rectified to DC by an AC to DC converter and then 'inverted' back to AC using an inverter. Here, the final AC output may be of a different frequency and magnitude than the input AC of the utility supply. The converter varies depending on the type of rectifier used: Pulse-width-modulated voltage source inverter (PWM-VSI) with a diode rectifier, Square-wave voltage source inverter (square-wave VSI) with a thyristor rectifier or Current source inverter (CSI) with a thyristor rectifier.

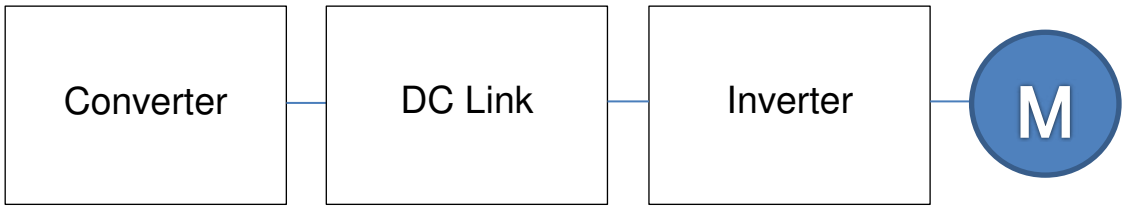

Figure 4-1: Typical AC Drive Block diagram

4.2 AC Drive technologies

AC drives can be classified according to their DC circuit structure to voltage-source, current-source, Six-step inverter and cycloconverter or matrix converter.

4.2.1 Voltage-source inverter

Figure 4-2 below shows a typical voltage source inverter structure where a constant DC voltage is formed by using an input diode rectifier. The output voltage with variable frequency and magnitude is produced by pulse-width modulating the inverter bridge. In more sophisticated inverters the input diode bridge can be replaced with a pulse-width modulation (PWM) bridge enabling a higher DC voltage, reactive power control, nearly sinusoidal supply network currents and regenerative operation of the inverter.

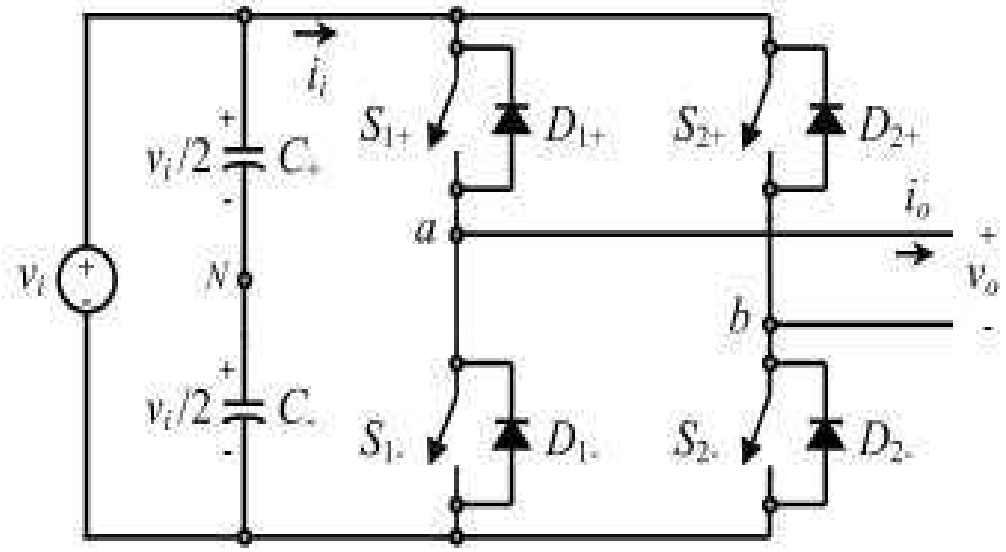

Figure 4-2: Voltage Source inverter [38]

4.2.2 Current-source inverter (CSI)

A CSI inverter [39] is a dual six-step voltage source inverter in which the DC power supply is configured as a current source rather than a voltage source. The converter section uses silicon-controlled rectifiers (SCRs), gate commutated thyristors (GCTs), or symmetrical gate commutated thyristors (SGCTs). This converter is known as an active rectifier or active front end (AFE). The DC link uses inductors to regulate current ripple and to store energy for the motor. The inverter section comprises gate turn-off thyristor (GTO) or SGCT semiconductor switches. These switches are turned on and off to create a pulse width modulated (PWM) output regulating the output frequency. The inverters SCRs are switched in a six-step sequence to direct the current to a three-phase AC load as a stepped current waveform. CSI inverter commutation methods include load commutation and parallel capacitor commutation.

The figure below illustrates a current source inverter. Due to high harmonic content the CSI design requires input and output filters.

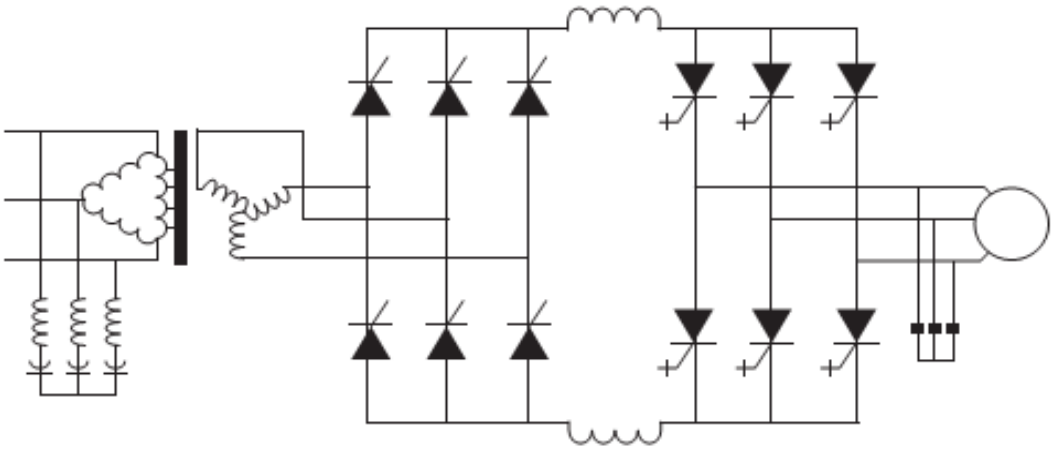

Figure 4-3: Current source inverter [40]

4.2.3 Six-step voltage source inverter

It is called “six-step inverter” because of the presence of six “steps” in the line to neutral (phase) voltage waveform. Harmonics of order three and multiples of three are absent from both the line to line and the line to neutral voltages and consequently absent from the currents. The Output amplitude in a three-phase inverter can be controlled by only changing the DC-link voltage. Figure 4-4 bellow illustrates a block diagram of a six step voltage source inverter.

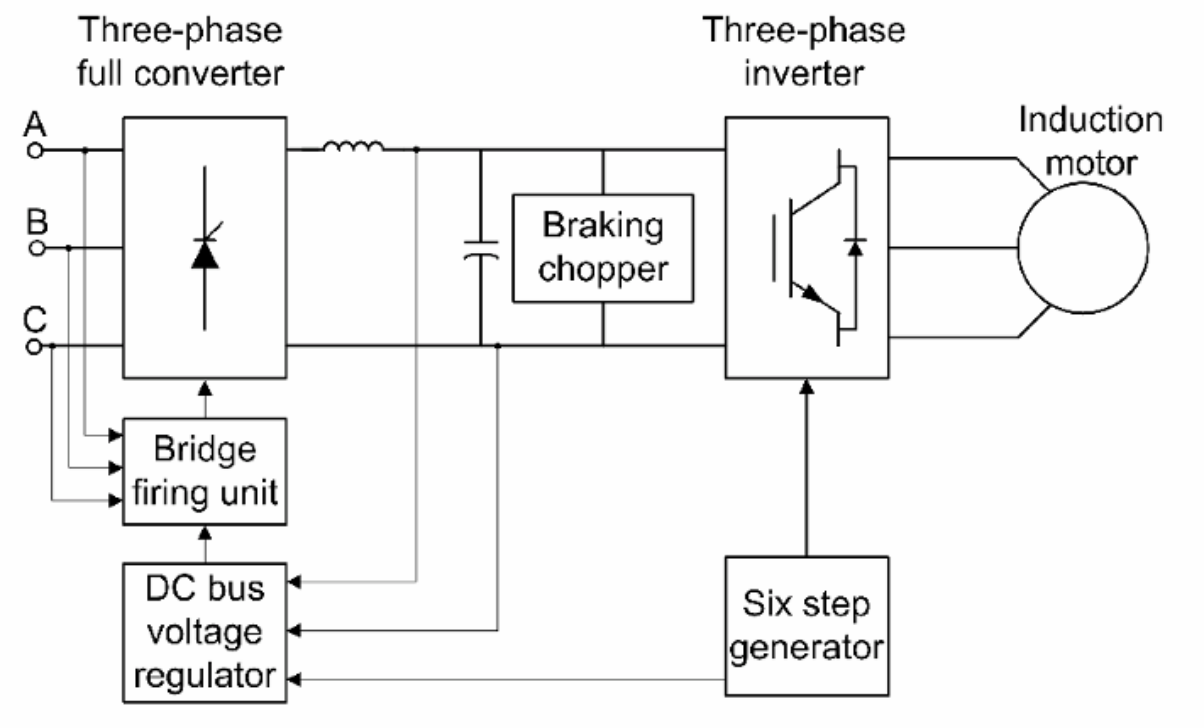

Figure 4-4: Six-Step VSI [41]

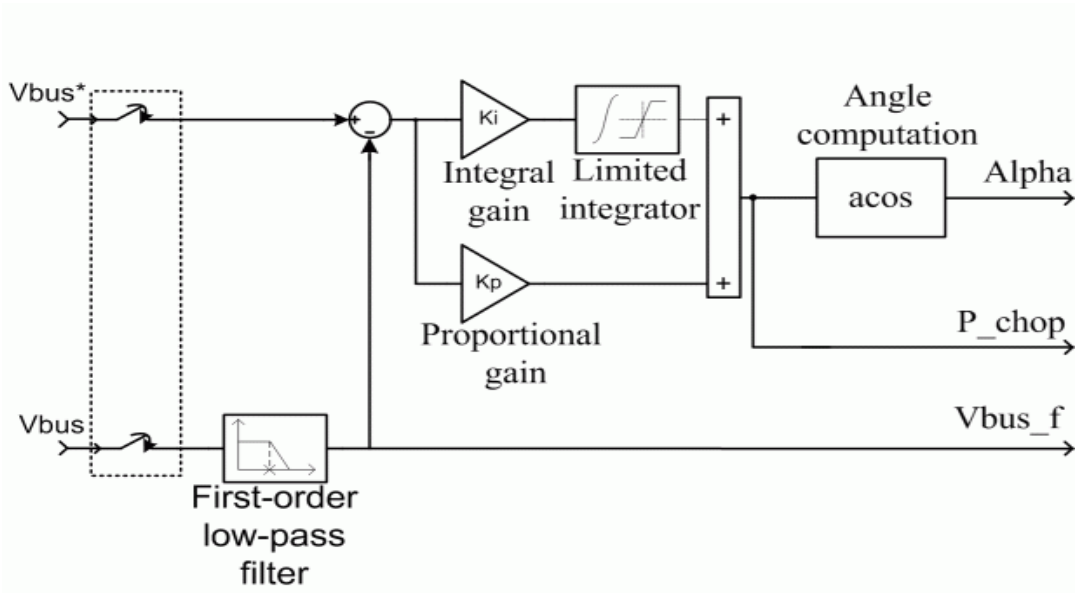

Figure 4-5: DC bus PI controller [41]

The DC bus voltage regulator is based on a PI controller shown on Figure 4-5 and hysteresis chopper logic. When the bus voltage decreases, the PI controller reduces the firing angle. When the bus voltage increases, the PI controller increases the firing angle. The chopper logic is based on

hysteresis control. If the voltage reaches the upper hysteresis limit, the DC voltage controller toggles to braking mode and the chopper is activated, whereas the Thyristor Bridge is shut off. In chopper mode, the proportional action remains active but the integral gain is set to zero because the chopper dynamics are very high and the integral gain is useless. When the bus voltage reaches the hysteresis lower limit, the braking chopper is shut down and the Thyristor Bridge is reactivated.

4.2.4 PWM inverter

With PWM inverters, a fixed dc input voltage is given to the inverter by means of a diode bridge rectifier and a controlled ac output voltage is obtained by modifying the width of the pulses in a pulse train in direct proportion to a small control signal; the greater the control voltage, the wider the resulting pulses become. By using a sinusoid of the desired frequency as the control voltage for a PWM circuit, it is possible to produce a high-power waveform whose average voltage varies sinusoidally in a manner suitable for driving ac motors as illustrated on Figure 4-6 bellow.

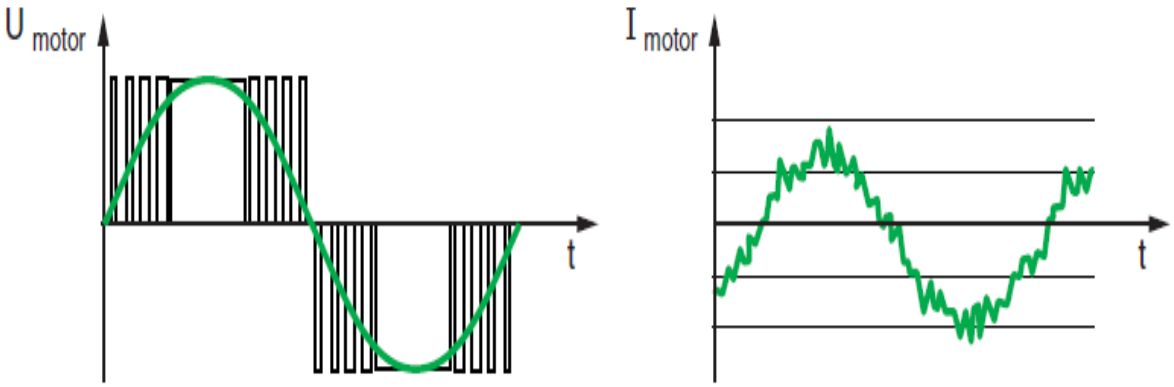

Figure 4-6: Pulse width modulation output waveforms [42]

As shown on the figure above, the triangular signal is the carrier or switching frequency of the inverter. The modulation generator produces a sine wave signal that determines the width of the pulses, and therefore the RMS voltage output of the inverter.

4.2.5 Cycloconverter or matrix converter

A matrix converter has several advantages over traditional rectifier inverter type power frequency converters. It provides sinusoidal input and output waveforms, with minimal higher order harmonics and no sub harmonics; it has inherent bidirectional energy flow capability; the input power factor can be fully controlled. It also has minimal energy storage requirements, which allows to get rid of bulky and lifetime limited energy storing capacitors. With the matrix converter, at any time one of the input lines has the voltage that is required for a PWM at the output line. Hence one only needs to connect the output line to the right input line at any time. To be able to connect each input with each output a matrix of 9 connection points is needed. Figure 4-7 below illustrates the structure of a matrix converter. Each connection point needs to be able to conduct current in both directions; therefore a bi-direction valve is required. These valves are shown as mechanical switches on the figure below for simplicity.

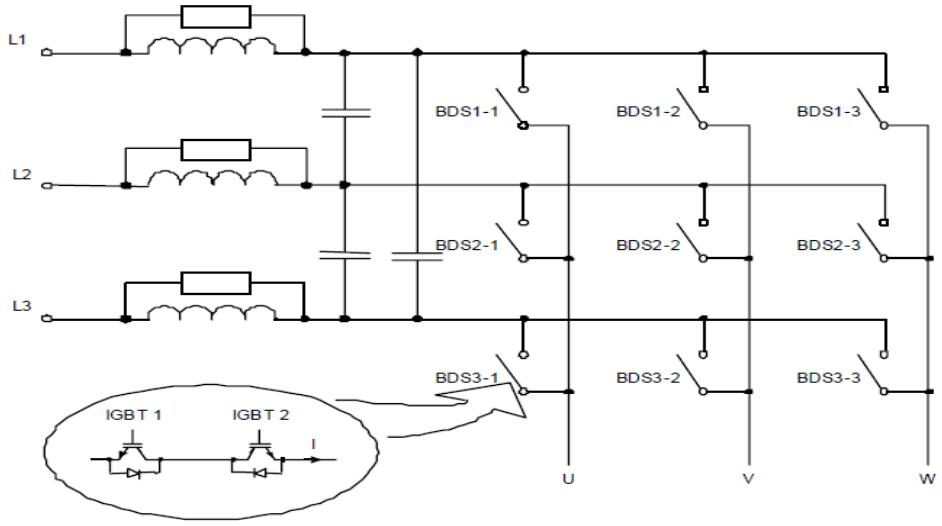

Figure 4-7: Simplified Structure of a matrix converter [43]

4.3 AC Drive control Platform

AC drives that use PWM techniques have varying levels of performance based on control algorithms. There are five basic types of controls for AC drives used these days in industry. These are Volts per Hertz, Sensorless Vector Control, Flux Vector Control, Sensorless Field Oriented Control and Field Oriented Control.

4.3.1 Volts/Hertz control

Volts/Hertz control is a basic control method for induction motors, providing a variable frequency drive for applications like fan and pump in which the v/f ratio is maintained constant in order to get constant torque over the entire operating range as illustrated on Figure 4-8 below. Very little knowledge of the motor is required for V/F control. It provides a reasonable speed and starting torque, at a cost effective price. This type of control is also called scalar control since only magnitudes of the input frequency and voltage are controlled. To increase starting torque, V/Hz drives use “Voltage Boost” to over-flux the motor to increase starting torque; but “Voltage Boost” over prolonged operating periods may result in overheating of the motor’s insulation system and result in damage or premature failure. Motor Insulation life is decreased by 50% for every 10°C above the insulation’s temperature capacity. Some of the drawbacks of this type of control are that the torque developed is load dependent as it is not controlled directly and the transient response is not fast due to the predefined switching pattern of the inverter.
These drawbacks can be overcome by vector control but it will make the system more expensive, and increase size and complexity.

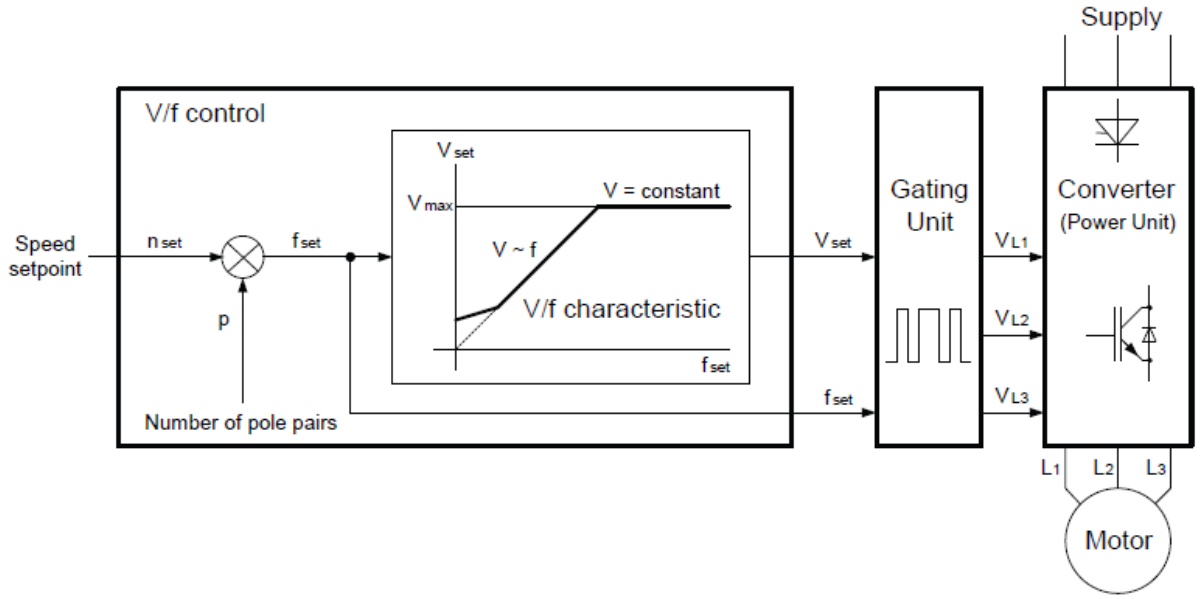

Figure 4-8: Diagram of the basic structure of the V/F control mode [44]

As seen on Figure 4-8, the voltage and the frequency are varied at a constant ratio up to the base speed. The gating unit generates pulse patterns to control the IGBTs in the three phases of the inverter's power unit. The flux and the torque remain almost constant up to the base speed. Beyond the base speed, the supply voltage cannot be increased. Increasing the frequency beyond the base speed results in the field weakening and the torque reduces.

4.3.2 Vector control

Performance levels can be significantly increased by using control electronics based on flux vector control, this feature is standard to most drives on the market these days. Vector control aims to achieve the same dynamic performance or better from and AC motor as from a DC motor but with certain limitation and the quantity that needs to be controlled is the torque. The torque (T) in all rotation electro mechanic machinery is proportional to the product of the current and (I) and the field flux (ψ). [$T \alpha I\psi$]

In order to achieve these levels of performance, some knowledge of the motor's parameters is required. On commissioning, the commissioning engineer must input the characteristics indicated on the motor rating plate into the drive adjustment parameters which are used to calculate the rotor characteristics. These include:

- Nominal motor voltage
- Nominal stator frequency
- Nominal stator current
- Nominal speed
- Motor cosine

Depending on the drive manufacturer the engineer might have to perform an autotune during commissioning or the drive will automatically perform an autotune on power up or start-up. There are two types of autotunes, stationary autotune and rotating autotune.

Rotating autotune spins the motor up to the maximum speed set by the user to identify all necessary motor characteristics and the motor must spin freely with no load during this method of autotune. This is the preferred method.

Stationary autotune only used when the motor cannot spin freely during the autotune feature hence a limited set of motor characteristics are identified. The commissioning engineer must enter the correct value of magnetising current as this is not identified with this method.

The following parameters are identified during autotune:

- Magnetising current. Not measured by Stationary autotune
- Per phase stator resistance
- Per phase stator leakage inductance
- Per phase mutual inductance

- Rotor time constant. This is identified from the magnetising current and motor nameplate rpm
- Encoder direction, Parameter is only set up if drive is configured to run as Closed-loop Vector control. This is not measured by Stationary autotune

This solution uses Park transformation as and can be used to control the current (Id) that provides the flux in the machine and the current (Iq) that provides the torque independently. The AC motor is controlled with this type of control in the same way as a DC motor. Figure 4-9 bellow illustrates a Simplified schematic of a drive with flux vector control with encoder feedback.

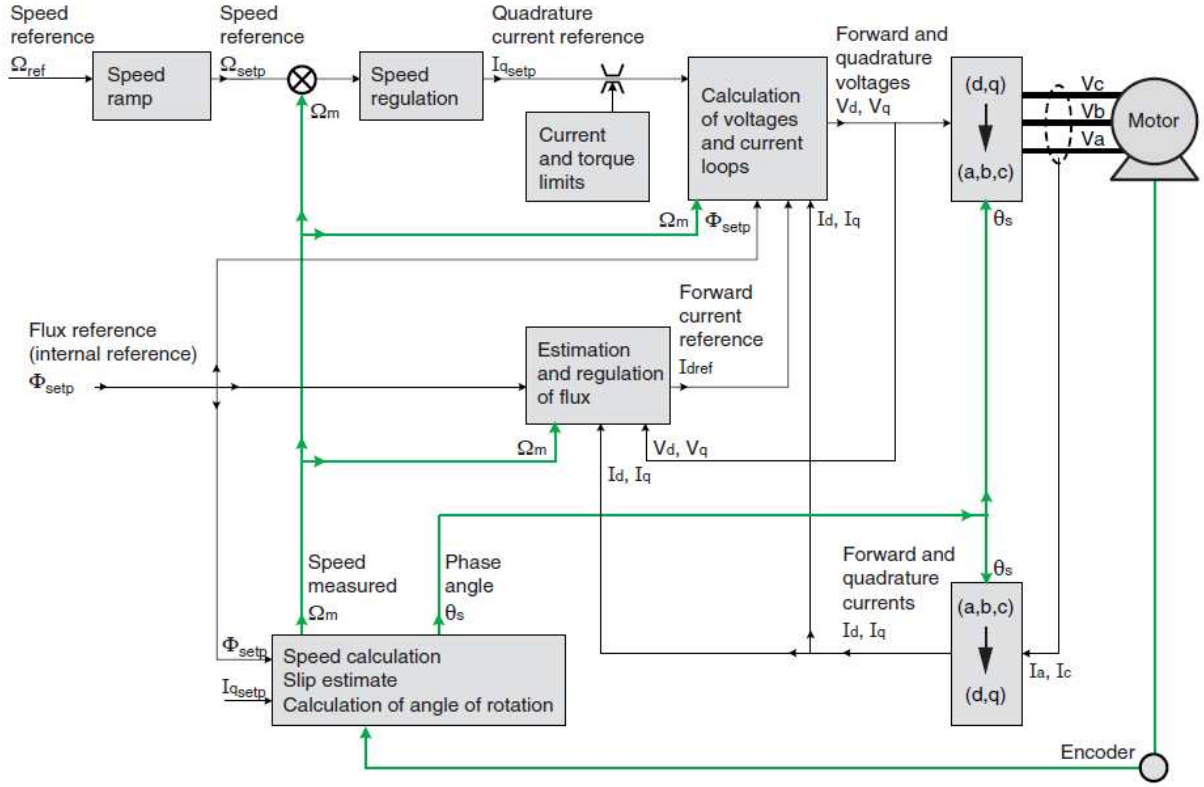

Figure 4-9: Simplified schematic of a drive with closed loop vector control [42]

4.3.3 Sensorless Vector Control

Vector control of an induction motor is usually implemented through measuring speed or position. However, speed and position sensors require the additional mounting space, reduce the reliability in harsh environments and increase the cost of motor.

Sensorless flux vector control illustrated on Figure 4-11 as its name says is a flux vector control without any sensor like an encoder, tachometer or any other speed or position feedback device; this is an improved V/F control as it uses direct field orientation to provide a higher performance.

This type of control relies heavily on speed or position estimation. They are various methods for speed estimation such as open-loop estimators, estimators using saturation third-harmonic voltage, estimators using saliency, model reference adaptive systems (MARS) with different kind of observers, estimators based on extended observers or estimators using artificial intelligence [45, 46]. MRAS [47, 48, 49] algorithm of them all has been proved to be effective and physically clear and is the method of speed estimation used in the test rig drive**.**

The classical rotor flux MRAS speed estimation shown in Figure 4-10 below consists mainly of a reference model, an adaptive model and an adaptation scheme which generates the estimated speed. The reference rotor flux components obtained from the reference model are given by [50]:

$$p_{\psi_{rd}} = \frac{L_r}{L_m}\{v_s D - R_s i_s D - \sigma L_s p i_s D\} \qquad \textbf{Equation 4-1}$$

$$p_{\psi_{rd}} = \frac{L_r}{L_m}\{v_s Q - R_s i_s Q - \sigma L_s p i_s Q\}$$

The adaptive model, usually represented by the current model, describes the rotor equation where the rotor flux components are expressed in terms of stator current components and the rotor speed. The rotor flux components obtained from the adaptive model are given by [50]:

$$p_{\hat{\psi}_{rd}} = \frac{L_r}{T_m} i_s D - \frac{1}{T_r}\hat{\psi} rd - \hat{\omega} r \hat{\psi} rq$$
$$p_{\psi_{rd}} = \frac{L_r}{T_m} i_s Q - \frac{1}{T_r}\hat{\psi} rq + \hat{\omega} r \hat{\psi} rd$$

Equation 4-2

$i_s D$, $i_s Q$	Stator current components in the stator frame
L_m	Mutual inductance
L_s, L_r	Stator and rotor self-inductances
p	Differential operator
R_s, R_r	Stator and rotor resistances
T_r	Rotor time constant
$v_s D$, $v_s Q$	Stator voltage components in the stator frame
σ	Leakage coefficient
$\hat{\psi} rq$, $\hat{\psi} rd$	Components of the rotor flux linkage vector
$\hat{\omega} r$	Angular rotor speed

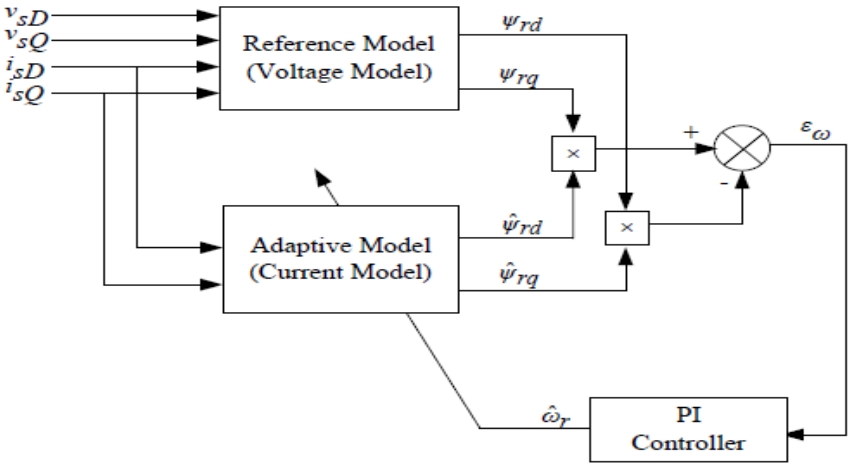

Figure 4-10: Simplified MRAS speed estimation [51]

The reference model above, usually expressed by the voltage model represents the stator equation. It generates the reference value of the rotor flux components in the stationary reference frame from the monitored stator voltage and current components. The output from the reference model and the adaptive model are fed into the vector cross product block to produce a vector error signal.
Knowledge of the motor parameters after autotune and motor model are used to calculate the ideal d and q axis voltage required to achieve the demanded magnetising current for varying motor load conditions. The identified stator resistance and inductance replace the requirement of voltage boost used in a traditional inverter drive.
The figure below illustrates a simplified block diagram of a drive with sensorless vector control, the control uses the d and q axis current components provided by the current feedback processing software block. The d axis current component represents the magnetising current and must remain constant in the constant torque region independent of the motor loading. The q axis current component represents the torque producing current and is used to achieve open loop slip compensation.

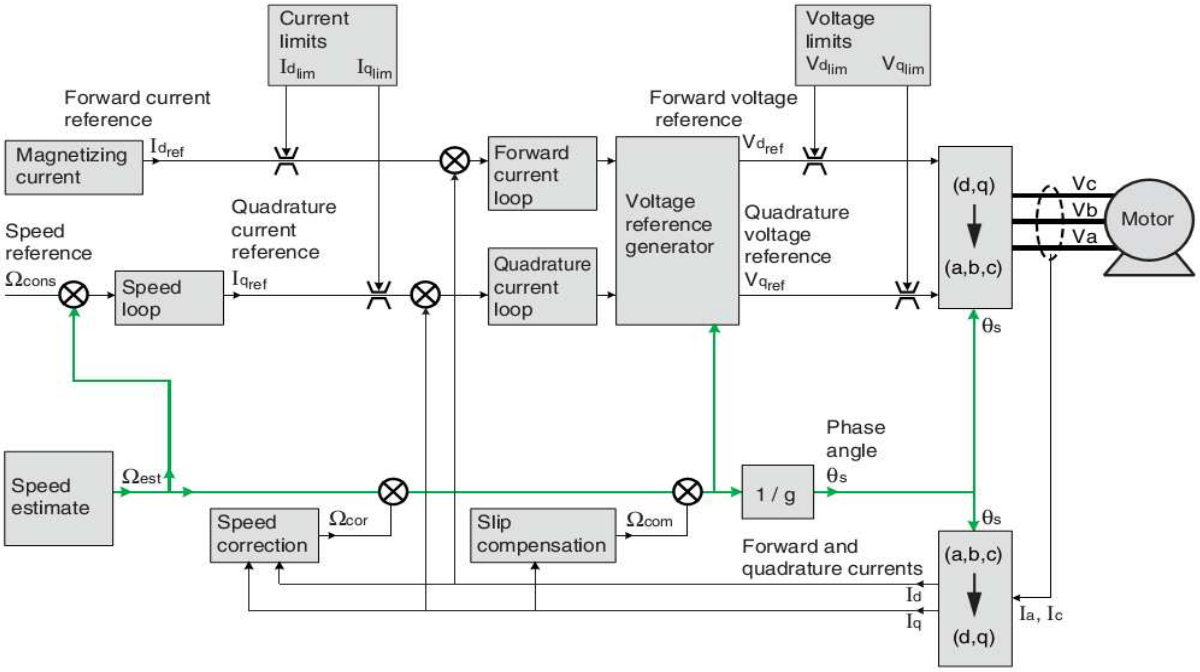

Figure 4-11: Simplified schematic of a drive with sensorless vector control [42]

4.3.4 Field oriented control

The main difference between a vector control and field oriented control (FOC) is the ability to separate and independently control (regulate) the motor flux and torque by using voltage feedback to adapt/optimise changes in motor temperature. This allows the induction motor to be controlled as a simple DC motor.

Field oriented control as shown on Figure 4-12 involves controlling the components of the motor stator current using a high bandwidth regulator represented by a vector, in a rotating reference frame (with a d-q coordinate system). The high bandwidth characteristics of this control help eliminate nuisance trips due to shock-loads and will continuously adapt to changes in the motor and load characteristics.

A separate adaptive controller uses information gained during autotuning, actual reference information and motor feedback information to give independent torque and flux control. This allows continuous regulation of the motor speed and torque.

In a special reference frame, the expression for the electromagnetic torque of the smooth-air-gap machine is similar to the expression of torque in a separately excited DC machine. In the case of induction machines, the control is normally performed in a reference frame aligned to the rotor flux space vector. To perform the alignment on a reference frame revolving with the rotor flux requires information about the modulus and the space angle (position) of the rotor flux space vector.

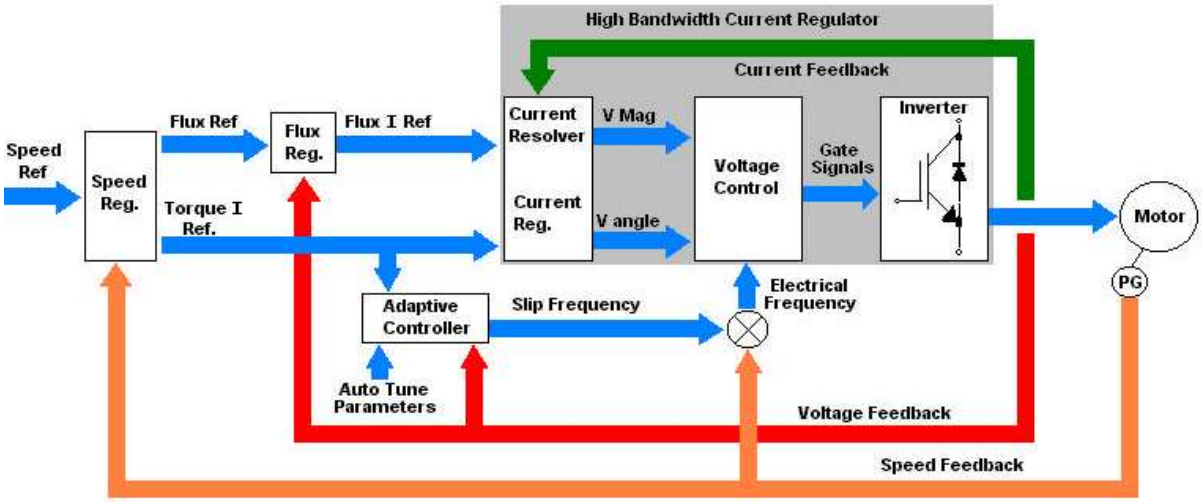

Figure 4-12: Simplified closed loop Field Oriented Control Block Diagram [52]

4.3.5 Sensorless field oriented control

This is effectively field oriented control without motor speed or position feedback as illustrated on Figure 4-13. A major difference is that the drive continues to operate with field oriented control instead of reverting back to volts/hertz control which provides significant benefits with dynamic performance, tripless operation, and torque regulation.

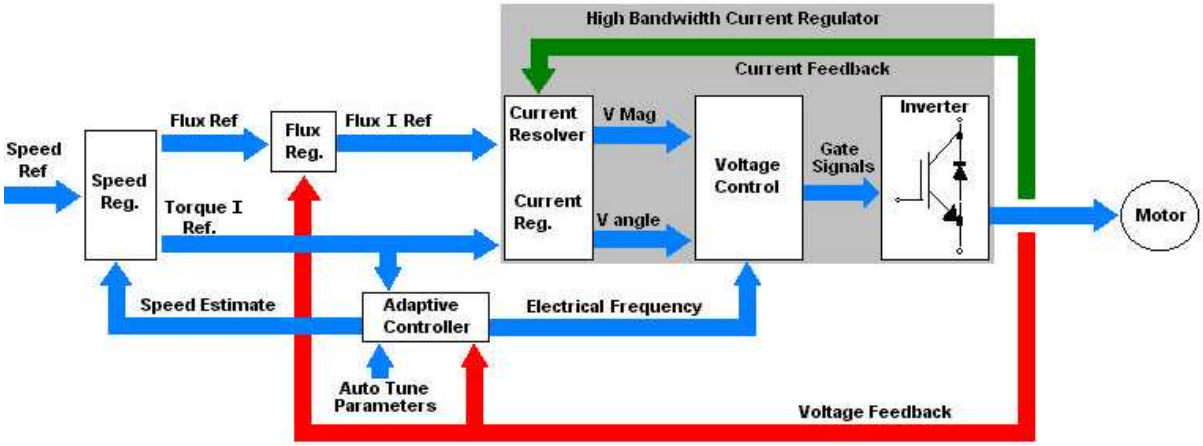

Figure 4-13: Simplified sensorless Field Oriented Control Block Diagram [52]

4.3.6 Direct torque control

Direct torque control (DTC) as shown on Figure 4-14 is the control of a three phase induction motor speed by controlling its torque. This involves calculating an estimate of the motor's magnetic flux and torque based on the measured voltage and current of the motor. DTC principles were first introduced by Depenbrock [43] and Takahashi [53]. With this method, Stator voltage vectors are selected according to the differences between the reference and actual torque and stator flux linkage. Torque is estimated as a cross product of estimated stator flux linkage vector and measured motor current vector. The estimated flux magnitude and torque are then compared with their reference values. If the estimated flux or torque deviates from the reference by more than the set tolerance, the transistor of the inverter will switch on and off at high speed in such a way that the errors will return to their tolerant bans as soon as possible. This high speed of switching is fundamental to the success of DTC. The DTC method is characterised by its simple implementation and a fast dynamic response.

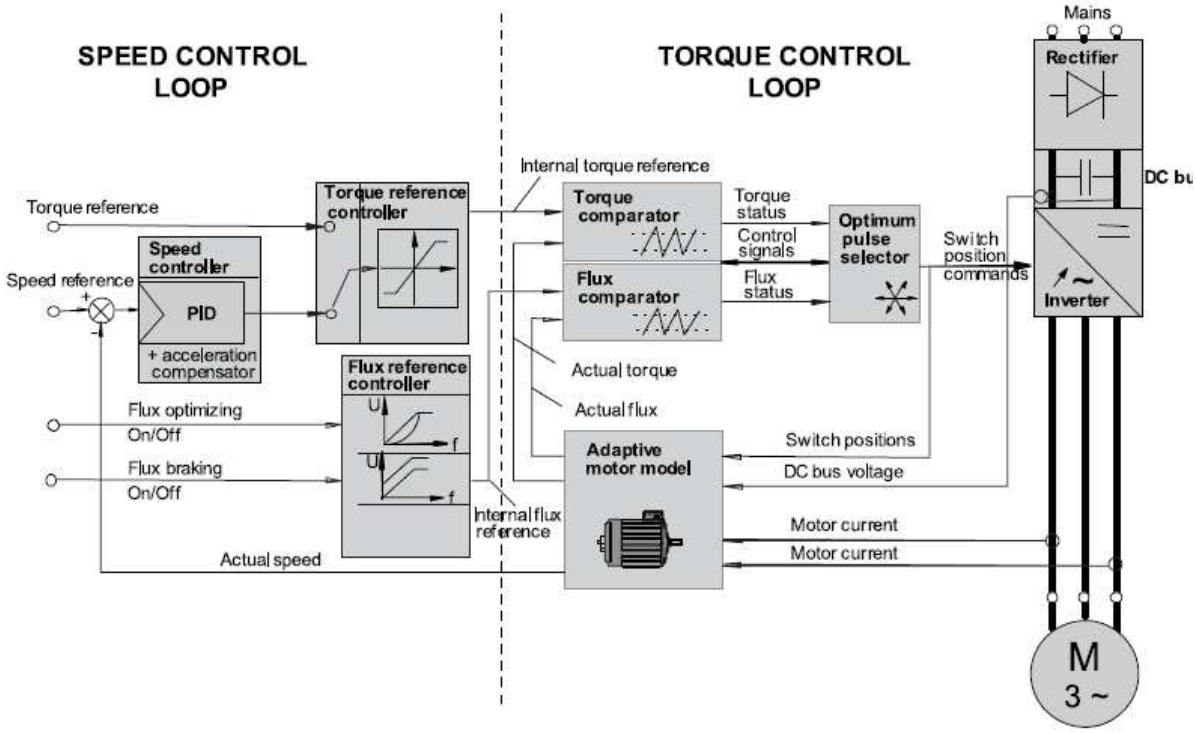

Figure 4-14: DTC block diagram [54]

4.4 Braking/Regeneration

When the rotor of an induction motor turns slower than the speed set by the applied frequency, the motor is transforming electrical energy into mechanical energy at the motor shaft. This process is referred to as 'motoring'. When the rotor turns faster than the synchronous speed set by a drive output, the motor is transforming mechanical energy from the motor shaft into electrical energy. It may be that the motor is ramping down to stop, a reduction in commanded speed for example the set speed is dropped and the motor is slowing down to its new set speed, or an overhauling load that causes the shaft speed to be greater than the synchronous speed. In any of these cases this condition is referred to as 'regeneration". The motor then becomes a generator. The energy or power generated by the motor may be dissipated as heat through a dynamic braking resistor (Resistive braking), or alternatively with the correct technology, it can be returned into the incoming power line (regenerative braking).
Cranes, hoists and elevators all require braking when load is descending. Regenerative braking is applicable for economy but for applications such as this, resistive braking is a necessary safety feature: as long as the motor field supply is intact, a resistive brake will provide backup should the mains supply be interrupted or the line fuses blow, or if the drive was to fail [55].

Chapter 5 Gearbox test rig

The test rig was mechanically designed by the university of Huddersfield engineering department. The control system on this test rig was designed and built by Optima Control Solutions my former employer, although I was not involved in the design I have worked with the control gears used on the rig for a number of years.
The test rig control system consists of a HMI connected to a PLC interface to enable specific timing and control setting functions to operate automatically. The AC inverter drive controls the test rig's AC motor over different speed settings from the HMI and the DC Drive controls the load to the AC motor. Figure 5-1 below shows the block diagram of the test rig.

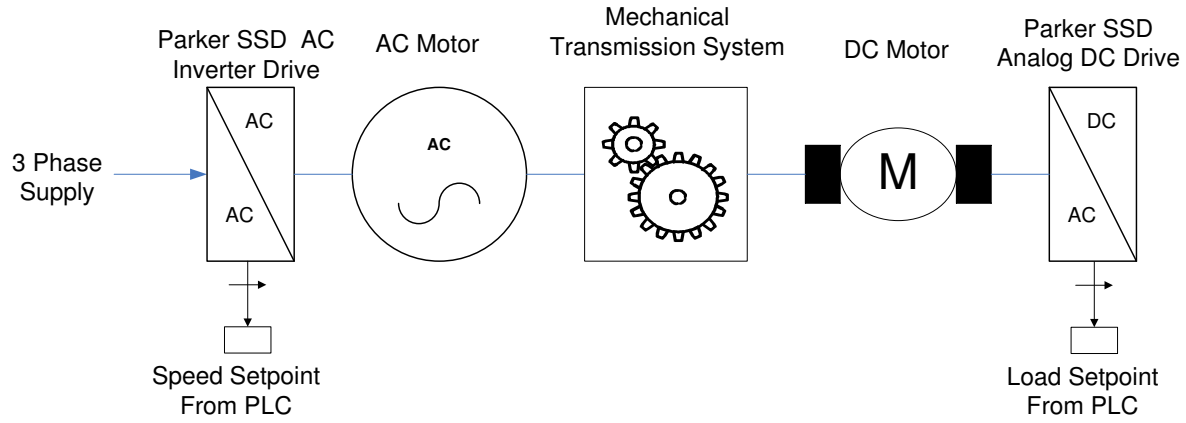

Figure 5-1: Gearbox test rig block diagram

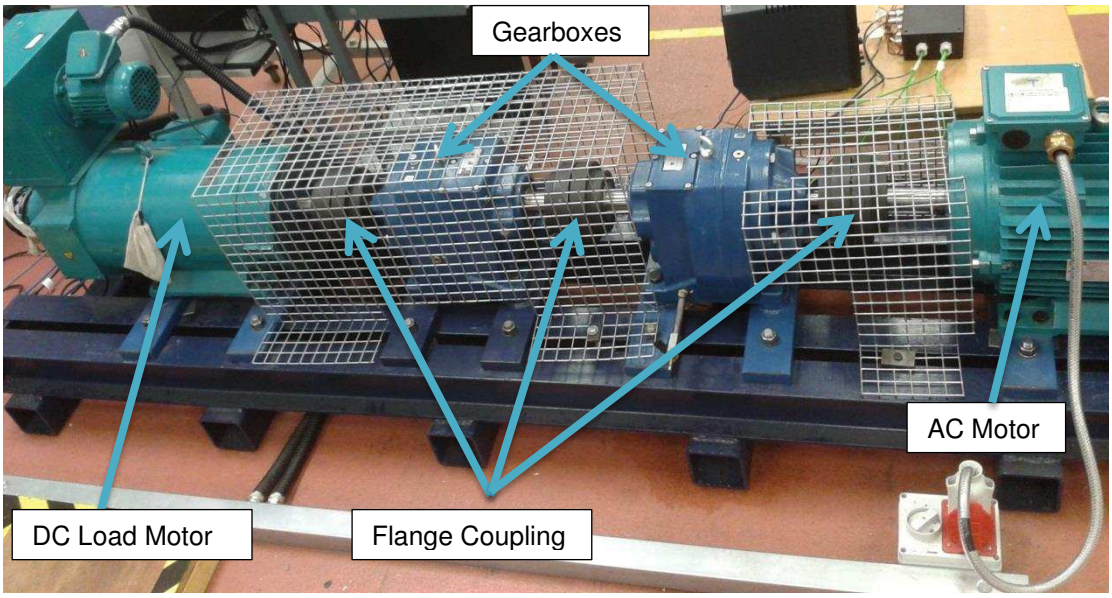

Figure 5-2: Gearbox Test rig

As shown on Figure 5-2 above the transmission system consist of two set of gearboxes connected between the AC motor and the DC load motor using flange couplings. The specification of each components of the test rig is explained below.

5.1 AC motor

Most motors come with a gearbox already attached to the shaft of the motor; however on this test rig the motor is a standalone attached to a separate gearbox by a flange coupling. This is due to the fact that the primary purpose of the rig was gearbox testing and it is easier to remove the gearbox when required. The specification of the AC motor used on the test rig is listed below in Table 5-1.

Table 5-1: AC Motor Specifications

DC Load Motor Specification	
Manufacturer	Brook Crompton
Type	T-DA160LA
kW rating	15
Speed (RPM)	1460
Cos Φ	0.87
Full load torque (Nm)	98.1
DOL Starting torque ratio	2.2
Rotor inertia (kgm^2)	0.129
Full load current at 380 (Amps)	29.6
Full load current at 400 (Amps)	28.2
Full load current at 415 (Amps)	27.13

5.2 DC Motor

The DC load motor provides load to the AC motor and is connected to the AC motor via a set of gearboxes. The specification of the DC motor used on the test rig is listed below in Table 5-2.

Table 5-2: DC Load Motor Specifications

DC Load Motor Specification	
Manufacturer	Brook Crompton
Size	MD132LC
kW rating	15
Speed (RPM)	2100
Armature Voltage (Volts)	460
Armature Current (Amps)	37.5
Armature Field Voltage (Volts)	360
Armature Field Current (Amps)	2.37
Form Factor	1.05

5.3 Gear boxes

Two identical David & Brown Radicon M series gearboxes are used on this rig each with a ratio of 3.678 t0 1.

5.4 DC drive and resistors bank

The parker 514 C DC controller is used to control the field of the test rig DC motor therefore providing the load to the AC motor. The DC motor act as a generator and the energy generated is converted into heat by the resistors bank. The field current setpoint is sent from the test PLC in the form of 0 to +10V (0-100% load) to provide a load to the test rig AC motor. The diagram of the DC load motor with the DC controller is illustrated on Figure 5-3: Test Rig DC load motor diagramFigure 5-3.

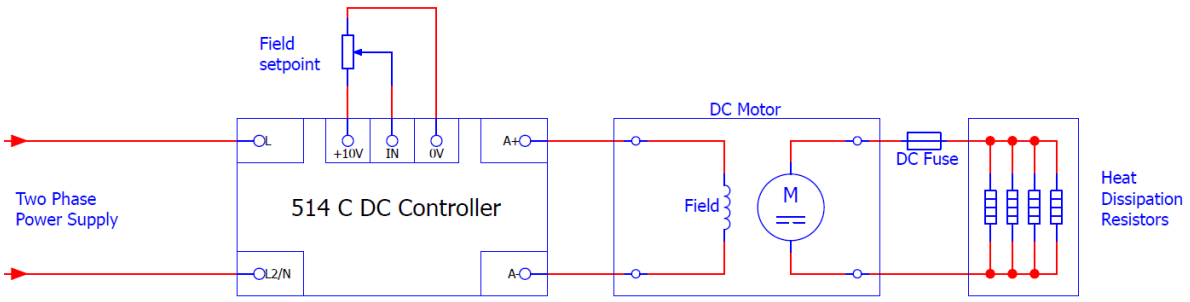

Figure 5-3: Test Rig DC load motor diagram

The 514C is a full four-quadrant regenerative controller designed to control the speed of a DC Shunt wound or permanent magnet motor; however in this application it is solely used as a field controller. It uses Closed Loop with Proportional Integral Control and adjustable Stability control of the output current and feedback voltage to give precise control of the motor field. The heat dissipation resistors were selected to cope with the maximum amount of energy generated by the DC motor.

5.5 Test rig AC drive

The drive used on this test rig is a Parker SSD 650 Vector drive; this is general purpose high performance AC drive ideal for standard AC motor control applications where the functionality of more complex drives is unnecessary and has the following control terminals:

- 2 x Analogue Inputs (Speed Control 0-10V, 0-10V/4-20mA),
- 3/5 Digital Inputs (User configurable Start/Stop/Direction/pre-set speeds),
- 1 Analogue output (User configurable output frequency/load 0-10V),
- 1/3 Digital outputs (one relay output 4A @ 240V and two programmable input/output).

SSD 650V AC Frequency Inverters are designed for AC motors in V/F (voltage/ frequency) or Sensorless Flux Vector. Sensorless vector is used on the test rig drive. These two control modes are discussed further in the next chapters.

Figure 5-4 illustrates a block diagram of the drive.

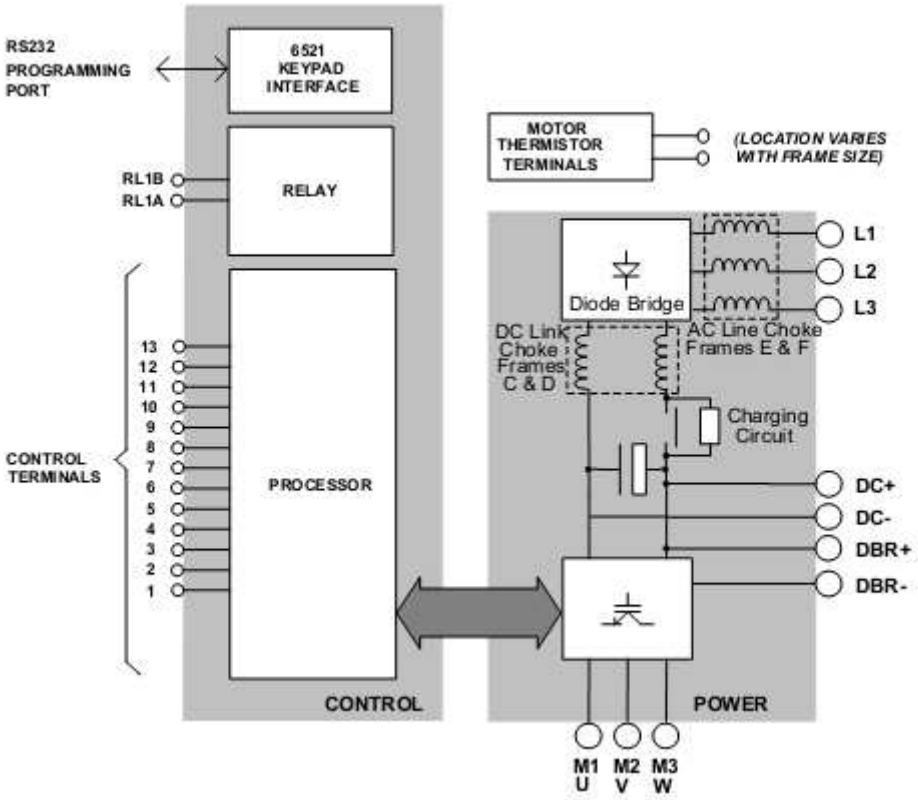

Figure 5-4: Block Diagram of 650V (drive Frames C, D, E, F) [56]

As shown on Figure 5-4 the drive consist of two main parts; a power board on the left and a control board on the right. On the power board DC link capacitors smooth the dc voltage output prior to the drive power stage. And the IGBT (Insulated Gate Bi-polar Transistor) output stage converts the dc input to a three phase output used to drive the motor.
The control board houses the processor, control relay and the communication interface via a keypad or a PC running Parker SSD Drives' "DSE Lite" windows-based configuration software. The processor provides for a range of analogue and digital inputs and outputs, together with their reference power supplies.
This drive is controlled and monitored via its terminal. Each control function or parameter been monitored has a dedicated terminal block and wire running between the drive and the PLC. The speed is adjusted by driving an analogue output from the PLC into one or both of the drive analogue input(s) and start/stop function is achieved by energizing a digital input of the drive from the PLC digital output. The status of the drive is monitored by sending digital outputs to the PLC digital inputs for running, tripped and stopped. Since this drive only has one analogue output, this can be configured to send one of the following signals to the PLC: current feedback, current demand, torque feedback, torque demand, speed demand etc. This type of communication between the drive and the control station (PLC on this rig) is called "Parallel communications" as multiple binary data can be transferred simultaneously and all communication paths are in parallel [55]. This is illustrated on the Figure 5-5 below.

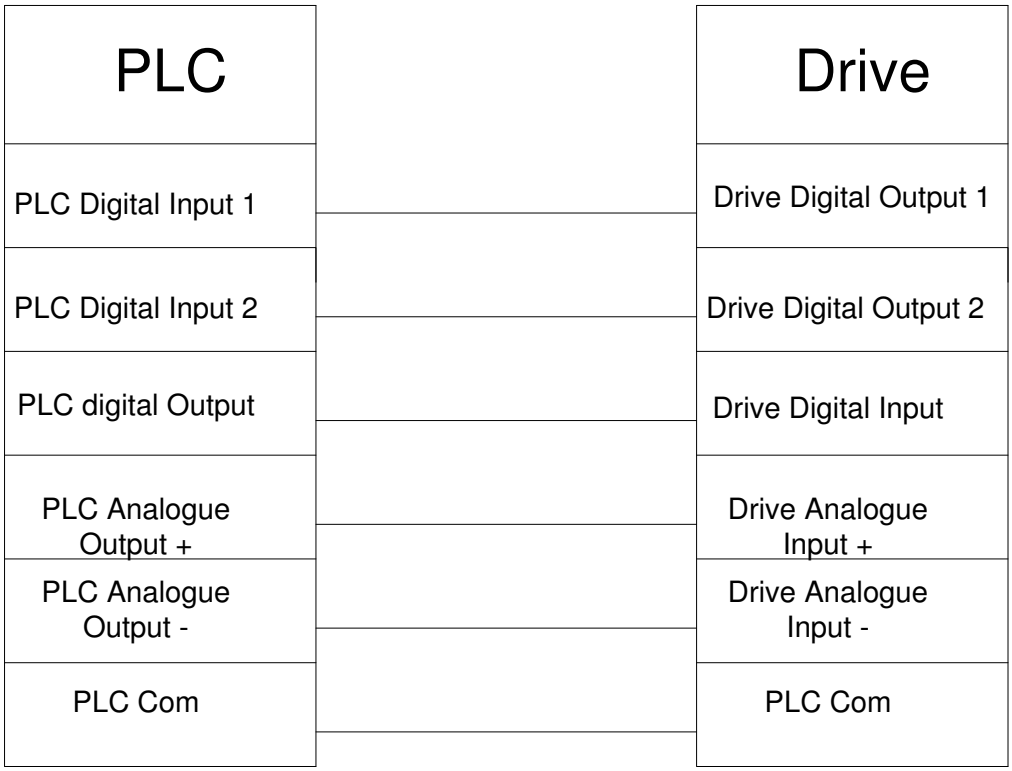

Figure 5-5: Parallel Communications illustration [55]

The advantage of this method is fast data transfer rate between the PLC or any other control device and the drive but the limited number of digital and especially analogue output terminals means than not a lot of parameters can be monitored using this method. On complex systems with multiple drives and control stations with a wider range control and monitoring parameters or a system that require more monitoring capability, the cost of wiring and additional hardware will make this method less cost effective. All data exchange between the drive and the PLC can be done by other means of communication as the drive support serial RS232/485 and profibus communication interface discussed further down.
As mentioned above this drive only has one analogue output therefore only one parameter can be monitored at a time which is really poor from a condition monitoring point of view given that various electrical parameters can be monitored from the following blocks:

5.5.1 Speed Loop block

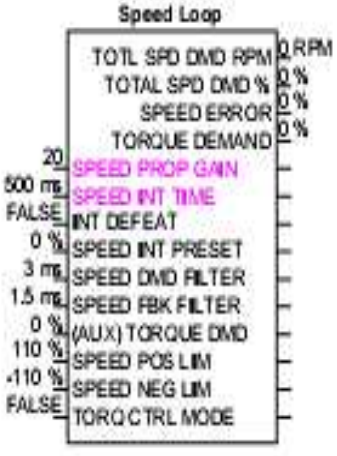

Figure 5-6: Speed loop block

In sensorless vector motor control mode the speed loop block above controls the speed of the motor by comparing the actual speed to the demanded speed, and applying more or less torque in response to the error. The following parameters can be monitored from above block.

5.5.1.1 Total Speed Demand

The total speed demand is the speed set point set by the operator from the HMI. It is called total speed demand because on some applications the can have various speed demand sources summed together and sometimes the speed can also have a trim.

5.5.1.2 Speed Error

The speed error is the difference between the speed demand and speed feedback and is calculated using a PI (proportional and integral) controller.

5.5.1.3 Torque Demand

The torque demand is the output of the PI controller.

5.5.2 Feedbacks block

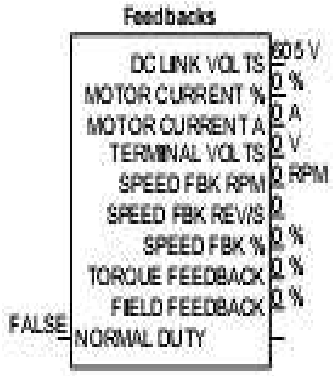

Figure 5-7: Feedbacks block

The above block displays feedback parameters of the drive and the following parameters can be monitored:

5.5.2.1 DC link voltage

The DC link voltage is the voltage at the output of the diode bridge rectifier after the DC Link capacitor; this is the voltage that gets converted into three phase motor supply by the IGBT (Insulated Gate Bipolar Transistor) output stage.

5.5.2.2 Motor current feedback

This is the amount of current being pulled by the motor, it can be expressed in percentage or in Amps.

5.5.2.3 Speed feedback

This is the calculated motor shaft speed feedback value which can be expressed in RPM or in percentage.

5.5.2.4 Torque feedback

This is an estimation of the motor torque as a percentage of the motor rated torque.

5.5.2.5 Field feedback

This is a measure of the motor magnetic field strength. A value of 100% indicates that the motor is fully fluxed and below that the motor will be operating in field weakening mode.

5.5.3 Energy metre block

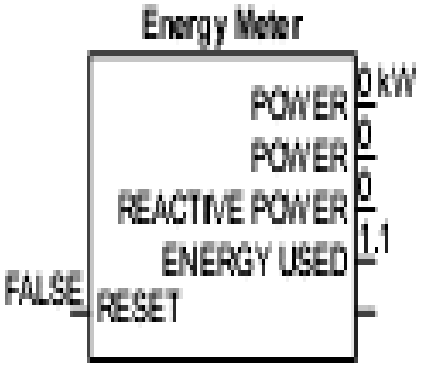

Figure 5-8: Energy Metre block

This block is used to measure the amount of energy being used by the motor. The energy delivered by the motor can be measured in kilowatts or kilowatts per hour.

There are other parameters that could also be monitored from this drive, some of which are normally hidden in the Parker SSD software as 95% of control systems designers don't necessarily need to know what these parameters do and where they are stored in the drive. I have been granted access to these parameters by the manufacturer for the purpose of this research. The two main parameters are the Id and Iq of the sensorless vector loop.

5.6 PLC

This PLC used on this test rig is a Siemens S7-200 PLC; it is a micro PLC used for less complex automation tasks. The extensive basic functionality offered by the five different CPUs can be expanded with a wide range of individual modules (digital inputs/outputs, analogue inputs/outputs and communication). Programming is based on Siemens STEP 7 Micro/WIN Software.

5.7 HMI

The HMI (Human Machine Interface) as its name says is an interface between the controlled machine and the operator, it allows the operator to set the test rig's speed, set the DC load, select control mode, test sequence or steps, starting and stopping of the machine. The HMI used on the gearbox test rig is a Siemens TP177A HMI device; this HMI supports three types of communication (profibus, MPI and PPI). PPI is currently used to communicate with S7-200 PLC, MPI and profibus.

Chapter 6 Proposed remote condition monitoring platform

As mentioned above this test rig only has one analogue output which means only one parameter from the drive control loop can be monitored at a given time. In order to get more parameters out of this drive; a PROFIBUS field bus communication card can be added into the 650V drive. This communication card will enable the drive to communicate with external devices i.e. data logger/data acquisition devices and data could be exchanged between the two devices. The block diagram below illustrates the proposed system.

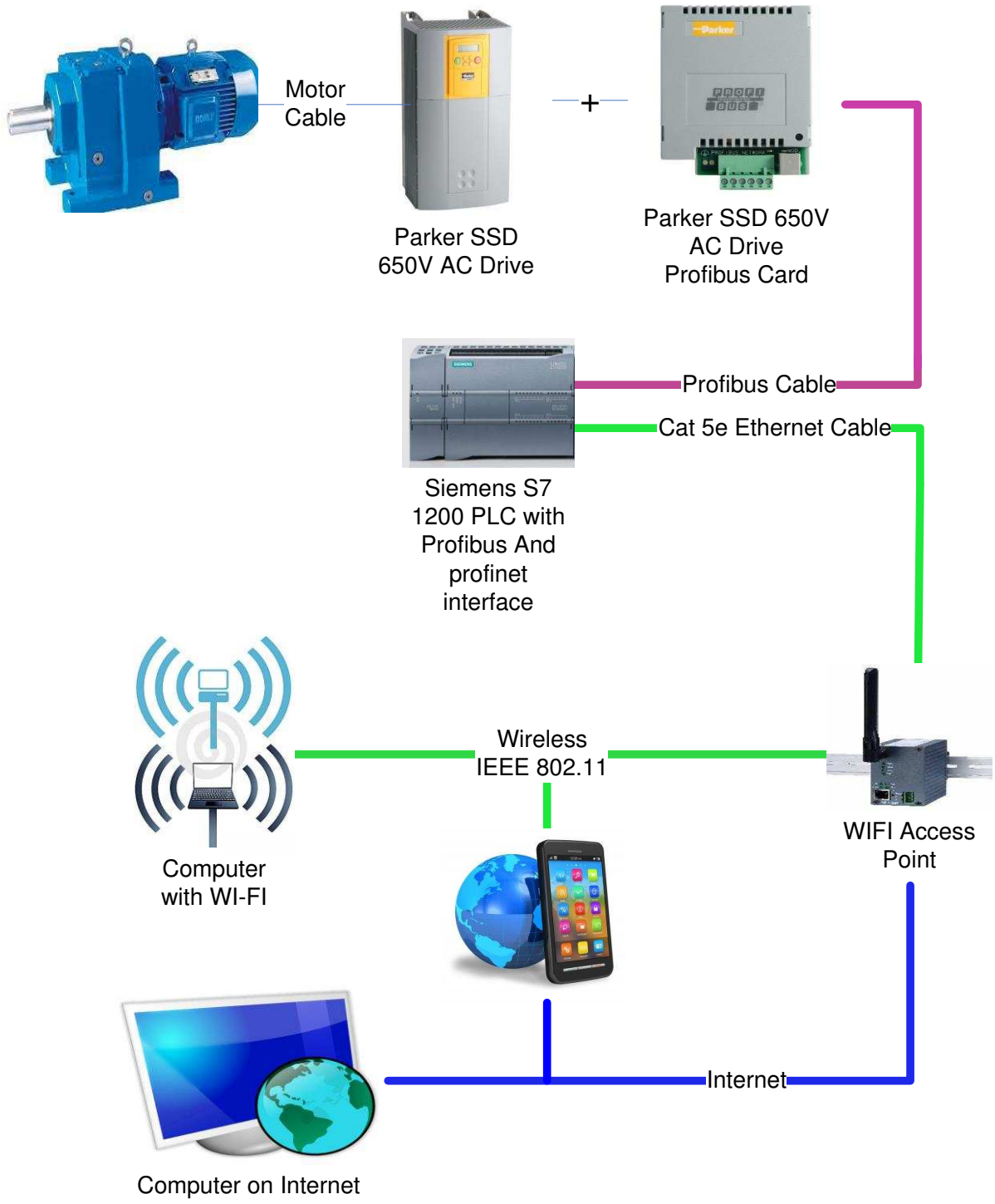

Figure 6-1: Proposed remote machine condition monitoring based on Gearbox Test Rig

Figure 6-1 shows that the proposed system consist of a Parker SSD 650V Drive profibus communication card, a Siemens S7-1200 PLC with profinet and profibus interface, an industrial wireless access point and a wireless enabled computer running a SCADA software. These devices will be added to the existing test rig.

6.1 Test Rig AC drive Profibus Communication

Since the 650V SSD drive does not have any built in fieldbus communication, a Profibus-DP Communications Interface module also has to be added to the drive on one of the serial ports. The parker SSD 650V drive has two serial ports, the first OP port protocol (RS232) is usually used for the drive's keypad but can also be configure to be used as a programming port and the second P3 port protocol (RS485) is used as a programming port by default but can be programmed for external keypad, Modbus commination port and fieldbus. As other students also use this test rig for their research and need to have access the drive programming port the OP port was configured to be both a keypad port and a drive programming port. The P3 port was configured to connect to the profibus communication card allowing the drive to be networked to other devices. Signals from the drive are converted by the drive profibus communication card into RS485, and vice versa, so that information can be shared between the Master (S7-1200 PLC) and 650V drive which is a slave on the profibus network. Figure 6-2 show a 650V Frame C, D, E and F Profibus communication card.

Figure 6-2: 650V Frames C, D E & F Profibus Card [57]

To enable the drive to communicate with the master PLC the drive "Comms Ports" function block has to be configured with the drive communication parameters as illustrated on Figure 6-3.

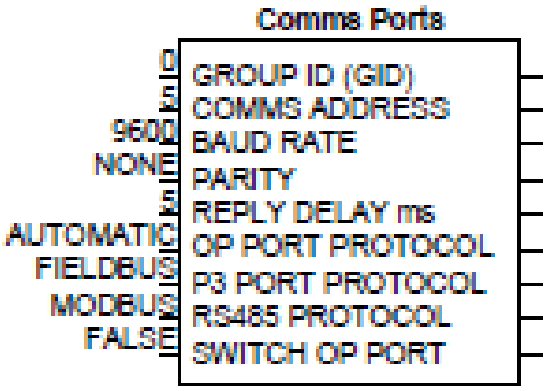

Figure 6-3: 650V Drive Comms Port Configuration

This function block configures the programming ports that allow connection to the keypad, to a personal computer and the master PLC. The parameters modified for the purpose of this research are the following:

- COMMS ADDRESS
  The SSD Drives protocol unit identity profibus node address in this case the node address of the drive is set to 5.
- REPLY DELAY
  The time in milliseconds between the drive receiving the complete request from the communications master and replying to this request.
- OP PORT PROTOCOL
  This is set to automatic and selects the protocol to be used by the keypad port on the front of the drive and also used as programming port.
- P3 PORT PROTOCOL
  This parameter is set to fieldbus allowing the drive to connect to the PROFIBUS communication card
- SWITCH OP PORT
  When TRUE, the keypad port on the front of the drive is disabled when the communications equipment is connected to the RS232 programming port on the drive's control board. This parameter is set to false so that the keypad port remains enabled when there is communication with the RS232 programming port.

With all these parameters set the drive is ready to communicate with the Siemens S7-1200 PLC over PROFIBUS while at the same time allowing communication with a computer via its keypad port

6.2 Siemens S7-1200 PLC

A Siemens S7 1200 PLC is proposed as it can communicate with the drive over PROFIBUS and has a built in data logging facility. As Siemens S7 1200 has an industrial Ethernet capable port for profinet which is the innovative open standard for Industrial Ethernet, developed by Siemens and the PROFIBUS User Organisation (PNO), it can therefore be connected to an industrial wireless network IEEE 802.11 and data can be access by any WI-FI enabled laptop or computer. With these features, and utilising the Ethernet's other services such as a web and ftp server, remote administration and monitoring of the PLC possible. The PLC will be setup to handle communication from both the local network as well as, handling messages from a wider network such as the internet. This is achieved by adding a gateway address to its Ethernet communication settings. Thereby, allowing it to send and receive IP messages that are not established inside the local network. This method is very common these days with automation engineers like myself and most large machines that I have designed and commissioned within the last few years have remote monitoring capability which allows an engineer to monitor and fix problem anywhere around the world from the comfort of their office.

Data logged can be access via its Profinet port in the form of CSV (comer separated values) file; this file format is supported by MATLAB, the signal processing software used at the University of Huddersfield. The S7-1200 PLC is a modular and expandable PLC as illustrated on Figure 6-4.

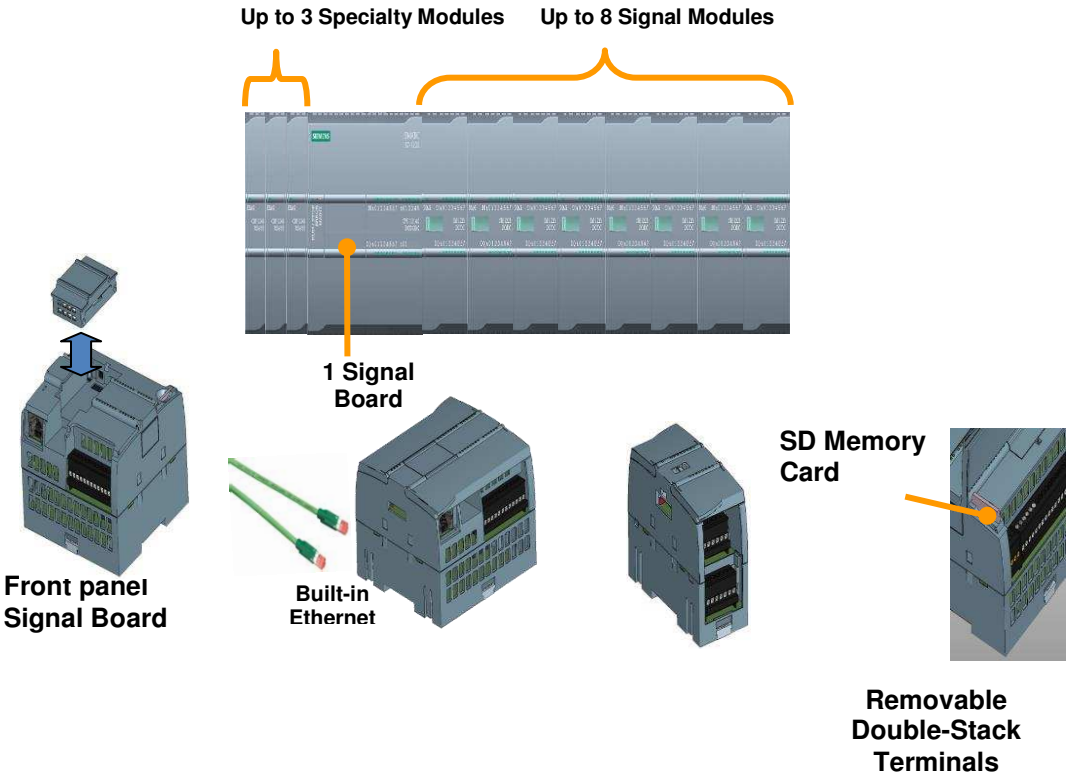

Figure 6-4: S7-1200 PLC Hardware

The S7-1200 PLC used for this project is CPU 1212C DC/DC/Rly; this PLC has the following specifications:

Table 6-1: Siemens S7-1200 CPU 1212c Specifications

Feature		**CPU 1212C**
Physical size (mm)		90 x 100 x 75
User memory	Work	50 Kbytes
	Load	1 Mbyte
	Retentive	10 Kbytes
Local on-board I/O	Digital	8 inputs/6 outputs
	Analogue	2 inputs
Process image Size	Inputs (I)	1024 bytes
	Outputs (Q)	1024 bytes
Bit memory (M)		4096 bytes
Signal module (SM) expansion		2
Signal board (SB), Battery board (BB), or communication board (CB)		1
Communication module (CM)(left-side expansion)		3
High-speed counters	Total	4 built-in I/O, 6 with SB
	Single phase	3 at 100 kHz 1 at 30 kHz SB: 2 at 30 kHz
	Quadrature phase	3 at 80 kHz 1 at 20 kHz SB: 2 at 20 kHz
Memory card		2MB
Real time clock retention time		20 days, typ. / 12 day min. at 40 degrees C (maintenance-free Super Capicator)
PROFINET		1 Ethernet communication port
Real math execution speed		2.3 µs/instruction
Boolean execution speed		0.08 µs/instruction

The S7-1200 PLC has a specialty master PROFIBUS communication module CM 1243-5 added which will allow it to communicate with other as master on a PROFIBUS network. The CM 1243-5 master determines the data communication on the bus and can send messages without an external request when it holds the bus access rights (the token). Masters are also called active stations in the PROFIBUS protocol. While the 650V PROFIBUS -DP Communications Interface module slave is a peripheral device capable of handling inputs and outputs data. PROFIBUS Input Data are values sent from the drive to the PLC whereas PROFIBUS Output Data are values sent from the master PLC to the drive.
With this card the drive becomes an intelligent slave. This means it will only respond to a master when requested to do so.
PROFIBUS is one of the largest open industrial fieldbuses in the world. As with most fieldbus systems, PROFIBUS can reduce operating costs, increase productivity, decrease time to market for new products, improve product quality, and for condition monitoring fast data transfer. And unlike standard 4-20mA controls, PROFIBUS can support up to 32 devices per segment and up to a total of 126 devices, depending on total system current.

6.2.1 S7-1200 Programming Basics

Siemens S7-1200 PLC range is programmed using STEP 7 Totally Integrated Automation Portal Software. STEP 7 provides the following standard programming languages for S7-1200 [58]:

- LAD (ladder logic) is a graphical programming language. The representation is based on circuit diagrams.
- FBD (Function Block Diagram) is a programming language that is based on the graphical logic symbols used in Boolean algebra.
- SCL (structured control language) is a text-based, high-level programming language.

When code block is created the programmer is prompted to select the programming language to be used by that block.

6.2.1.1 Ladder Logic

Ladder logic is a graphical programming language that represents a program by a graphical diagram based on the circuit diagrams of relay logic hardware. This standard programming language for most PLC used in industrial automation. The elements of a circuit diagram, such as normally closed and normally open contacts, and coils are linked to form networks. The drawing below represents a ladder logic electrical circuit for stop and start control using a normally open push button for start, a normally closed push button for stop, a relay for the output and a contact from the relay for latching.

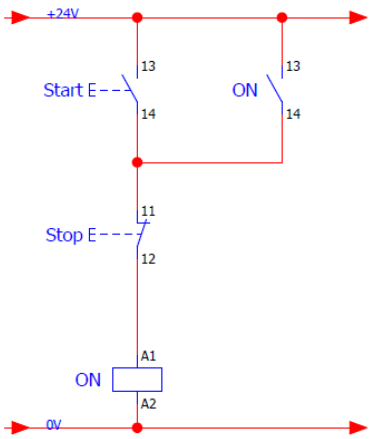

Figure 6-5: Hardwire Electrical Start/Stop Circuit

Figure 6-6 represents the equivalent of the electrical circuit in ladder logic. This shows how ladder logic resembles electrical circuit diagram, here the stop and start are also done by means of push buttons wired into the PLC and the output can be an internal coil wire to a physical output.

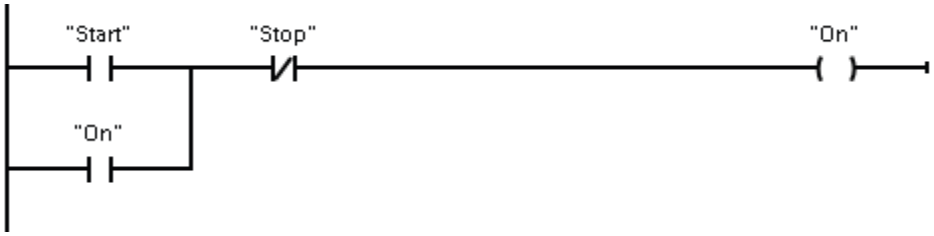

Figure 6-6: Ladder Start/Stop logic

For complex operations branches can be inserted to create the logic for parallel circuits. Parallel branches are opened downwards or are connected directly to the power rail and can be terminated upwards.

6.2.1.2 Function Block Diagram (FBD)

Like LAD, FBD is also a graphical programming language. The representation of the logic is based on the graphical logic symbols used in Boolean algebra. Function Block Diagrams (FBDs) are another part of the IEC 61131-3 standard. The primary concept behind a FBD is data flow. The figure below shows the FBD representation of hardwire electrical circuit above.

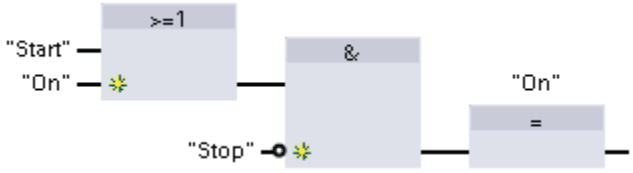

Figure 6-7: FBD Start/Stop Diagram

Mathematical functions and other complex functions can be represented directly in conjunction with the logic boxes.

6.2.1.3 Structured Control Language (SCL)

SCL is a high-level, PASCAL-based programming language for Siemens SIMATIC S7 CPUs. SCL supports the block structure of STEP 7. Program blocks written in SCL can be included with program blocks written in LAD and FBD. SCL instructions use standard programming operators, such as for assignment (:=), mathematical functions (+ for addition, - for subtraction, * for multiplication, and / for division). SCL uses standard PASCAL program control operations, such as IF-THEN-ELSE, CASE, REPEAT-UNTIL, GOTO and RETURN. Any PASCAL reference can be used for syntactical elements of the SCL programming language. Many of the other instructions for SCL, such as timers and counters, match the LAD and FBD instructions.
Since SCL like PASCAL offers conditional processing, looping, and nesting control structures, you can implement complex algorithms in SCL more easily than in LAD or FBD.
Arithmetic operators can process various numeric data types. The data type of the result is determined by the data type of the most-significant operands. For example, a multiplication operation that uses an INT operand and a REAL operand yields a REAL value for the result.

6.2.2 S7-1200 PLC Hardware Configuration

The test rig drive has to be configured in the S7-1200 PLC hardware configuration in order for the PLC to request communication with the drive. In the hardware configuration the drive GSD (General Station Description) file will be inserted and configured with it node address as show on Figure 6-8 below.

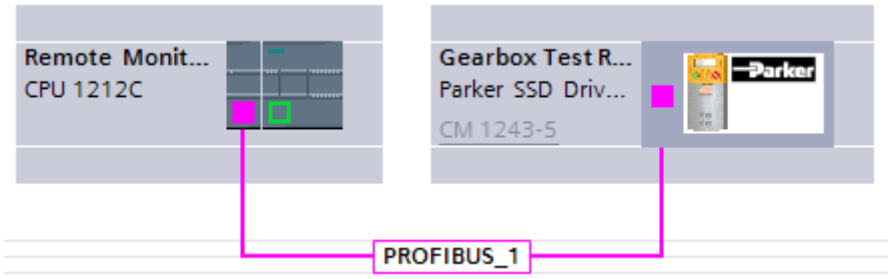

Figure 6-8: S7-1200 PLC and 650V Parker SSD Drive PROFIBUS Communication

On the above figure the purple line represents PROFIBUS communication cable which is a specifically designed shielded twisted pair cable for the cabling of industrial field bus systems, particularly developed for factory automation applications. The PROFIBUS topologies utilised in the industrial environment include the following configurations: line, tree and star (and combinations of these topologies). Standard connections are made through use of a 9-pin D-Sub miniature connector. Transmission speeds are selectable starting at 9.6kbs.
The input and output data mixture used by a given slave device is defined by the GSD file. GSD files contain information about the basic capabilities of a device. All devices are shipped with a GSD file, or a file can be downloaded from PROFIBUS & PROFINET International (PI) web site or the vendor's own web site. With a GSD file, system designers can determine basic data such as the communications options and the available diagnostics. For simple devices such as digital or analogue I/O blocks, this is fixed. However, since more complex devices like the test rig drive often have a much wider choice of possible values to send, it is usually possible to edit the GSD file to change the mapping of device parameters onto PROFIBUS inputs or outputs. This is the case with the gear box test rig drive, which also allows access to parameter data not in the GSD Input/output data file. Figure 6-9 bellow illustrates the GSD configuration for the test rig drive.

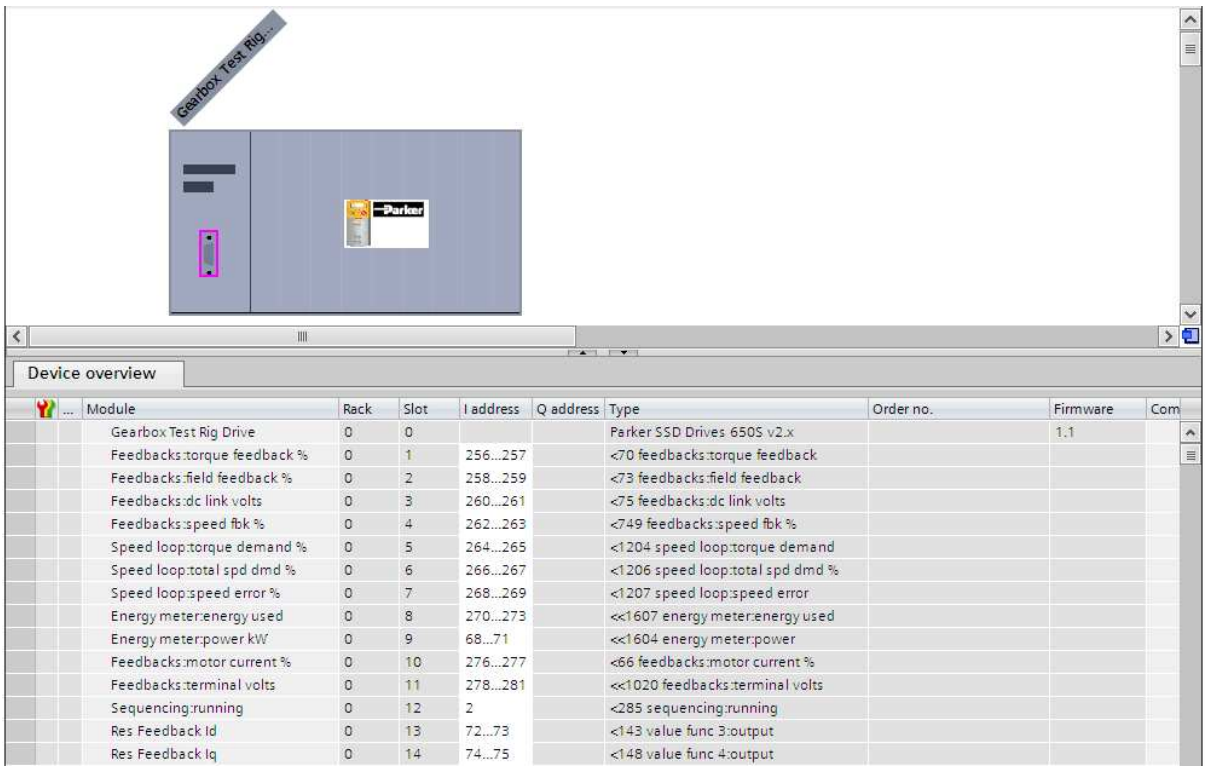

Module	Rack	Slot	I address	Q address	Type	Order no.	Firmware	Com
Gearbox Test Rig Drive	0	0			Parker SSD Drives 650S v2.x		1.1	
Feedbacks:torque feedback %	0	1	256...257		<70 feedbacks:torque feedback			
Feedbacks:field feedback %	0	2	258...259		<73 feedbacks:field feedback			
Feedbacks:dc link volts	0	3	260...261		<75 feedbacks:dc link volts			
Feedbacks:speed fbk %	0	4	262...263		<749 feedbacks:speed fbk %			
Speed loop:torque demand %	0	5	264...265		<1204 speed loop:torque demand			
Speed loop:total spd dmd %	0	6	266...267		<1206 speed loop:total spd dmd %			
Speed loop:speed error %	0	7	268...269		<1207 speed loop:speed error			
Energy meter:energy used	0	8	270...273		<<1607 energy meter:energy used			
Energy meter:power kW	0	9	68...71		<<1604 energy meter:power			
Feedbacks:motor current %	0	10	276...277		<66 feedbacks:motor current %			
Feedbacks:terminal volts	0	11	278...281		<<1020 feedbacks:terminal volts			
Sequencing:running	0	12	2		<285 sequencing:running			
Res Feedback Id	0	13	72...73		<143 value func 3:output			
Res Feedback Iq	0	14	74...75		<148 value func 4:output			

Figure 6-9: Parker SSD 650V GSD Configuration

For the purpose of this research only 14 parameters are extracted from the test rig's drive but there is scope to get more data if required. The GSD file contains the addresses of all Input/output on the data file. For example the address of torque feedback is IW 256, where IW is input word because this is an integer.

This PLC could also be used to control the drive but we are only interested in using it for condition monitoring which is the reason why only input data appears on the above GSD configuration. The parameters being monitored by the proposed system are the following:

- Torque feedback
- Field feedback
- DC link volts
- Speed feedback
- Torque demand
- Total speed demand
- Speed error
- Energy used
- Power kW
- Motor current
- Terminal volts
- Drive running
- Iq current
- Id current

This communication will allow us to extract more parameters from the test rig drive and sent to the PLC for condition monitoring. This data can be accessed directly from the PLC and a SCADA (supervisory control and data acquisition) system can also access and log the data as the PLC has limited memory for data logging.

6.2.3 Process Data Acquisition and monitoring with S7-1200 PLC

The SIMATIC S7-1200 used for condition monitoring on the test rig includes the data logging function with “Data log” instructions. With these instructions, the process data can be stored in the flash memory (CPU or memory card) in CSV format. The files are then accessible via the integrated PLC web server and available for analysis, e.g. using Microsoft Excel as illustrated on Figure 6-11. This PLC is suitable for routing operations and enables remote access via the Internet. To ensure secure communication a suitable hardware components and connection over a VPN tunnel can be used. Figure 6-10 illustrates an overview of the automated task of remote condition monitoring.

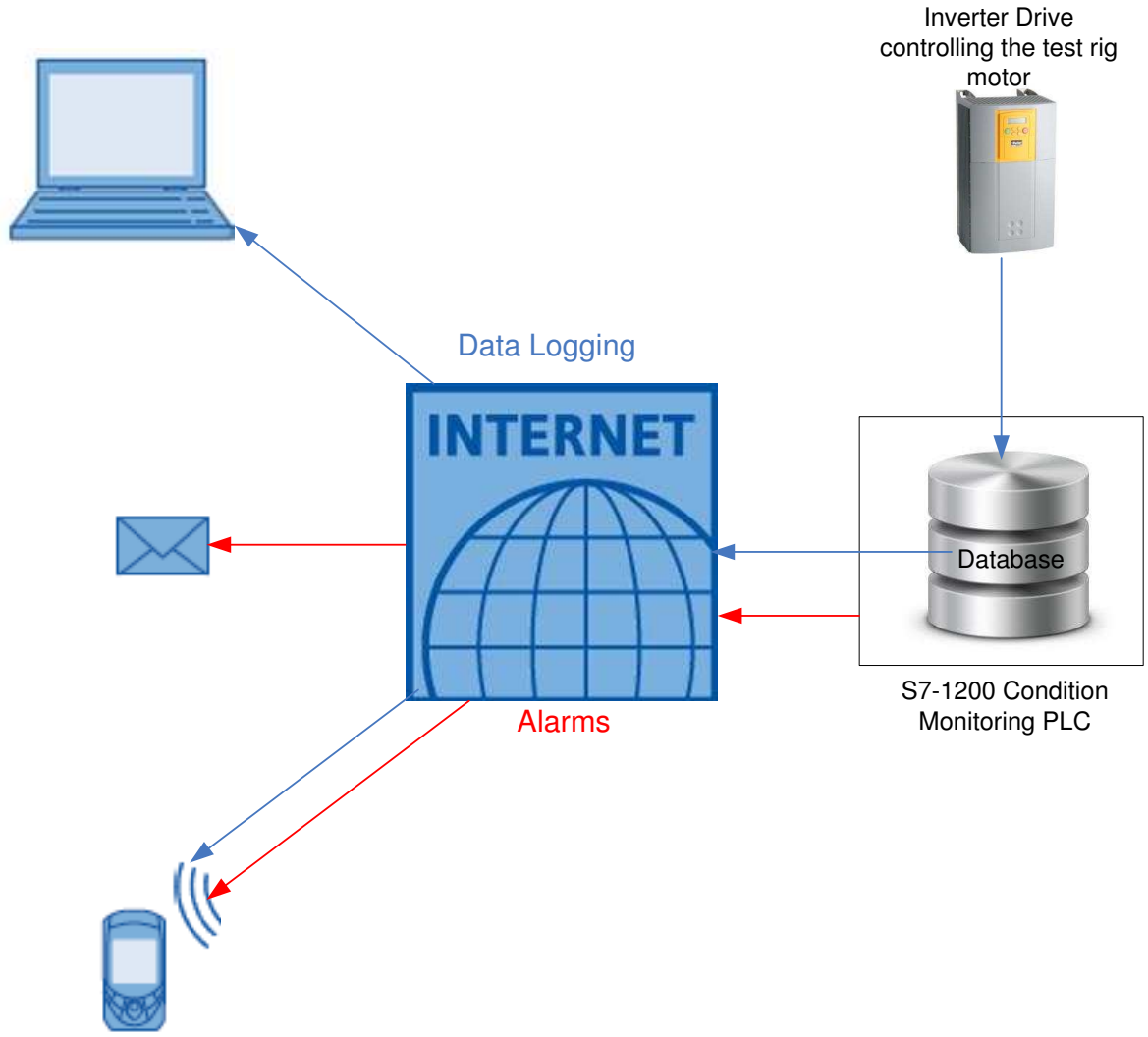

Figure 6-10: Overview of remote condition monitoring with S7-1200 PLC

As shown on the above figure, process data from the drive are acquired using special data logging instructions and stored on the PLC database. The PLC analyses the process values using Equation 7-3 generated from the motor model (refer to 0) and generates an alarm which triggers massage to be automatically send to the configured addresses on the PLC. When this message is received the data logs can be access via the internet for further analysis.
Figure 6-11 illustrates the data logging process with the condition monitoring PLC.

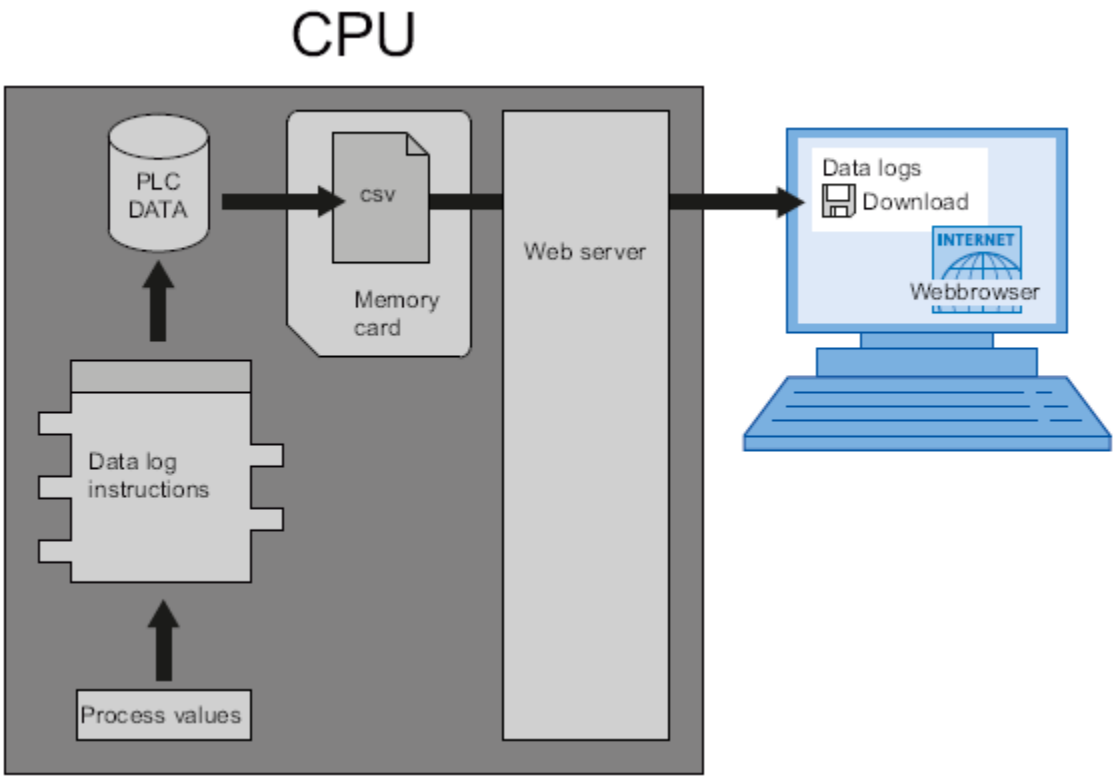

Figure 6-11: Data Logging with S7-1200 PLC [59]

In the condition monitoring PLC program, the data log instructions are used to store process values collected from the drive in log files. These data log files can be stored on the memory card (MC) or in the internal load memory of the CPU but for this research a 2 MB memory card is used for this purpose. The data log files are stored in CSV format. The CSV files can be accessed with the help of a card reader, or if accessed via web server, they can be downloaded via a web browser using any WI-FI enable device (smartphone, PDA, laptop etc.).
When connected to the secured WI-FI network or VPN setup on the test rig; access to the web server is achieved typing the address of the remote condition monitoring PLC which 192.168.0.10, this will take the user to the web server but will not allow them to get any information unless they have logged on to the web server. This double security (secured network and secured web server) ensures no unauthorised access to the PLC. The type of protection used on this CPU is write/read protection No write or read access is possible when the device switched online. Only the CPU type and the identification data can be displayed in the on the web server. Display of the log files or any control on the PLC will be disabled.

The instruction "DataLogCreate" illustrated in Figure 6-12 is used to create a data log file under the directory “\DataLogs” in the load memory of the PLC, whereby the “NAME” and the maximum number of data records (Parameter “RECORDS”) is predefined. With the “TIMESTAMP” parameter set to 1 a date and time stamp is registered for each data record. The data to be recorded is specified by the parameter “DATA”. The parameter “HEADER” is used to define the headers (column headings) in the data log for the data to be recorded. When creating the data log file with name allotment, a number (parameter “ID”) for file identification will be created.
Figure 6-13 illustrates the diagnostics block used to monitor any errors that occurs during the execution of the instruction "DataLogCreate"

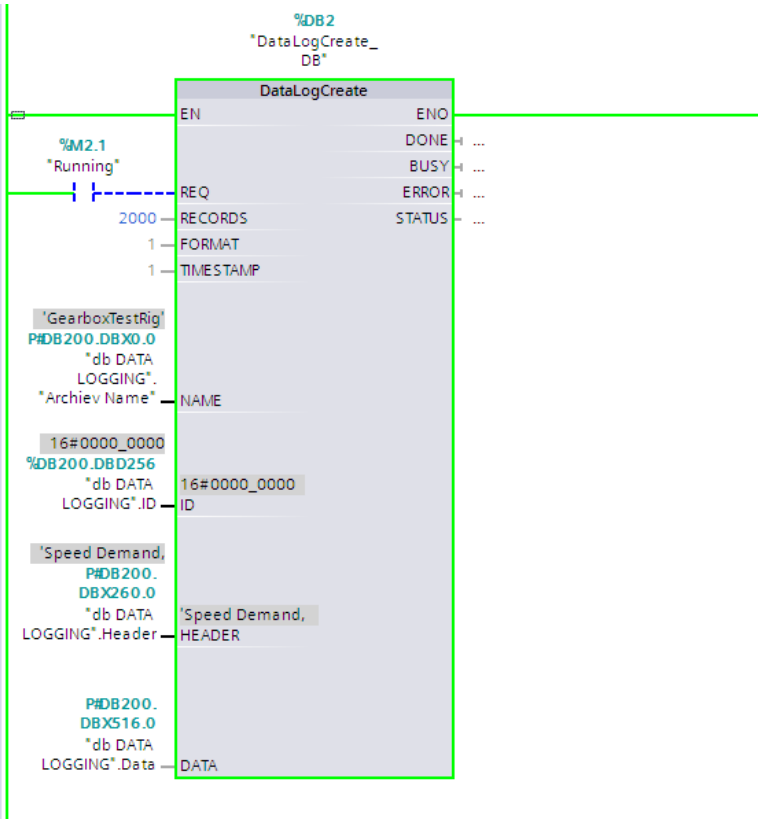

Figure 6-12: Create Data Log Function Block

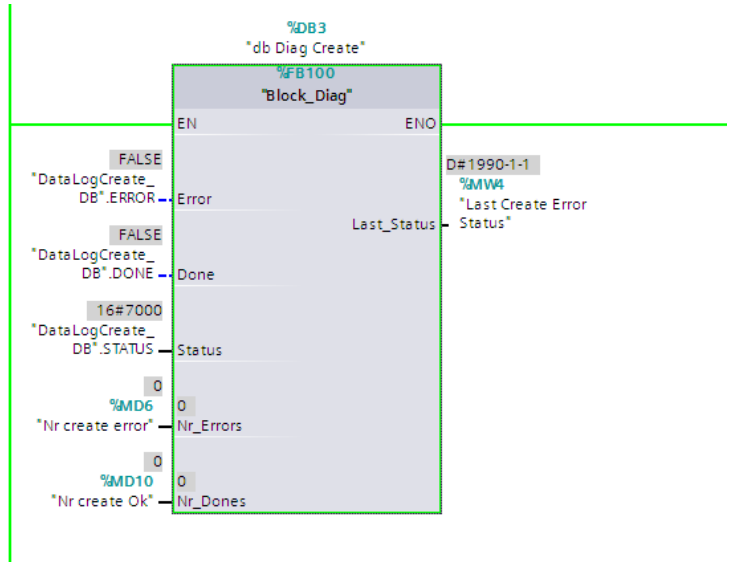

Figure 6-13: Data Log Diagnosis Function Block

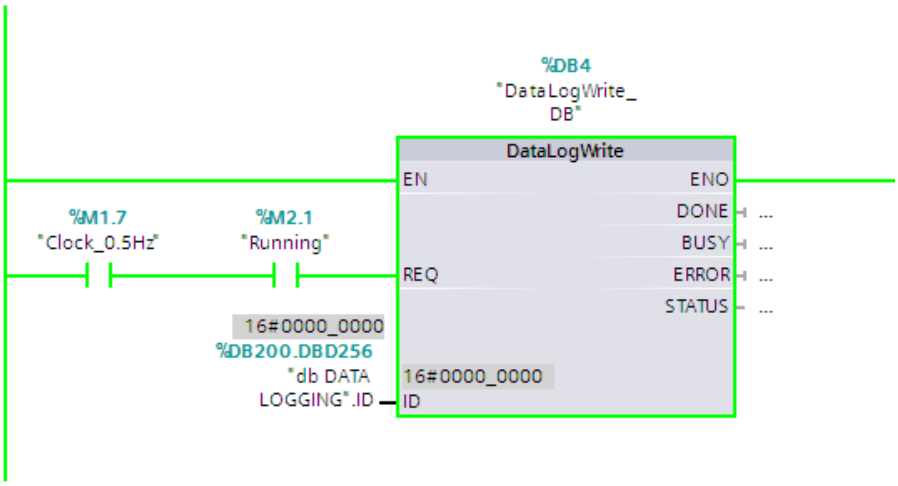

Figure 6-14: Write Data Logs Function Block

The instruction “DataLogWrite” is used to write a data record into the specified data log. The DataLogWrite” instruction can be executed only, if the previously created target data log has been opened. Use the parameter “ID” to select the data log.
Figure 6-15 illustrates a flowchart for data logging with the condition monitoring PLC.

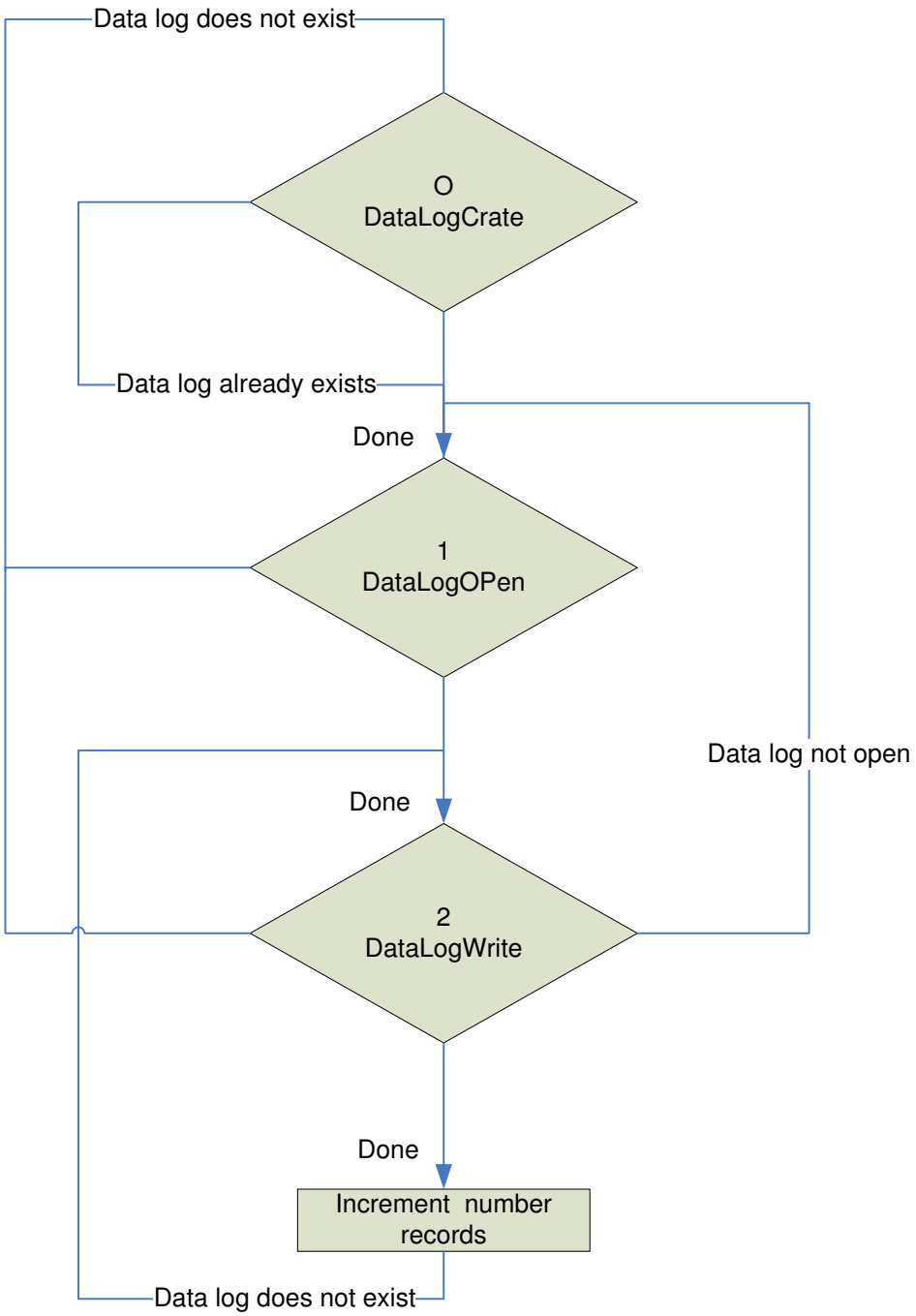

Figure 6-15: S7-1200 PLC Data Logging flowchart

The S7-1200 PLC is an intelligent device that can communicate with the test rig drive monitor, acquire and log real time data. However this device has some limitation. Firstly the memory card installed in the PLC is 2 MB; this means that the maximum data size will not exceed 2 MB. When dealing with condition monitoring system where data is logged on value change or every second, the size of this memory could be exceeded in a couple of hours. Secondly the only way to view this data in real time on this PLC time is by using the Siemens programming software which means the user will have to know how to go online with the device to interrogate it. To get around this a web page was designed and hosted on the PLC that could display trends and values from the test rig but the refresh rate was very slow.

To ensure that the maximum amount of data could be logged and viewed, while at the same time having access to real time data from the PLC, I opted for the use of a site computer running SCADA software and communicating with the S7-1200 PLC wirelessly over profinet. All the data is accessed in real time and also stored on the site computer with tens of gigabytes of hard drive capacity which means a lot more data can be logged.

6.3 Site Computer with SCADA system

6.3.1 Introduction to SCADA

SCADA is an acronym for supervisory control and data acquisition; a computer based industrial control system for gathering and analysing real time data. SCADA systems are used to monitor and control plant or equipment in many industries including telecommunications, water and waste control, energy, oil and gas refining and transportation. InduSoft SCADA software technology uses the Internet to access data that is stored on industrial devices and test and measurement equipment. In addition, InduSoft tools and technologies can convert personal computers, web browsers, and such remote productivity devices such as cell phones, pagers, and personal digital assistants (PDAs) into industrial automation, diagnostic, test and measurement systems.
In order for InduSoft Web Studio to communicate with S7-1200 a communication driver has to be configured to enable this process

6.3.2 InduSoft Web Studio Industrial Ethernet Driver Configuration for Siemens PLC

When process and machines need to interact with Human Beings, they need to speak a common language. The part of the SCADA systems that will be responsible to access the process data from the PLC is OPC client/server.
OPC is a software interface standard that allows Windows programs to communicate with industrial hardware devices. The acronym "OPC" comes from "OLE (Object Linking and Embedding) for Process Control". Since OLE is based on the Windows COM (Component Object Model) standard, under the hood OPC is essentially COM. Over a network, OPC relies on DCOM (Distributed COM), which was not designed for real-time industrial applications and is often set aside in favour of OPC tunnelling.

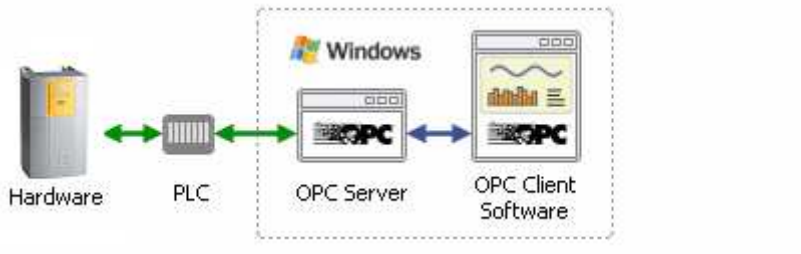

Figure 6-16: Typical OPC Server

OPC is implemented in server/client pairs. The OPC server is a software program that converts the hardware communication protocol used by a PLC into the OPC protocol. The OPC client software is any program that needs to connect to the hardware, such as an HMI or SCADA. The OPC client uses the OPC server to get data from (or send commands to) the hardware. The OPC is an open standard, which means lower costs for manufacturers and more options for users. Hardware manufacturers need only to provide a single OPC server for their devices to communicate with any OPC client. Software vendors simply include OPC client capabilities in their products and they become instantly compatible with thousands of hardware devices. Users can choose any OPC client software they need, resting assured that it will communicate seamlessly with their OPC-enabled hardware, and vice-versa.
Error! Reference source not found. illustrates a typical system where a PLC read data from ardware and the data is access by the OPC client software via the OPC server. However there are more possibilities. For example, one might need to:

- Connect an OPC client to several OPC servers. This is called OPC aggregation.
- Connect an OPC client to an OPC server over a network. This can be done with OPC tunnelling.

- Connect an OPC server to another OPC server to share data. This is known as OPC bridging.

Some SCADA manufacturers have an OPC server and client built into one package design to communicate with a specific PLC Hardware range; this is called a communication driver.
The InduSoft communication driver used for communication with Siemens PLCs over industrial Ethernet is the SIETH Communication Driver.
In InduSoft Web Studio (IWS) each communication driver has its own syntax for station and register addressing. Some communication drivers may have protocol-specific parameters like the SIETH driver. However, all communication drivers supported by IWS share the same configuration interfaces.

Figure 6-17 below shows communications parameters for Siemens PLC which contains network information.

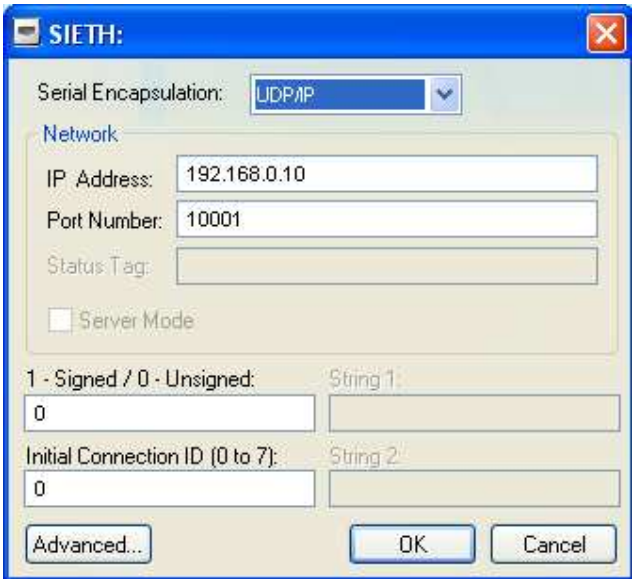

Figure 6-17: PLC Driver communication parameters settings

When the driver is inserted into the application, the MAIN DRIVER SHEET is automatically added to the driver folder. The MAIN DRIVER SHEET provides a simple way to associate IWS tags to addresses in the PLC.
After communication parameters have been set, The MAIN DRIVER SHEET can be configure as shown on Figure 6-18. The worksheet contains the name of each tag (variable from the PLC), the station address (address of the S7-1200 PLC) and the I/O address of the variable. In the worksheet the scan rate for all variables can also be set and the variable can also be scaled.

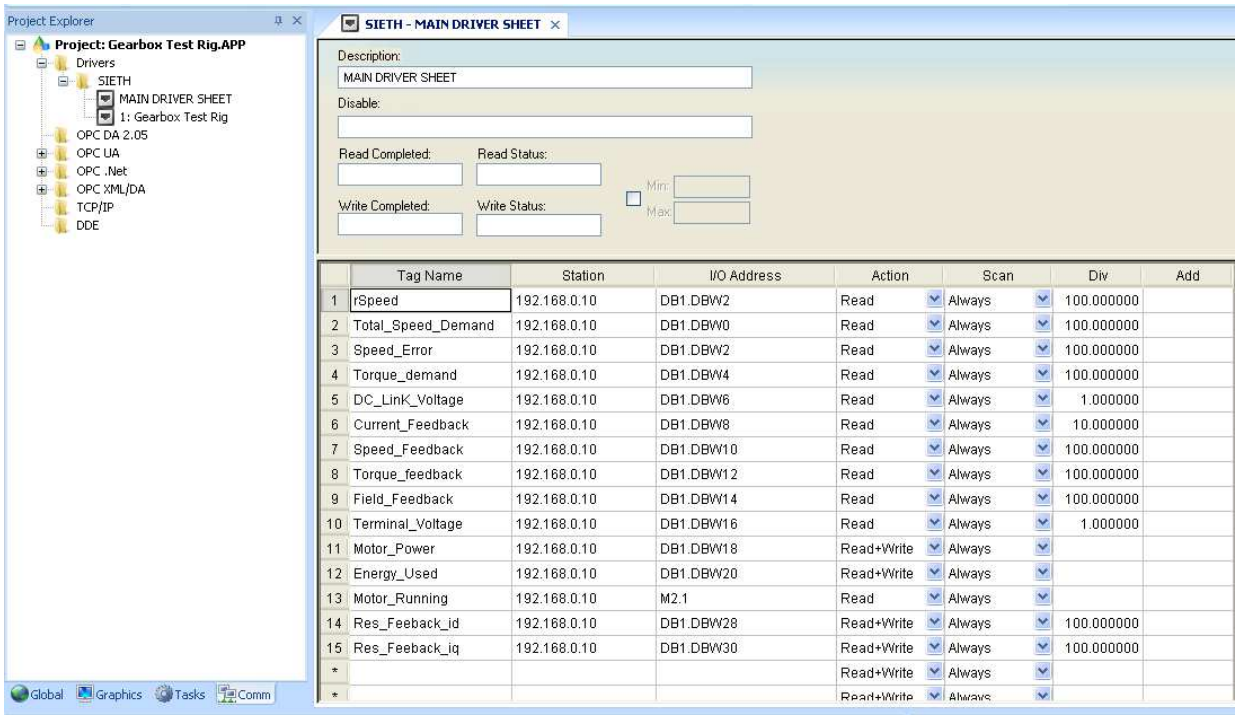

	Tag Name	Station	I/O Address	Action	Scan	Div	Add
1	rSpeed	192.168.0.10	DB1.DBW2	Read	Always	100.000000	
2	Total_Speed_Demand	192.168.0.10	DB1.DBW0	Read	Always	100.000000	
3	Speed_Error	192.168.0.10	DB1.DBW2	Read	Always	100.000000	
4	Torque_demand	192.168.0.10	DB1.DBW4	Read	Always	100.000000	
5	DC_LinK_Voltage	192.168.0.10	DB1.DBW6	Read	Always	1.000000	
6	Current_Feedback	192.168.0.10	DB1.DBW8	Read	Always	10.000000	
7	Speed_Feedback	192.168.0.10	DB1.DBW10	Read	Always	100.000000	
8	Torque_feedback	192.168.0.10	DB1.DBW12	Read	Always	100.000000	
9	Field_Feedback	192.168.0.10	DB1.DBW14	Read	Always	100.000000	
10	Terminal_Voltage	192.168.0.10	DB1.DBW16	Read	Always	1.000000	
11	Motor_Power	192.168.0.10	DB1.DBW18	Read+Write	Always		
12	Energy_Used	192.168.0.10	DB1.DBW20	Read+Write	Always		
13	Motor_Running	192.168.0.10	M2.1	Read	Always		
14	Res_Feeback_id	192.168.0.10	DB1.DBW28	Read+Write	Always	100.000000	
15	Res_Feeback_iq	192.168.0.10	DB1.DBW30	Read+Write	Always	100.000000	
*				Read+Write	Always		
*				Read+Write	Always		

Figure 6-18: SIETH Driver Worksheet

6.3.3 InduSoft Web Studio data logging and trending

The Trend folder enables you to configure history groups that store trend curves. The Trend worksheet is used to declare which tags must have their values stored on disk, and to create history files for trend graphs as shown on Figure 6-19. Since all the data are stored on the computer running IWS, there is no disk space restriction as on a PLC, however the project stores the samples in a binary history file (*.hst), and shows both history and on-line samples in a screen trend graph. The Trend worksheet is executed by the Background Task module and it handles the saving of trend data to the history. By default, IWS saves trend history files in a binary format (.hst). As you may want to have these files in .txt format, IWS provides the HST2TXT.EXE program to convert trend history files from binary into text format.

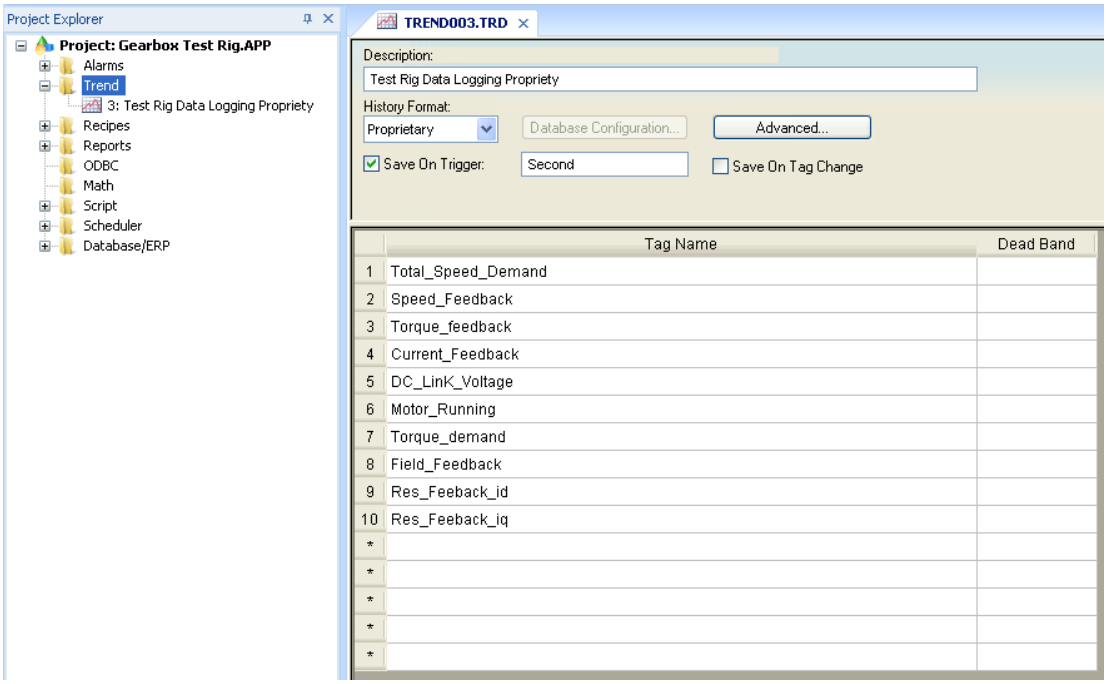

Figure 6-19: Trend worksheet

Chapter 7 Experimental shaft misalignment diagnostic on test rig

7.1 Shaft misalignment theory

Misalignment is one of the predominant failures of rotating machines driven by induction motors [60]. Optimised shaft alignment increases the operating life span of rotating machinery. To achieve this, components that are the most likely to fail must be made to operate within their acceptable design limits.
While misalignment has no measurable effect on motor efficiency, correct shaft alignment ensures the smooth, efficient transmission of power from the motor to the driven equipment. Incorrect alignment occurs when the centrelines of the motor and the driven equipment shafts are not in line with each other. Misalignment produces excessive vibration, noise, coupling, and bearing temperature increases, and premature bearing, coupling, or shaft failure.
There are two types of misalignment [60] parallel and angular misalignment as shown on the figure below. With parallel misalignment, the centre lines of both shafts are parallel but they are offset. With angular misalignment, the shafts are at an angle to each other. The parallel misalignment can be further divided up in horizontal and vertical misalignment. Horizontal misalignment is misalignment of the shafts in the horizontal plane and vertical misalignment is misalignment of the shafts in the vertical plane. Parallel horizontal misalignment is where the motor shaft is moved horizontally away from the pump shaft for example, but both shafts are still in the same horizontal plane and parallel. Parallel vertical misalignment is where the motor shaft is moved vertically away from the pump shaft, but both shafts are still in the same vertical plane and parallel. Similarly, angular misalignment can be divided up in horizontal and vertical misalignment. Angular horizontal misalignment is where the motor shaft is under an angle with the pump shaft but both shafts are still in the same horizontal plane. Angular vertical misalignment is where the motor shaft is under an angle with the pump shaft but both shafts are still in the same vertical plane.

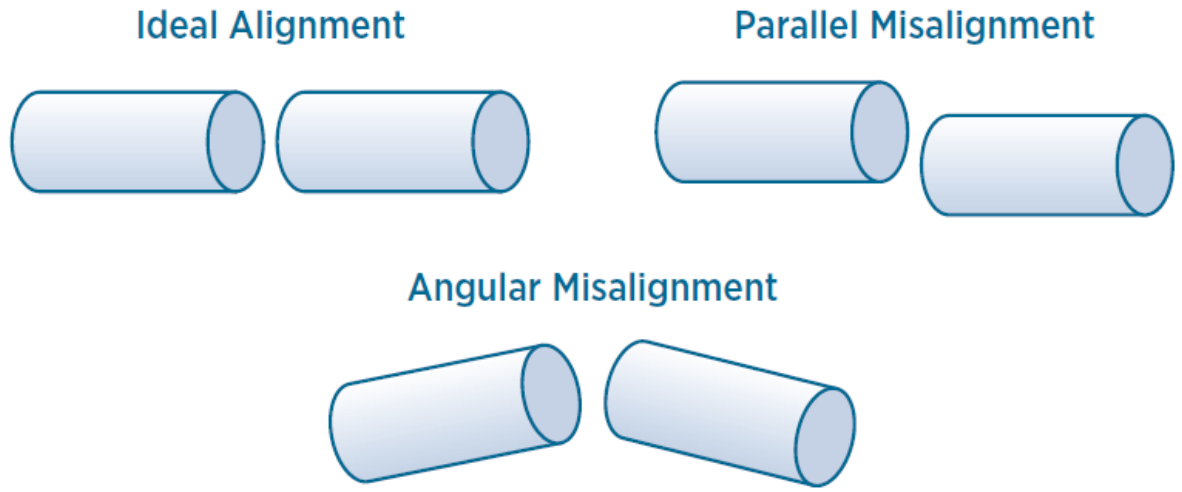

Figure 7-1: Types of Alignment

In practice, ideal alignment is difficult or almost impossible to achieve without using alignment specialised equipment such as dial indicators or laser alignment tools. The proper shaft alignment procedure is to secure the driven equipment first and use it as reference because moving a pump, for example, would stress the connecting piping. Next, install the coupling to the driven equipment. The motor should then be moved into proper alignment and joined to the coupling.
Machine conditions change from the time the machine is off line to when it is running under normal operating conditions. Some of these changes are due to process forces (e.g., fluid pressures, airflow, etc.). The most notable of these changes is the change in the temperature of the machine bearings and supports. This is called the machines thermal growth**.** Thermal growth is the change in the length of a particular metal as a result of the change in temperature of that metal. Typically, when a metal bar is heated, it will get longer. These changes can be very small or they can be very large,

depending on the length of the piece of metal and its coefficient of linear expansion. The formula used to calculate thermal growth is often referred to as the T x L x C formula. T represents the change in the materials temperature in degrees Fahrenheit, L represents the length in inches of the material, and C represents the materials coefficient of linear expansion. Different materials have different C values. Using the formula, we can anticipate the change in a machines shaft alignment based on the expected changes in machine temperature.

There are several methods for detecting misalignment including vibration monitoring, acoustic noise measurements, temperature monitoring, Motor Current Signal Analysis etc.

7.2 Measurement of experimental data for shaft misalignment

For repeatability and reliability of the measurement procedures multiple sets of test will be conducted; a set for a healthy machine (baseline) with no misalignment and another set for a 2 mm misalignment. The results will be compared and the most repeatable and reliable will be selected for further analysis.

Table 7-1: Simulation data set for 2mm shaft misalignment

Step	Speed Set (%)	Load Set (%)	Time (s)
1	25	0	60
2	50	30	60
3	75	50	60
4	100	70	60
5	100	80	60

The parameters been monitored from the drive for the purpose of this test are the following: Speed Demand (%)', 'Speed Feedback (%)', 'Torque Feedback (%)', 'Motor Current (%)','DC Link Volts, 'Torque Demand (%)','Field Feedback (%)','Id Current(%)', 'Iq Current(%)', 'Speed Setpoint (%)' and 'Load Setpoint (%)'.

Table 7-2 below gives more information on each of these signals collected:

Table 7-2: Data plot signals and scaling factors

Value	Description	Scaling
Speed demand	In this application the speed demand will be the speed setpoint.	0 – 100% = 0 to 1460 RPM
Speed Feedback	AC motor speed feedback from test rig inverter	0 – 100% = 0 to 1460 RPM
Torque feedback	AC motor torque feedback from test rig inverter	0 – 100% =0 to 98.1 Nm
Motor current	AC motor torque feedback from test rig inverter	0 – 100% = 0 to 27.13 A
DC Link Volts	Test rig inverter DC Link voltage	Volts
Torque Demand	AC motor torque demand from test rig inverter	0 – 100% = 0 to 98.1 Nm
Field Feedback	AC motor field feedback from test rig inverter	0 – 100% =0 to 100% of motor field
Id Current	Magnetising current from test rig inverter	0 – 100% = 0 to 11.9A Magnetising current
Iq Current	Quadrature current from test rig inverter	0 – 100% of motor torque producing current
Speed Setpoint	Speed set by the test rig PLC and output to the DC motor field controller	0 – 100% = 0 to 1460 RPM
Load Setpoint	Load set by the test rig PLC and output to the DC motor field controller	0 – 100% = 0 to 2.37A Field current

7.2.1 Baseline tests

As mentioned above multiple test are carried out under the same condition and machine settings and the results of the two most repeatable tests are displayed below in figures Figure 7-2 to Figure 7-9. The results from the two tests will not be 100 % identical in the real world because it is almost impossible to create identical environmental conditions for both tests. The aim is to get results that are as close to one another as possible (no major differences between the measured values) for the test to be deemed repeatable.

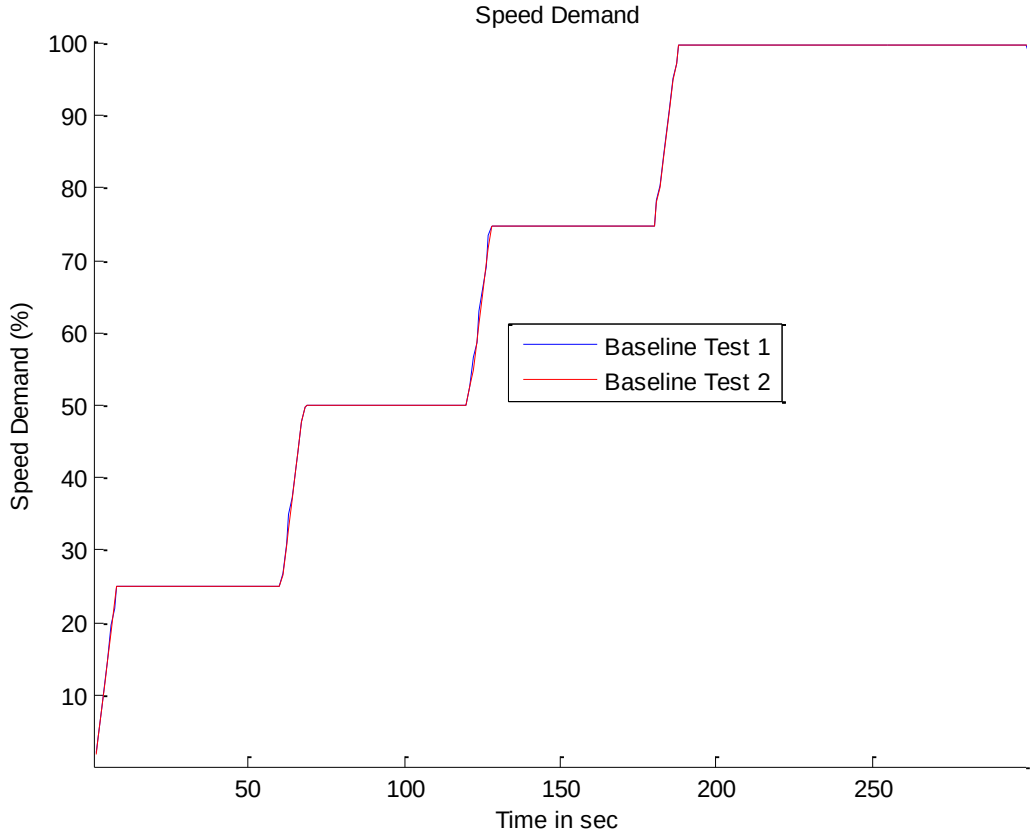

Figure 7-2: Baseline Speed demand

Figure 7-2 illustrates the graph of the speed demand read from the drive, notice that both signals are almost identical due the fact that the two test are conducted under the same settings. The speed demand is effectively the speed set to the drive by the test rig PLC.

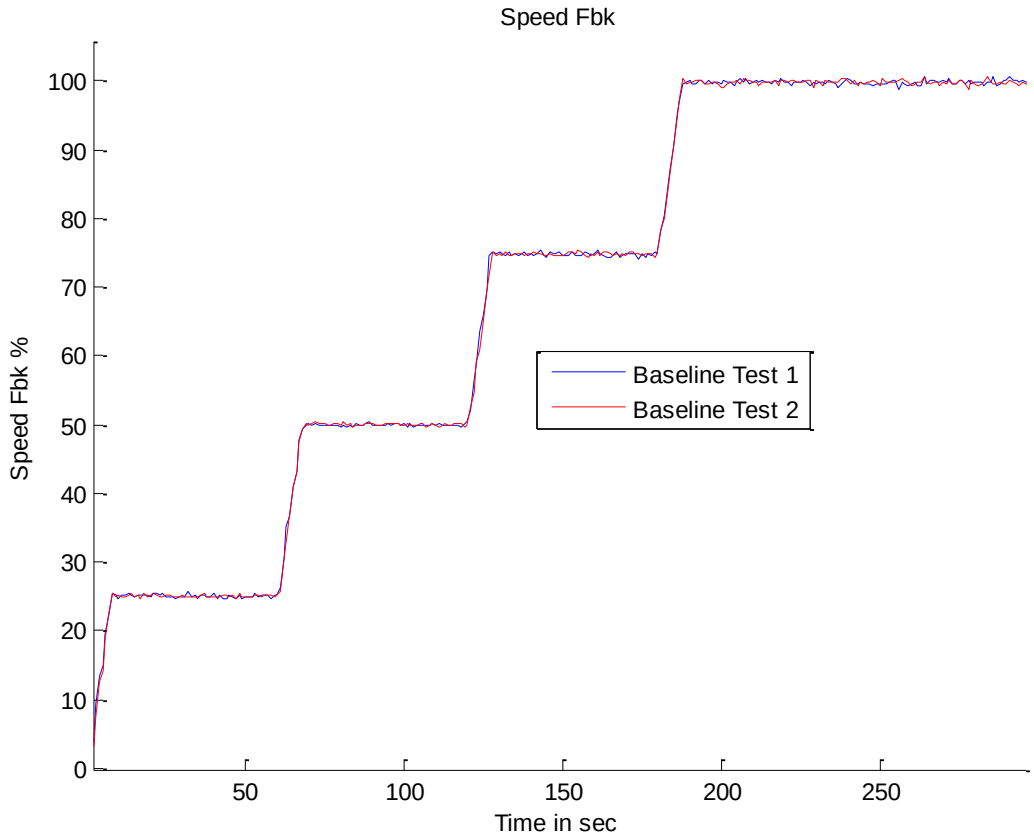

Figure 7-3: Baseline Speed feedback

The control mode used by the test rig drive is sensorless vector detailed in section 4.3.3; the drive uses motor parameters to calculate the speed of the shaft and tries to get the speed error as close as possible to zero by adding or subtracting the torque demand to the motor. This is why the speed feedback on Figure 7-3 is very similar to the speed demand on Figure 7-2 as the speed sequence for this test is 25%, 50%, 75% and 100%.

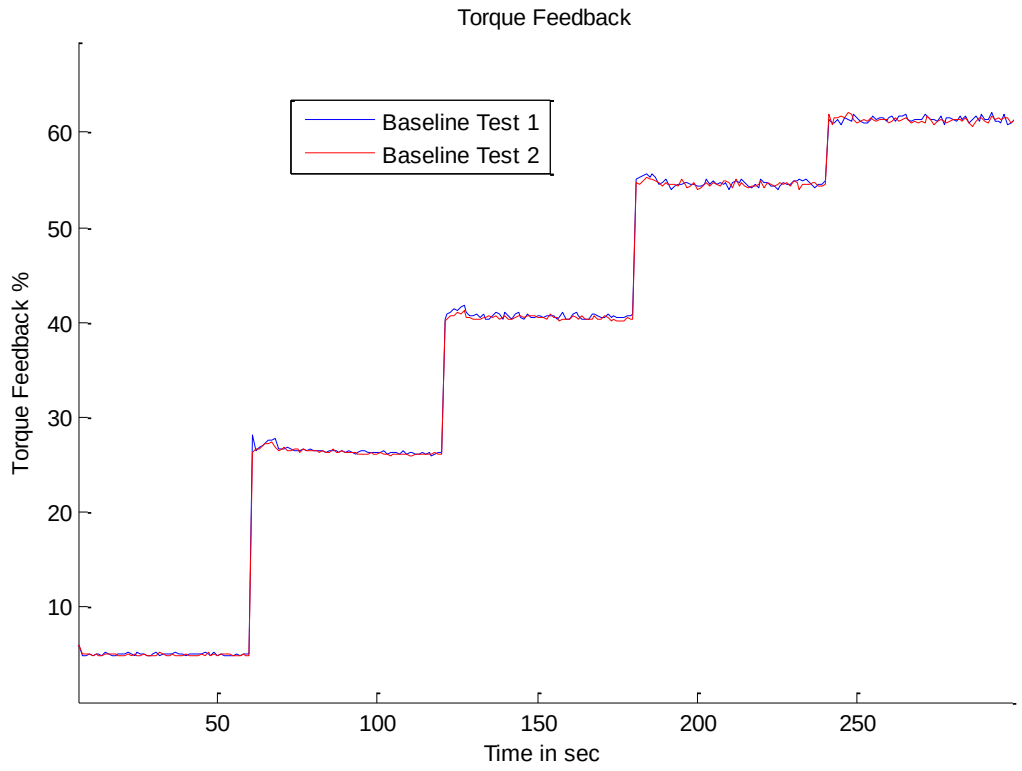

Figure 7-4: Baseline Torque Feedback

Figure 7-4 above shows the baseline torque feedback from both tests and there are no major differences between the two signals. As seen on this figure there are five step changes on the torque feedback in which step one is the feedback from the motor at 25% speed and no load. Step two to four are the response to speed changes (50, 75, 100%) respectively and load change (30, 50, 70%) respectively. On the final smaller step is because the speed stays at 100% however the load increases from 70 to 80%.

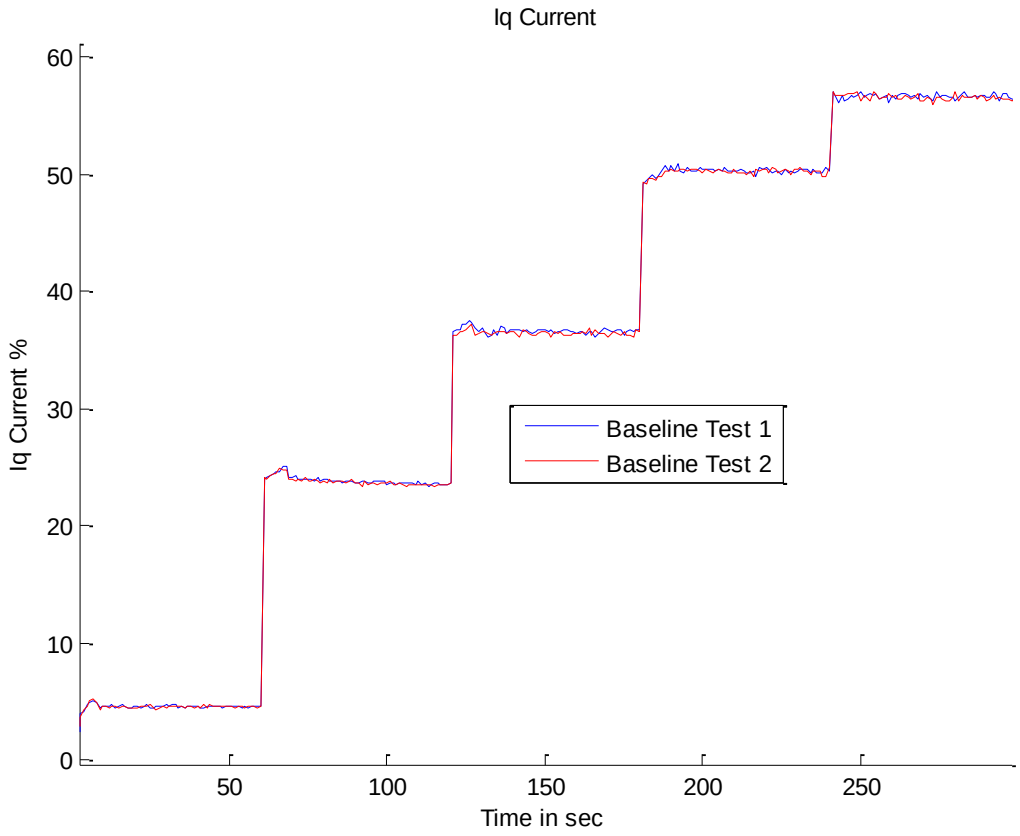

Figure 7-5: Baseline Iq Current

Figure 7-5 above shows the baseline Iq from both tests and there are no major differences between the two signals. The Iq current, also called quadrature current is the torque producing current as it can be noticed by the similarity between the curves for the Iq current and that of the torque feedback on Figure 7-4.

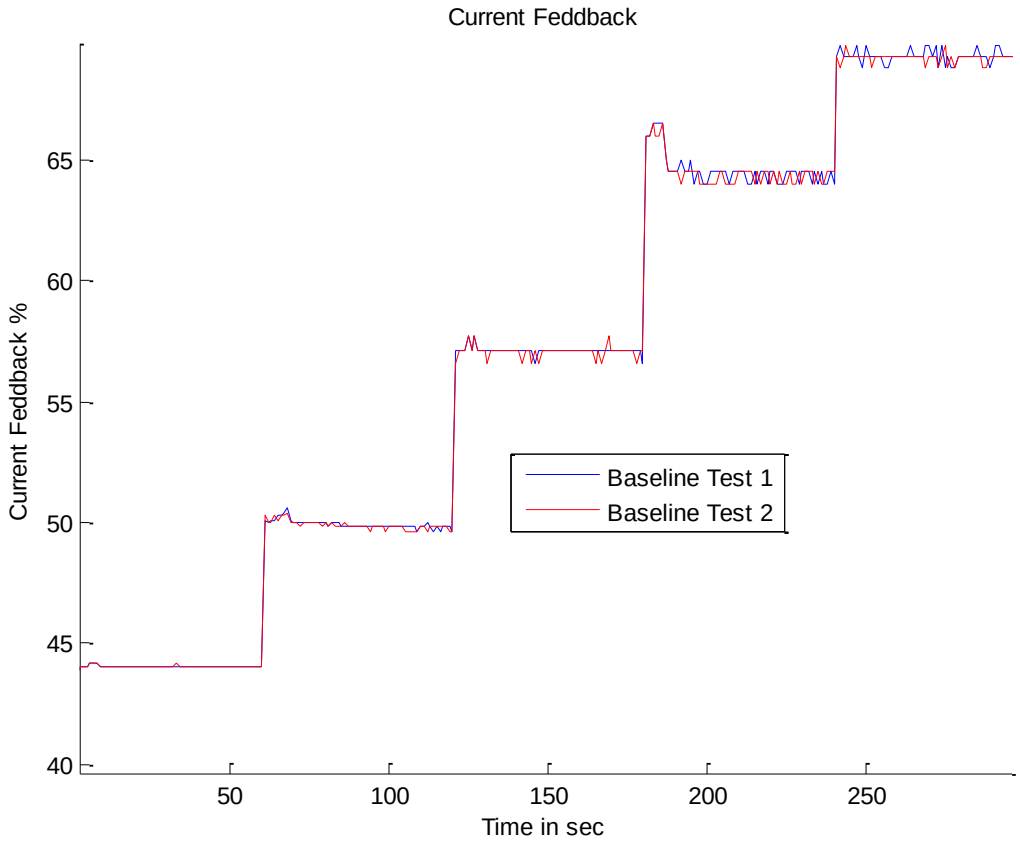

Figure 7-6: Baseline Current feedback

Figure 7-6 above shows the baseline current feedback from both tests and there are no major differences between the two signals. There are a few data spikes but none of them stays on for a considerable length of time therefore they can be considered as noises. Also note that there are five step changes all for the same reason as on the torque feedback curves.

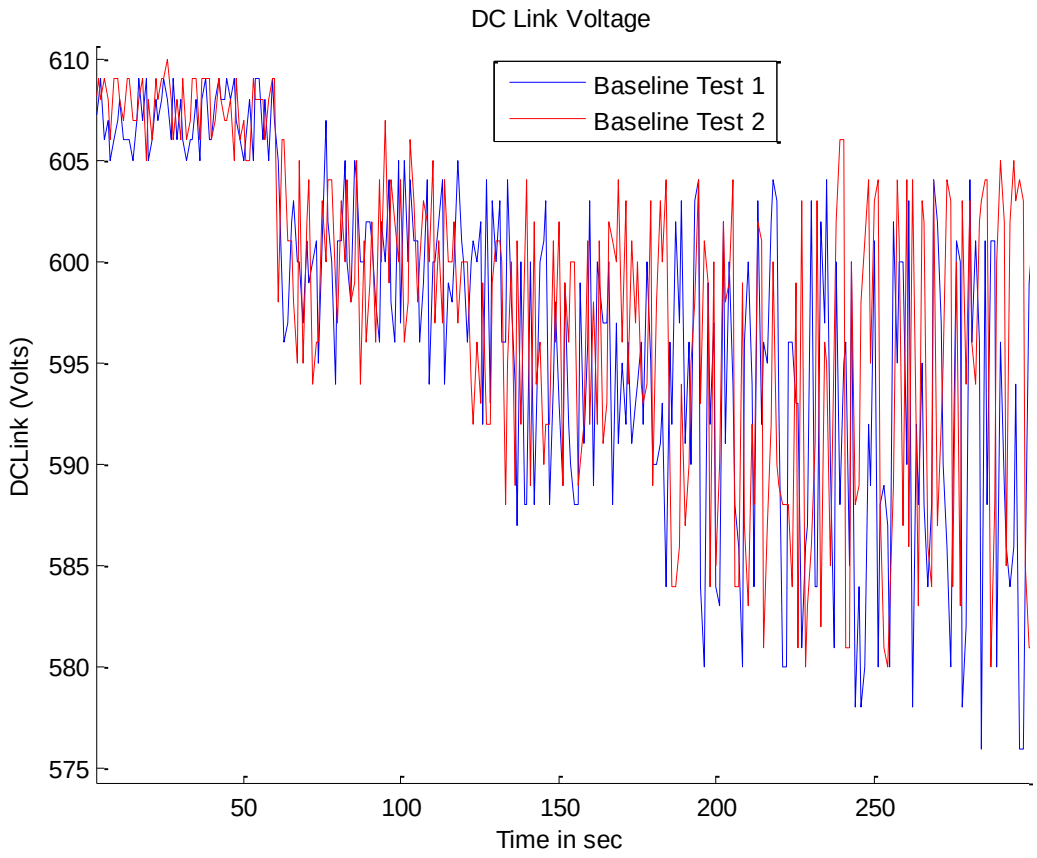

Figure 7-7: Baseline DC Link Voltage

The DC Link Voltage is derived from the rectified and smoothed three phase supply to the inverter. The smoothing is achieved by the used of DC Link capacitors to limit the ripple.
Figure 7-7 above shows the baseline DC Link Voltage from both tests and there are no major differences between the two signals.

The first thing to notice here is that the DC Link voltage varies with the load and speed of the motor. At 25% speed and no load the DC link voltage varies between 605 to 610 Volts. When the speed goes up to 50% with a 30% load the voltage drops and varies between 595 and 605 Volts. At a speed of 75% and a load set point of 50%, the voltage drop again and varies between 587 and 603 Volts. Then at full speed and load between 70 and 80% the voltage drops again and now varies between 577 and 603 Volts. The drop in DC Link Voltage at each stage is due the motor speed and load increase which cause the DC Link capacitor to discharge as the load increases. When the motor stopped the DC Link Voltage is $(rms) \times \sqrt{2}$. Where Vac is the Root Mean Square of the supply voltage.

The DC Link Voltage ripple also changes with motor speed this is caused by harmonics and the harmonics frequency vary with the motor speed. When the test rig motor is running at 25% speed, the ripple is just over 5 Volts. At 50% speed the ripple goes up to just over 10 Volts. At 70% Speed the ripple is around 15 Volts then when the speed reaches 100% the ripple goes up to 25 Volts approximately.

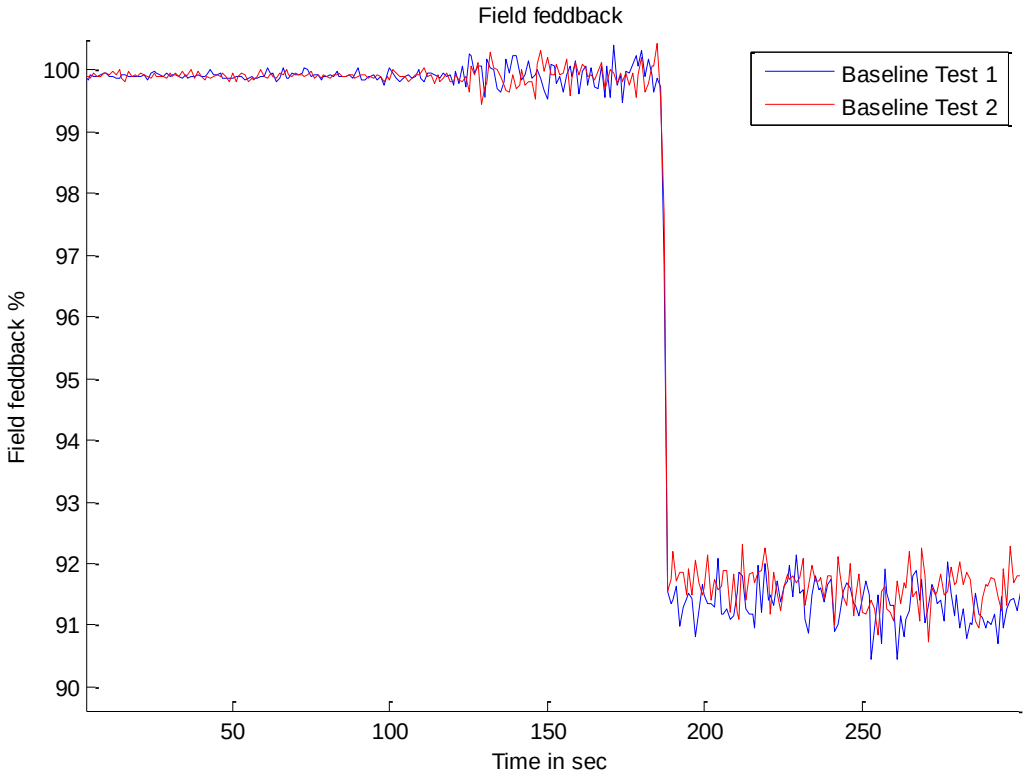

Figure 7-8: Baseline Field feedback

The baseline field feedback from the two tests is displayed on Figure 7-8 above; the results from both tests show there are no major differences. A field feedback value of 100% indicates the motor is operating at rated magnetic flux (field) and when the field drops below 100% this is called field weakening. The sudden drop on the field feedback from 100% to between 91-92% will be explained.

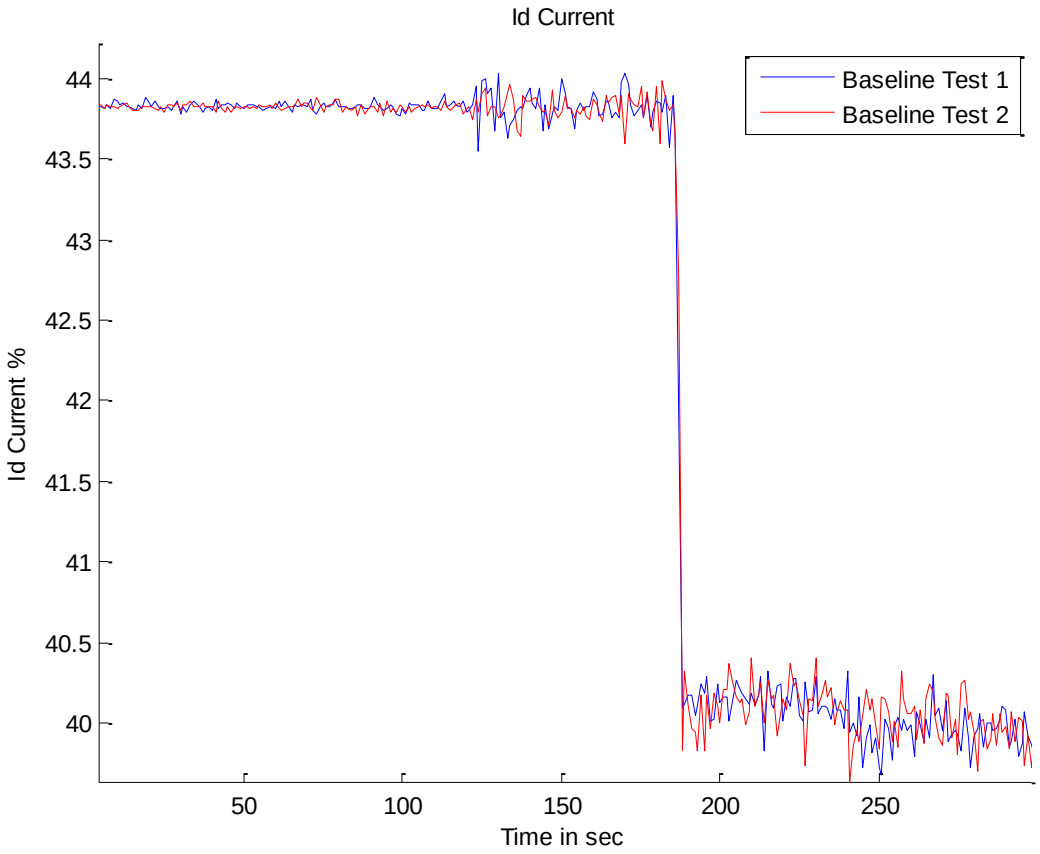

Figure 7-9: Baseline Id Current

Figure 7-9 shows the results of Id current from the two tests which also follow the same pattern with no major differences. The Id current is the field producing current which means that this current is proportional to the field feedback. The rated Id Current for this motor is 43.9% as shown on page 7 of the drive software in Appendix A. At the rated Id current the motor will be fully fluxed i.e. the field feedback will be 100%.

Notice that the field on Figure 7-8 drops about the same time when the Id current drops. The algorithm in the 650V drive will automatically weaken the field of the motor when needed to improve operational efficiency and for control purposes. On this drive 0 to 100% speed set point represent 0 to 1500 RPM where 1500 RPM is the calculated maximum speed of the motor during autotune as shown on page 7 of the drive software on Appendix A block (res autotune). On the other hand, on page 2 of the drive software block (Motor Data) the motor nameplate RPM is set as 1460 therefore when the drive is ask to run the motor at 100% i.e. 1500 RPM, the drive automatically goes into field weakening mode. I could have changed the automatically calculated RPM to 1460 to stop the drive going into field weakening but I decided to leave it as other students also used the rig and it might affect their test results.

Field weakening is a motor control technique that allows a motor to run faster than its rated speed and this will normally decrease torque production. The torque of an induction motor is expressed by the following equation.

$$T = \frac{3}{2} * \frac{P}{2} * \frac{1}{1+\sigma_R} \Psi_{mR} * I_q$$ **Equation 7-1**

Where:

T is the torque, P the number of poles, Ψ_{mR} the magnetising flux and I_q the torque producing current. $\sigma_R = \frac{L_R}{L_M} - 1$ Where: L_R is the rotor inductance and L_M the mutual inductance.
From the above equation if the magnetising flux (producing the field) decreases provided that we are in the constant torque zone where the torque producing current can still increase (by increasing the supply voltage to the motor) this will not affect the torque production. In the constant power zone (Field weakening zone) the supply voltage is constant at the maximum the drive can supply; this means that any decrease in magnetising flux to increase speed will decrease the motor torque. The breakdown torque is constant for the entire range of speeds below the field weakening region limit and once the speed increases above this limit, the breakdown torque value begin to decrease as shown on Figure 7-10.

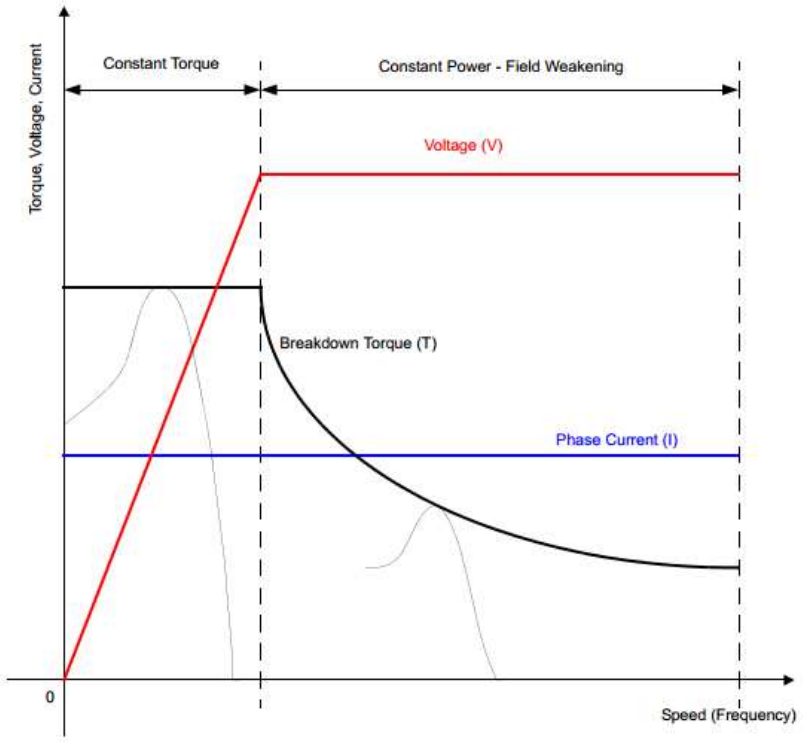

Figure 7-10: Theoretical Characteristic of induction motor [61]

All the baseline results above show that there are no major differences between the results obtained from both tests so we can therefore conclude the baseline test results are acceptable and repeatable.

7.2.2 2 mm misalignment tests

An identical test sequence to that performed for the baseline is also done here but with the shaft misaligned by 2 mm. the results are displayed on Figure 7-11 to Figure 7-17.

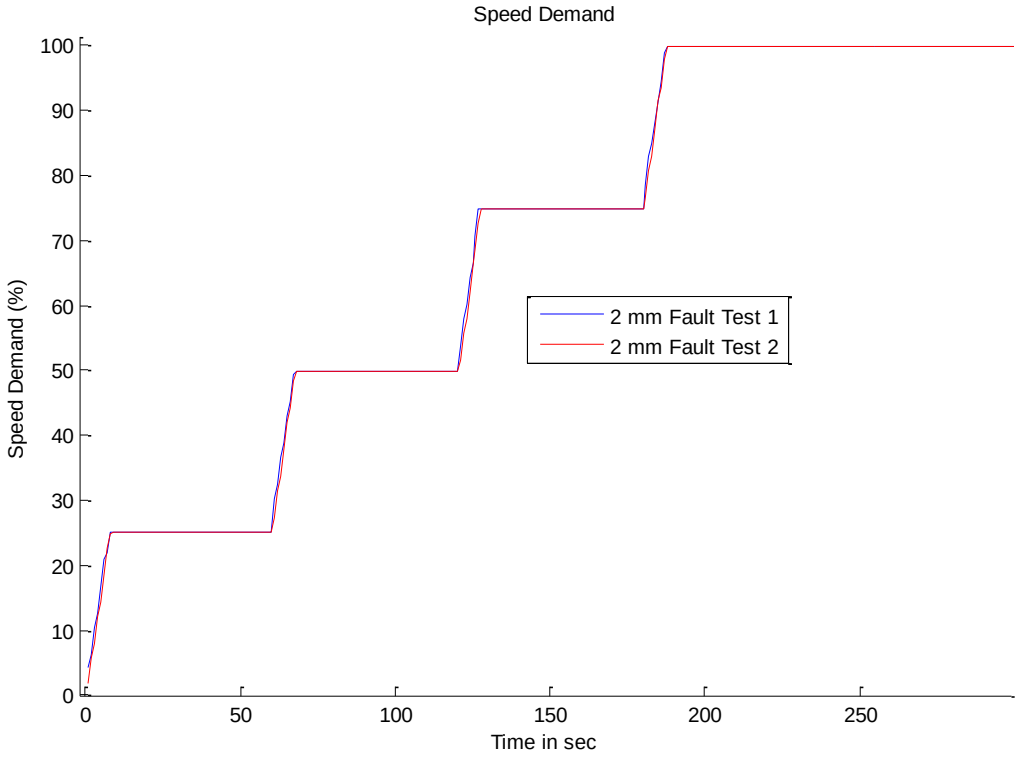

Figure 7-11: Fault test Speed Demand

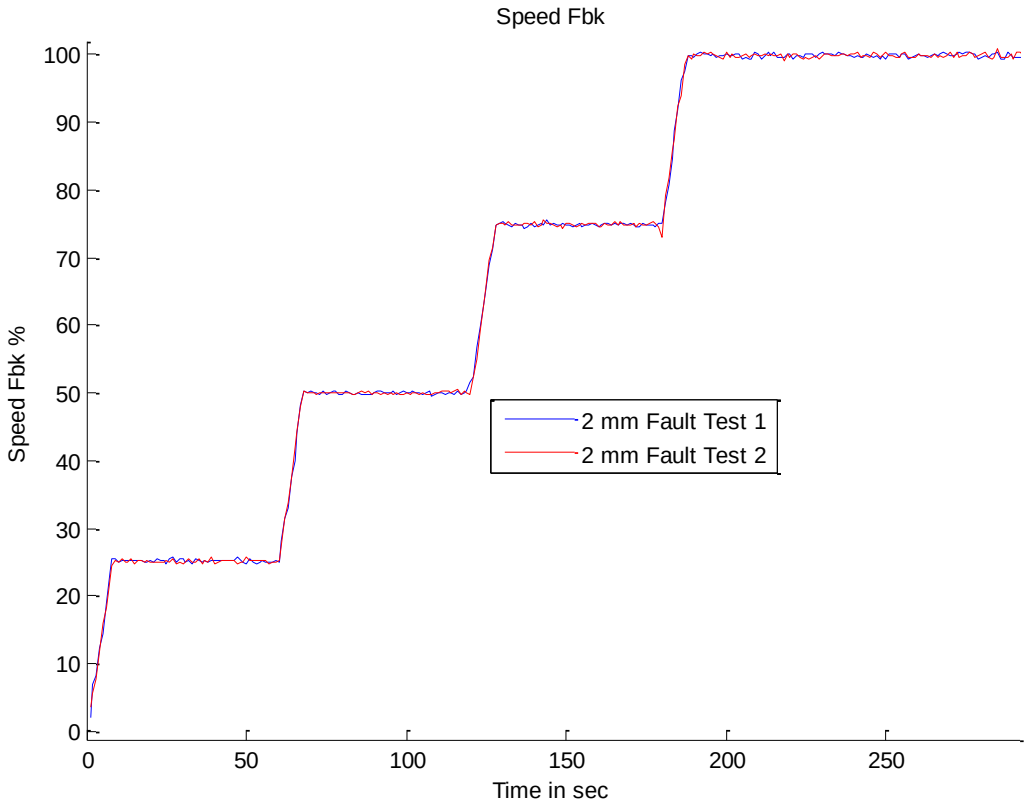

Figure 7-12: Fault test Speed Feedback

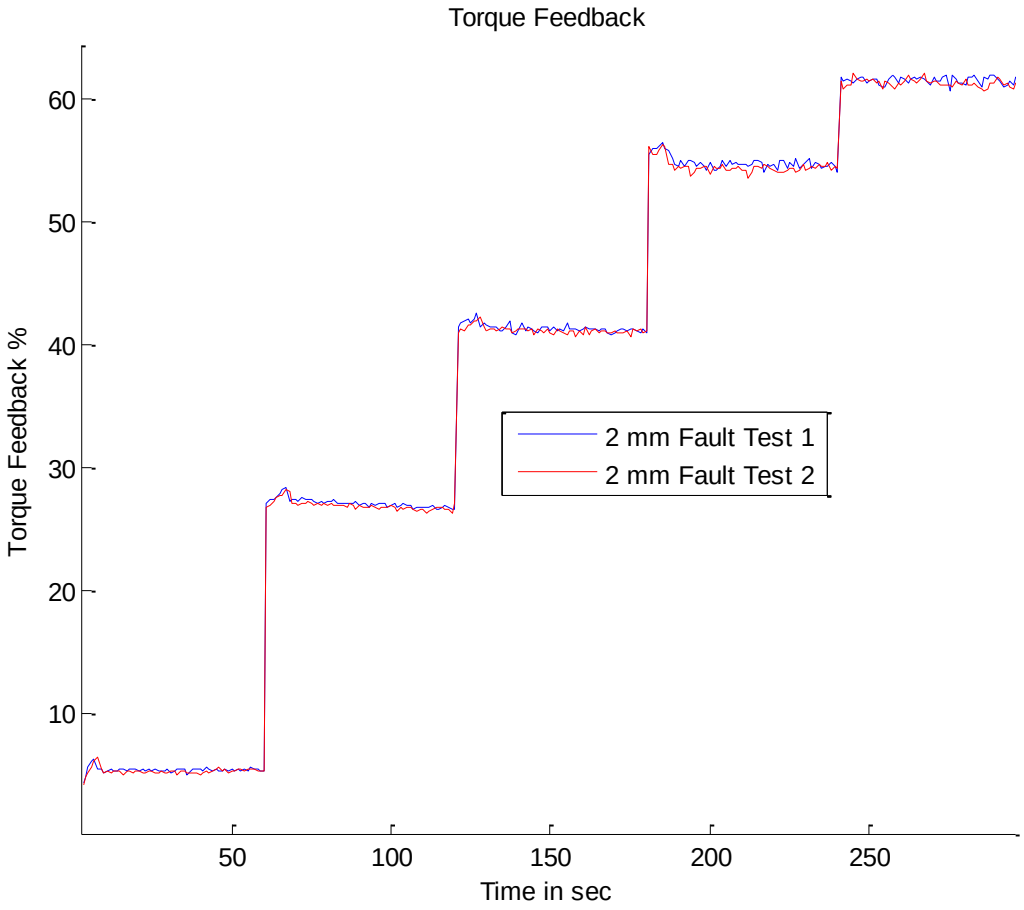

Figure 7-13: Fault test Torque Feedback

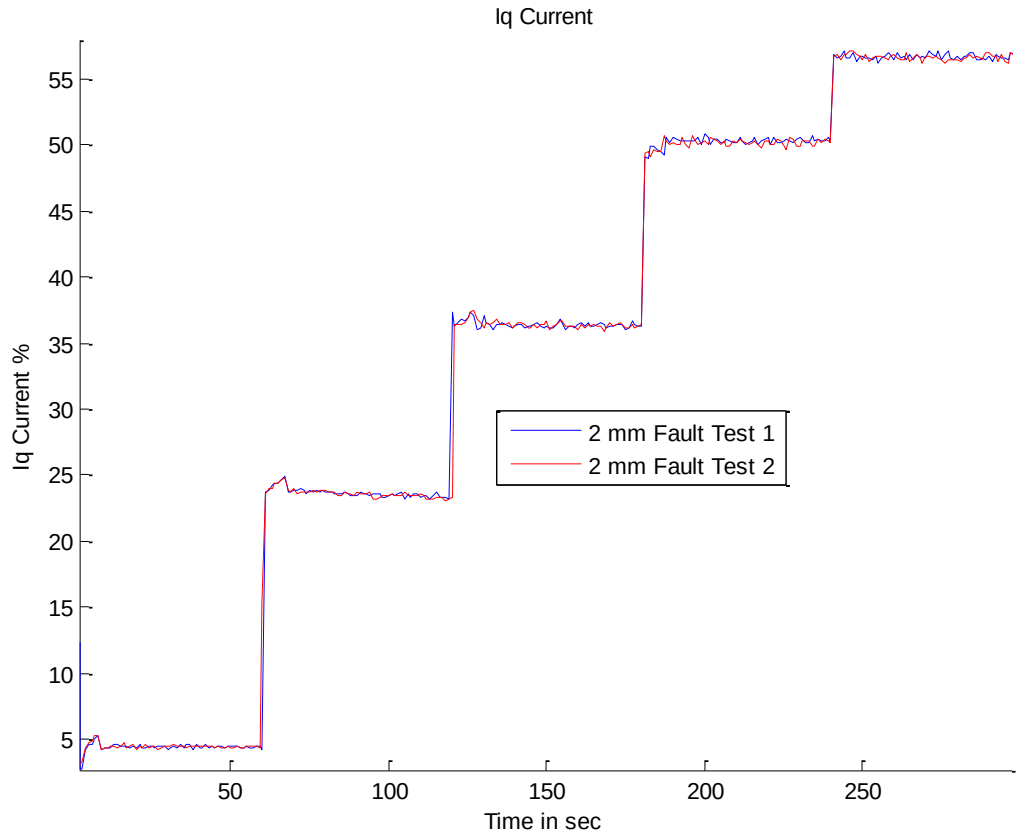

Figure 7-14: Fault test Iq Current

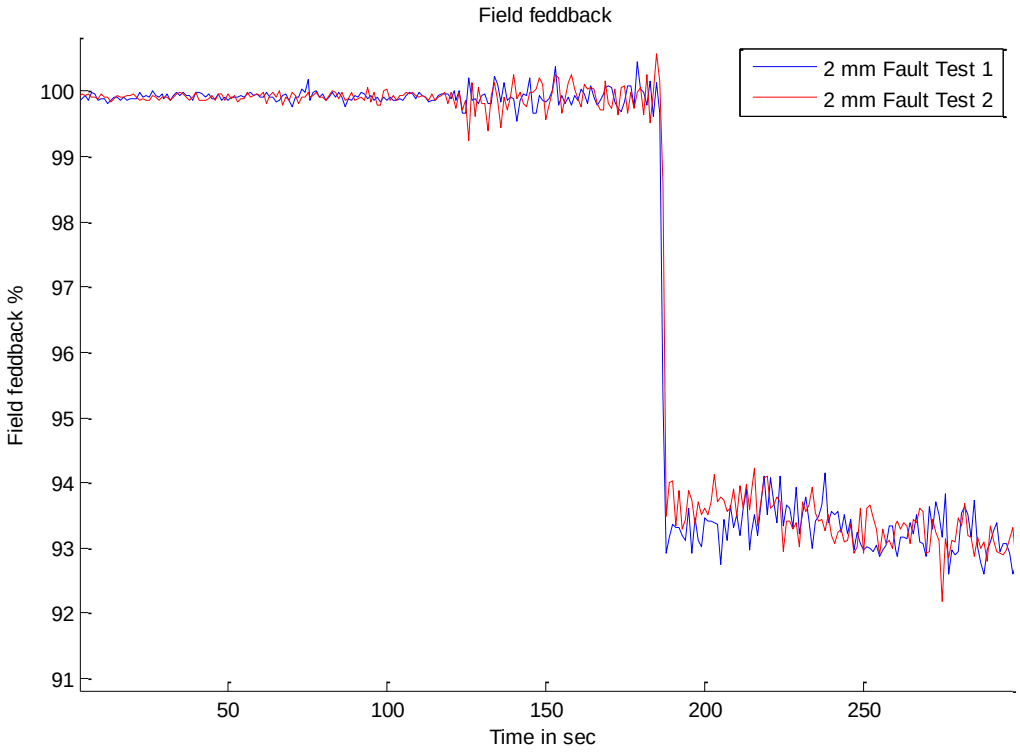

Figure 7-15: Fault test Field Feedback

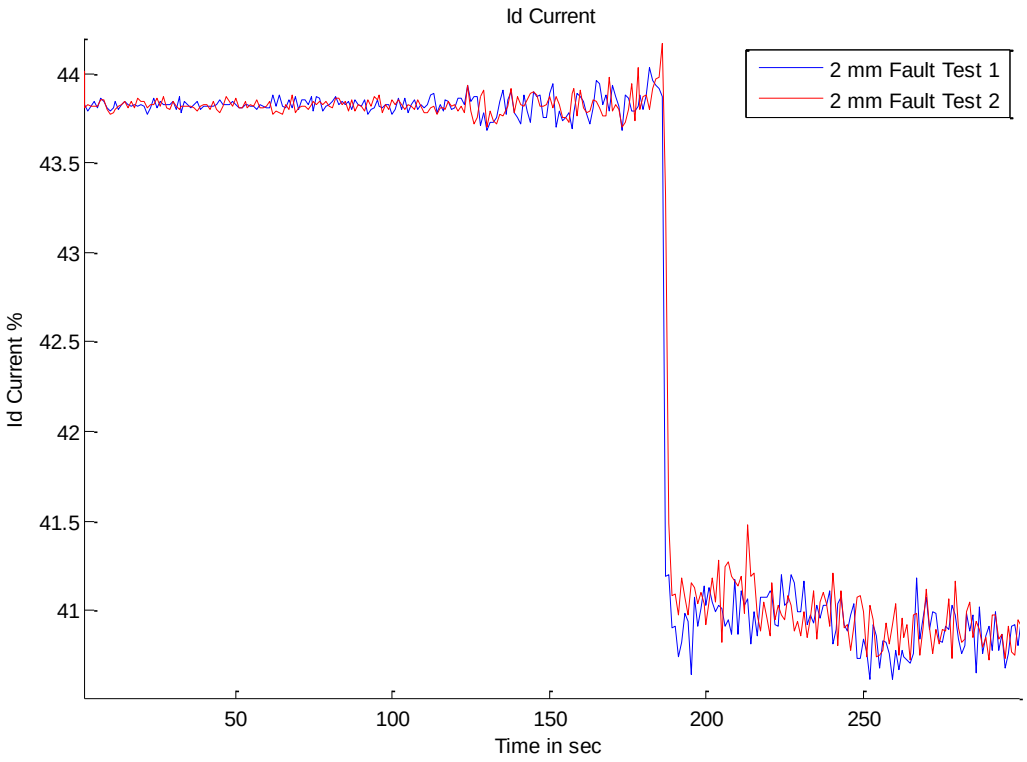

Figure 7-16: Fault test Id Current

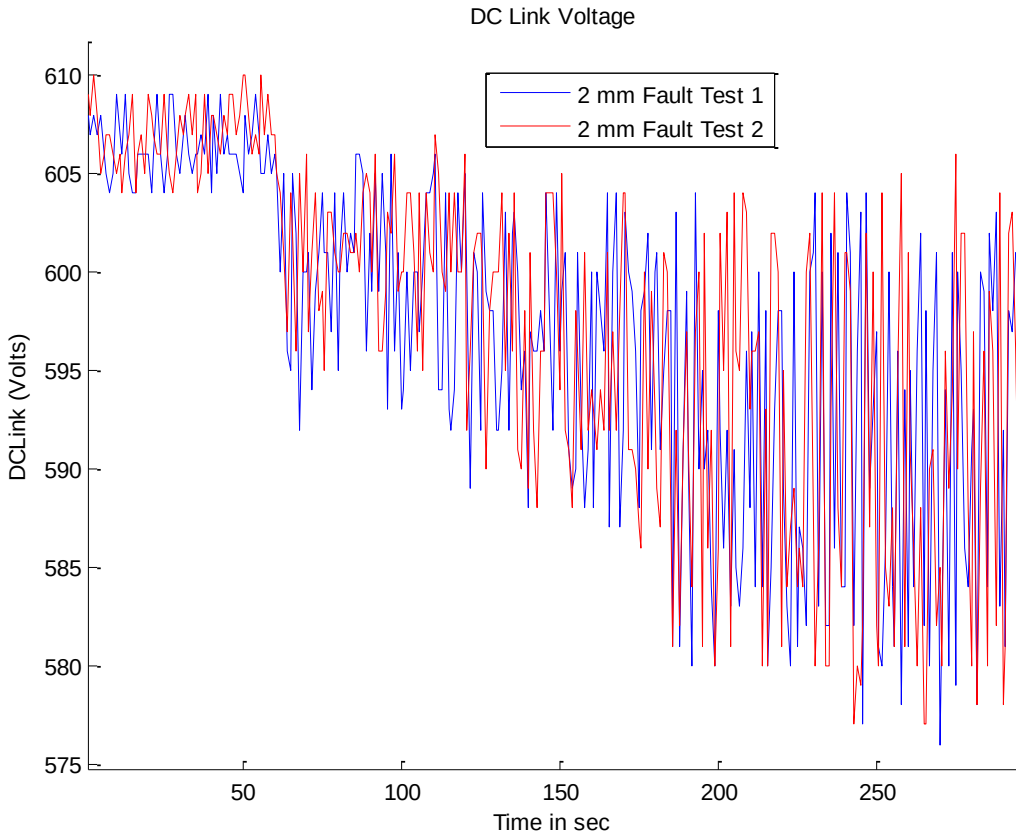

Figure 7-17: Fault test DC Link Voltage

By using a similar analogy to that used on the baseline tests it can also be said that all the results show that there are no major differences between the results obtained from both tests so 2 mm misalignment test results are acceptable and repeatable. The voltage ripple and drop is explained under Figure 7-7.

7.2.3 Test Results Comparison

The baseline results measured from the machine in a healthy state will be compared to those from the same machine with a 2 mm misalignment on the shaft.

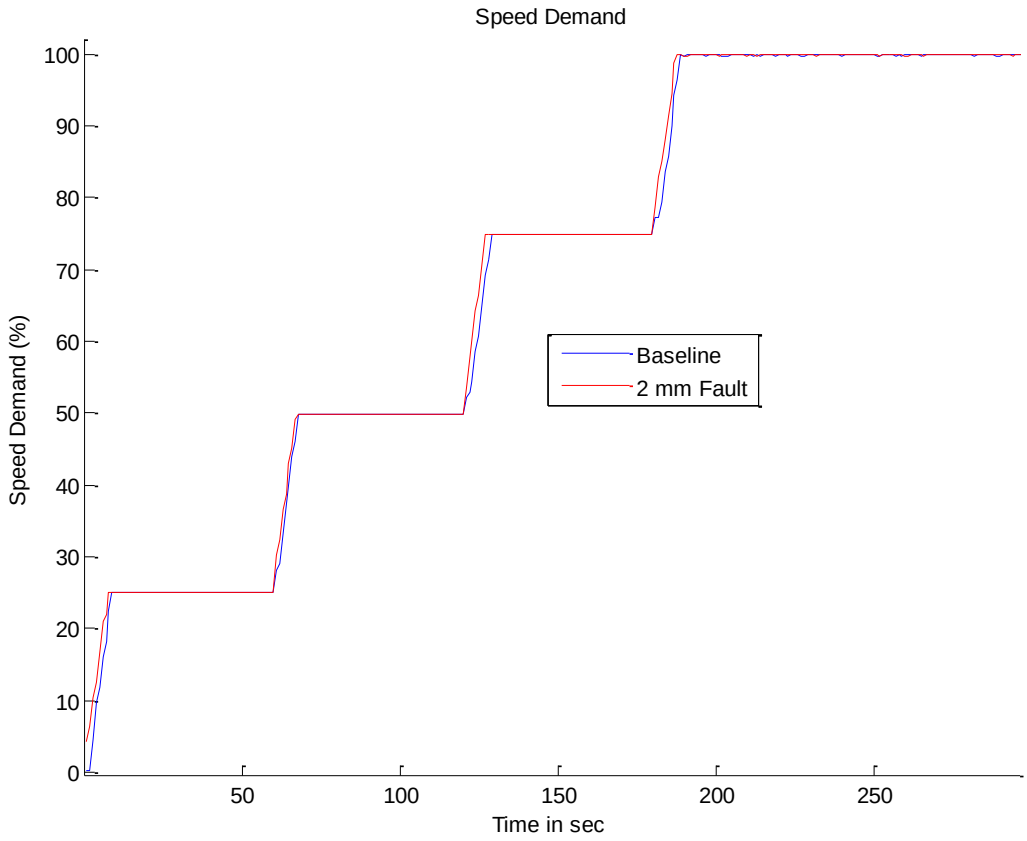

Figure 7-18: Baseline vs 2 mm Fault Speed Demand

As expected the speed demands from both tests illustrated on Figure 7-18 are the same since the same speed settings are used.

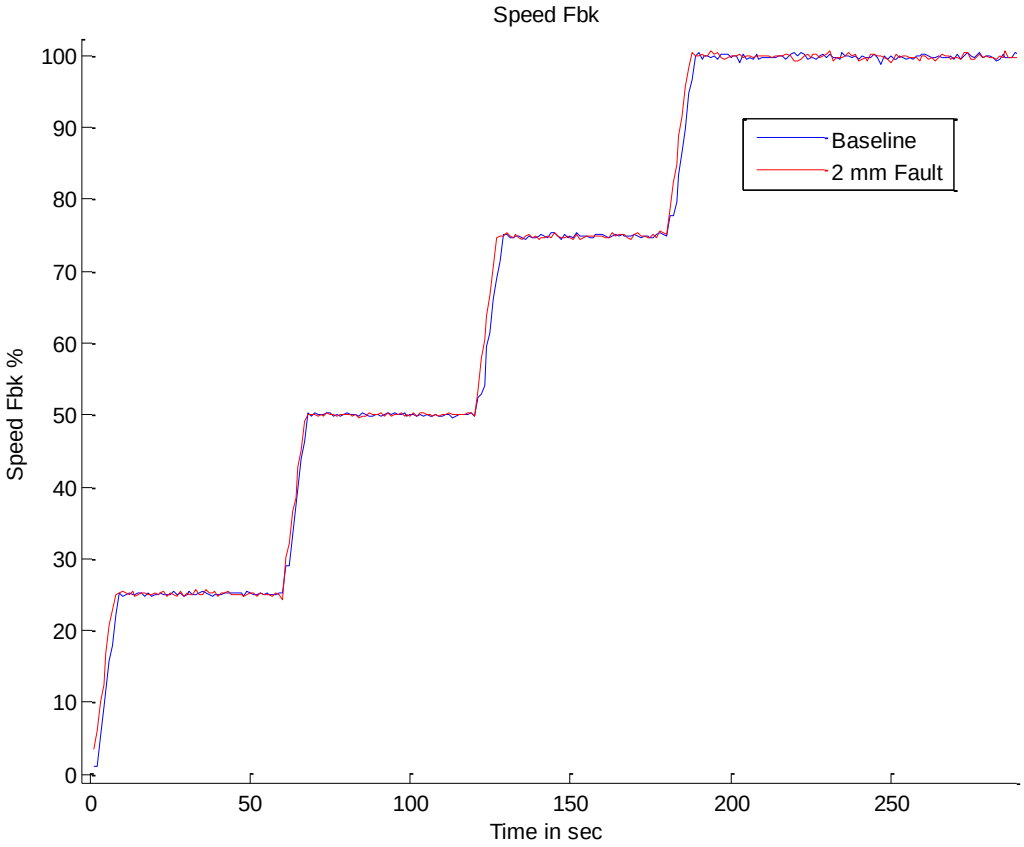

Figure 7-19: Baseline vs 2 mm Fault Speed Feedback

The speed feedback curves on Figure 7-19 are also very similar because the inverter automatically compensates for any speed change caused by increased load from misaligned shaft; by producing more torque to get the motor to go to the set speed as illustrated on Figure 7-20. Also notice that the speed feedback curves are similar to that of the speed demand.

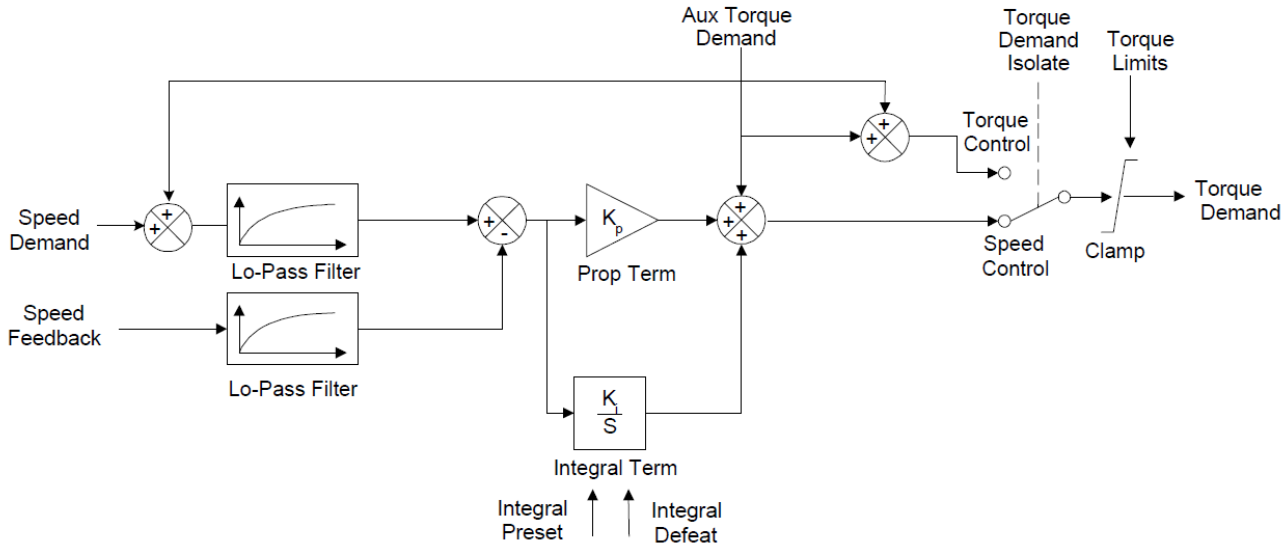

Figure 7-20: Test rig drive speed loop [62]

The speed error (speed demand minus speed feedback) is calculated and processed via a proportional + integral (PI) controller. The output of the PI controller is a torque demand, which is passed directly to the torque control block. The speed demand is derived from the Setpoint from the

PLC stored in the drive Scale block. When the drive is in SENSORLESS VECTOR mode, the speed feedback is calculated from the voltages and currents in the motor.

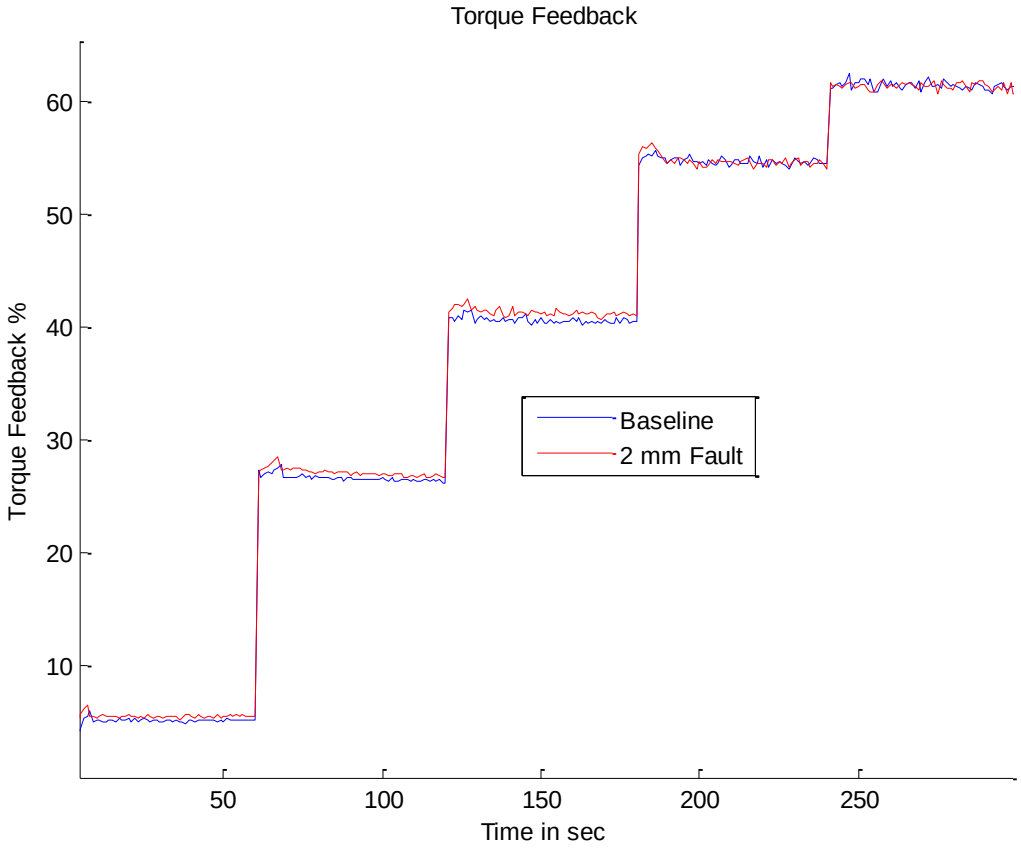

Figure 7-21: Baseline vs 2 mm Fault Torque Feedback

The misaligned shaft will create some form of resistance, the inverter will respond to this resistance by producing more torque so that the motor can achieve the demanded speed as explained above. One thing to notice here is that the fault can be detected between 0-75% speeds, however at 100% the motor is running at its base speed. The motor cannot produce any extra torque to achieve the set speed hence the field weaken just enough to achieve the set speed.

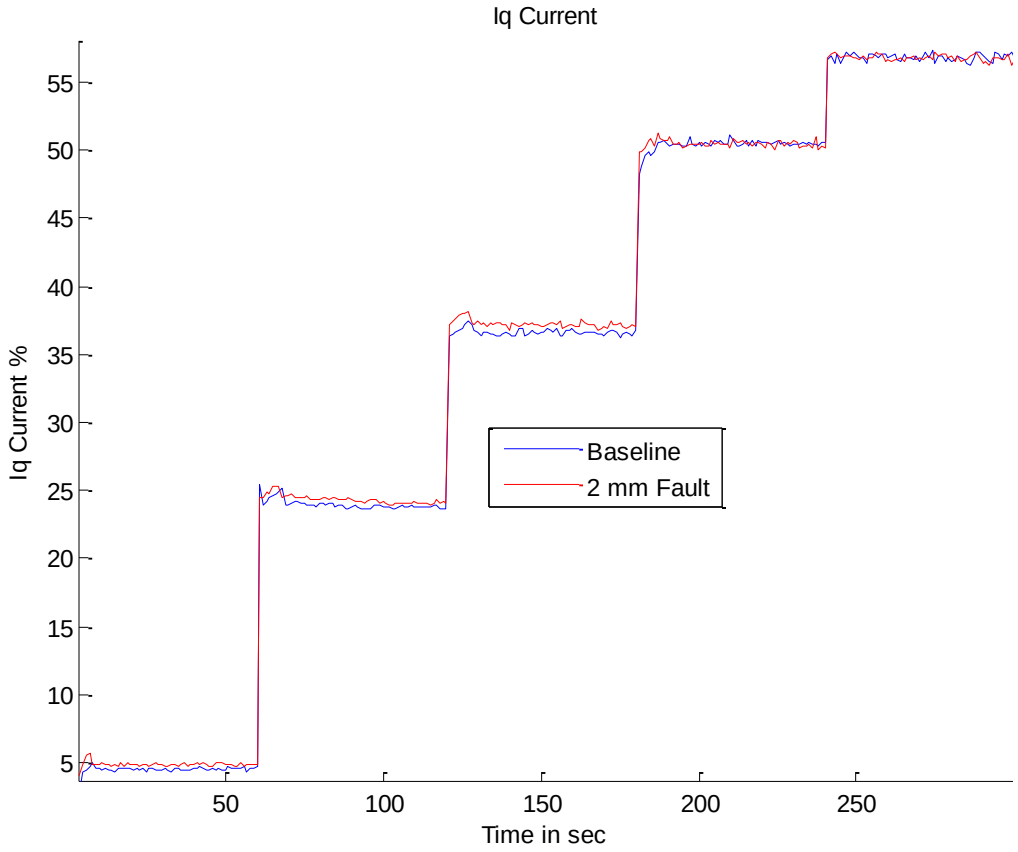

Figure 7-22: Baseline vs 2 mm Fault Iq Current

The same explanations for the torque feedback apply for the Iq current as they are proportional.

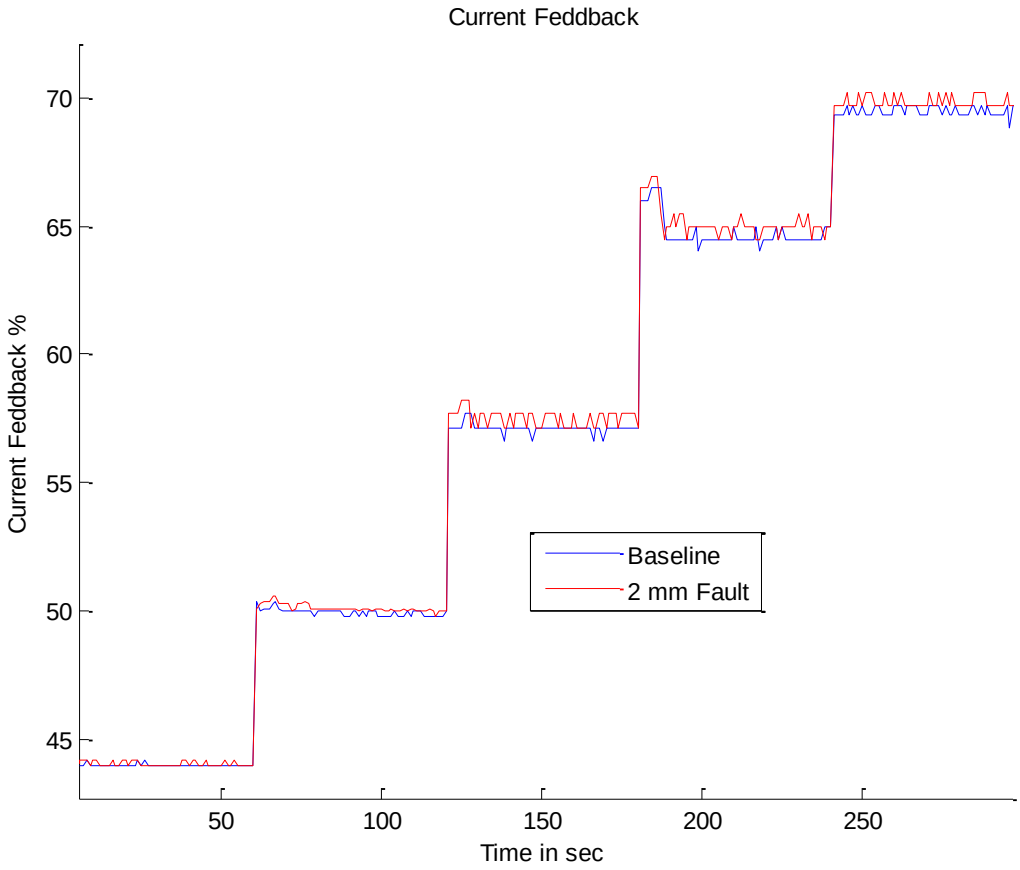

Figure 7-23: Baseline vs 2 mm Fault Current Feedback

Figure 7-23 shows that the motor pulls slightly more current when the shaft is misaligned than when the system is healthy. It is more noticeable at higher speed and load set points than it is at low speed with no load.

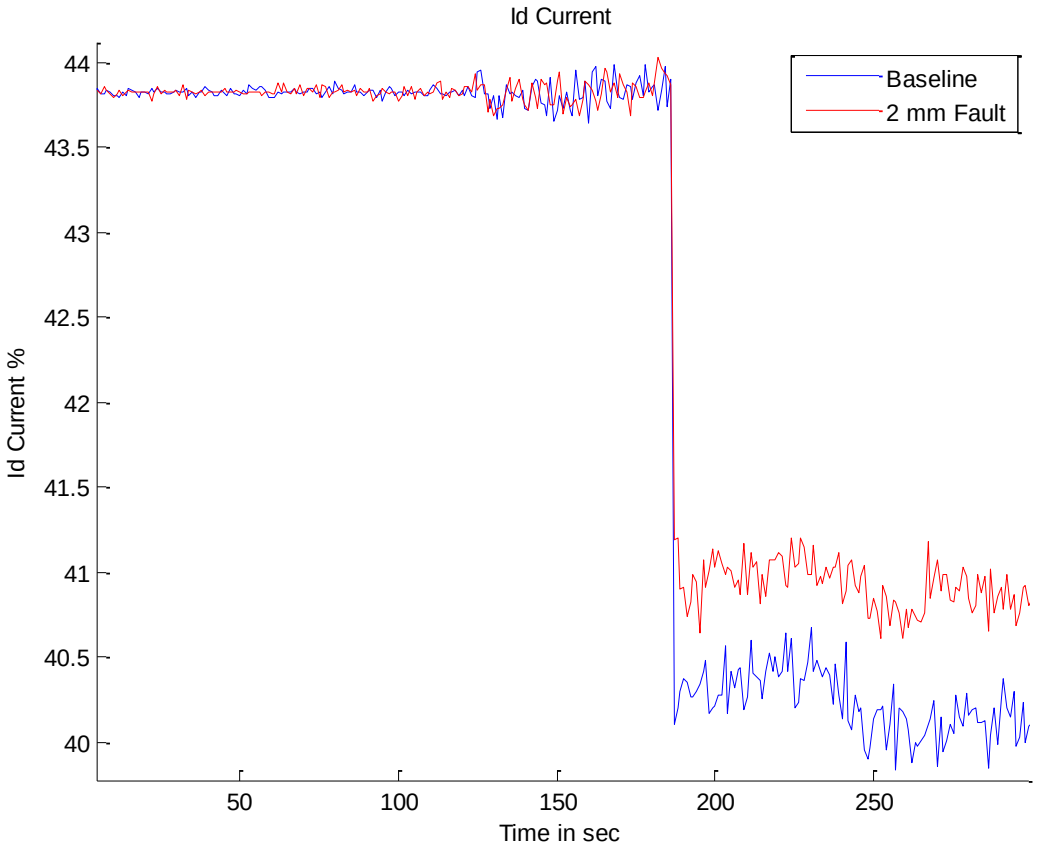

Figure 7-24: Baseline vs 2 mm Fault Id Current

The motor runs at the rated Id current as shown on Figure 7-24 to produce 100% field as shown on Figure 7-25; however at 100% speed set point, the field is weakened to enable the motor to achieve the set speed. Notice that with the shaft misaligned there is less field weakening as this will affect the torque required to turn the load to the set speed.

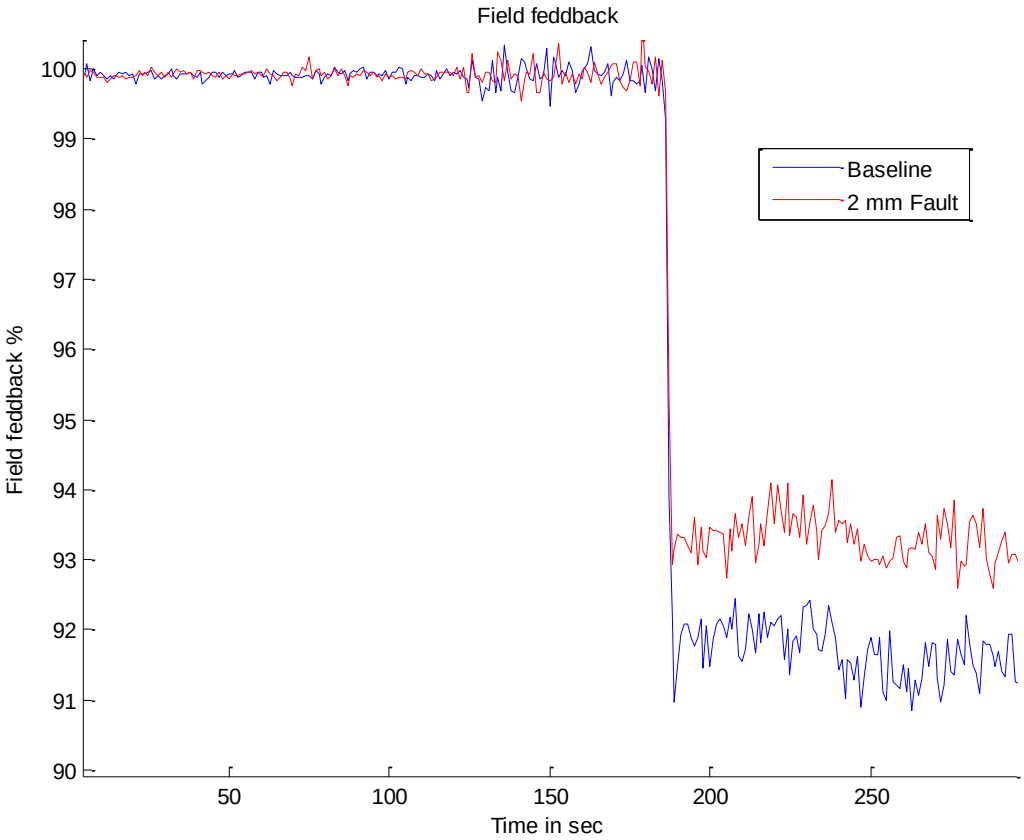

Figure 7-25: Baseline vs 2 mm Fault Field Feedback

7.2.4 Model based fault detection and diagnosis

Model-based fault detection and diagnosis is a monitoring procedure of fault detection and diagnosis in a system by comparing the system's available measurements with a priori information represented by the system's mathematical model. The system's mathematical model is generated using baseline measurements obtained from the system in a healthy state.

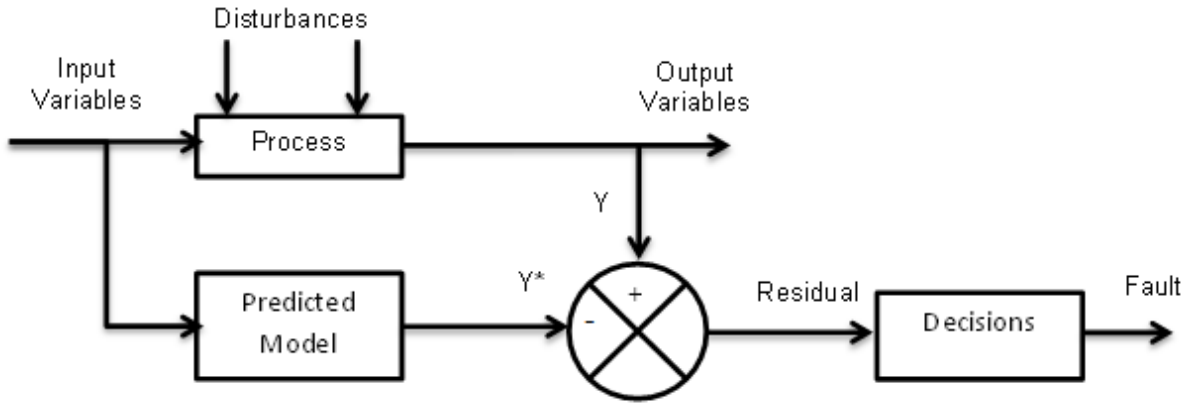

Figure 7-26: Model based Fault Detection and Diagnosis system

The residuals are examined for the likelihood of faults, and a decision rule is then applied to determine if any faults have occurred and which fault(s) have occurred. A decision process may consists of a simple threshold test on the instantaneous values or moving averages of the residuals, or comparing the residuals to a set of patterns (signatures) known to belong to simple faults, or by the use of more complex logical procedures like statistical decision theory, e.g., generalised likelihood ratio (GLR) testing or sequential probability ratio testing (SPRT) [63]. A number of residuals can be

designed with each configured to be sensitive of individual faults occurring in different locations in the system as illustrated on Figure 7-26. Ideally when there is no fault the residual should be zero but when a fault occurs and changes above zero in the presence of a fault.

After careful analysis of the results from the above tests, the current feedback is the parameter with the most variations over different speed and load settings and will be used for model base fault diagnosis. Figure 7-27 illustrates a bi-linear equation of the baseline current feedback as a function of the speed and load settings.

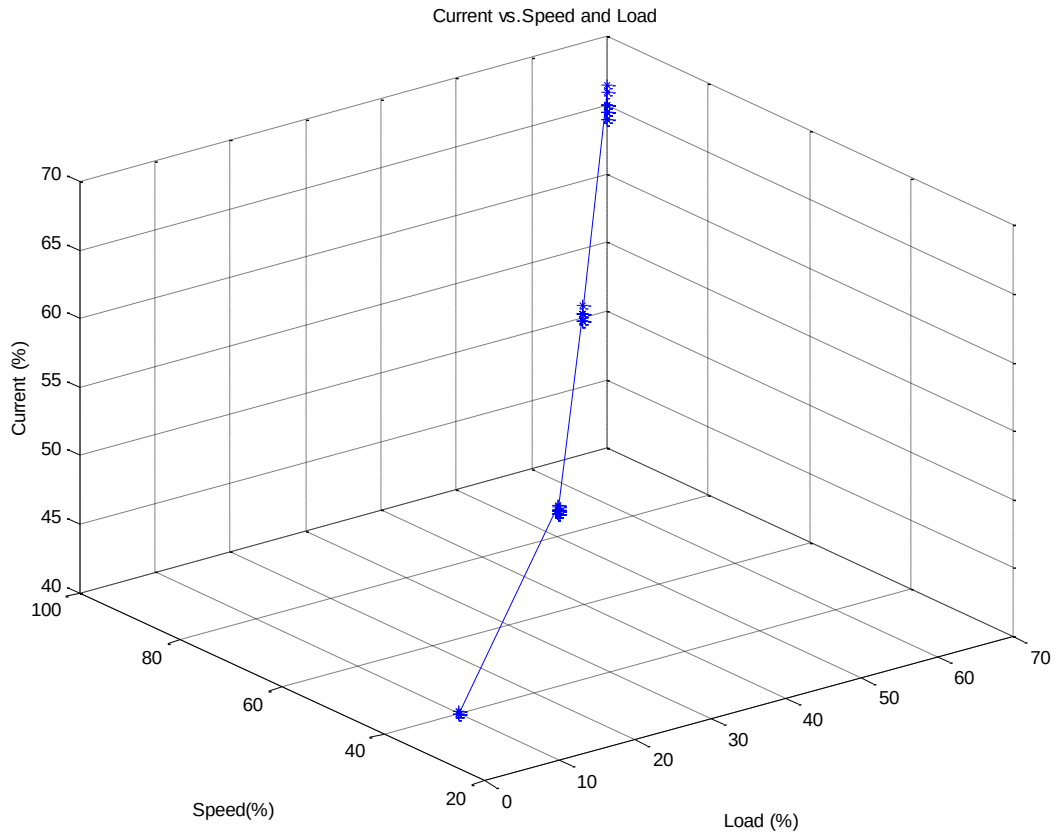

Figure 7-27: Bi linear equation of current feedback vs. Speed and load set points

The above information is then used to generate the model characteristics of the system as illustrated on Figure 7-28.

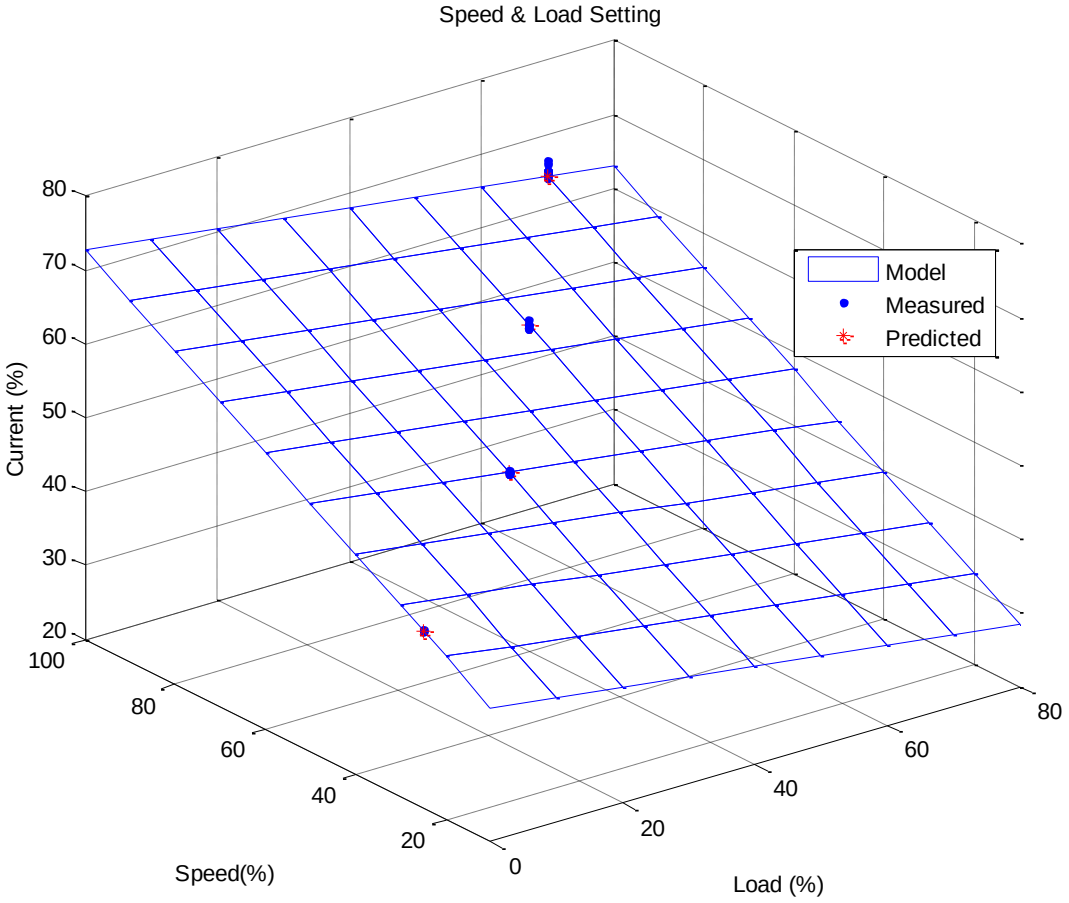

Figure 7-28: Model Characteristics

The first half of the data is used to produce the model and the model is verified by the select part of the data as illustrated in the figure below. The model equation is:

$$yhat = beta(1) + \ldots beta(2) * x(:,1) + beta(3) * x(:,2) \qquad \textbf{Equation 7-2}$$

The beta coefficients: -0.0166, 1.3754 and -0.4029. This means that the current feedback is expressed as a function of the load and speed setpoints as follows.

$$Current\ Feedback = -0.0166 + 1.3754 * speed - 0.4029 * load \qquad \textbf{Equation 7-3}$$

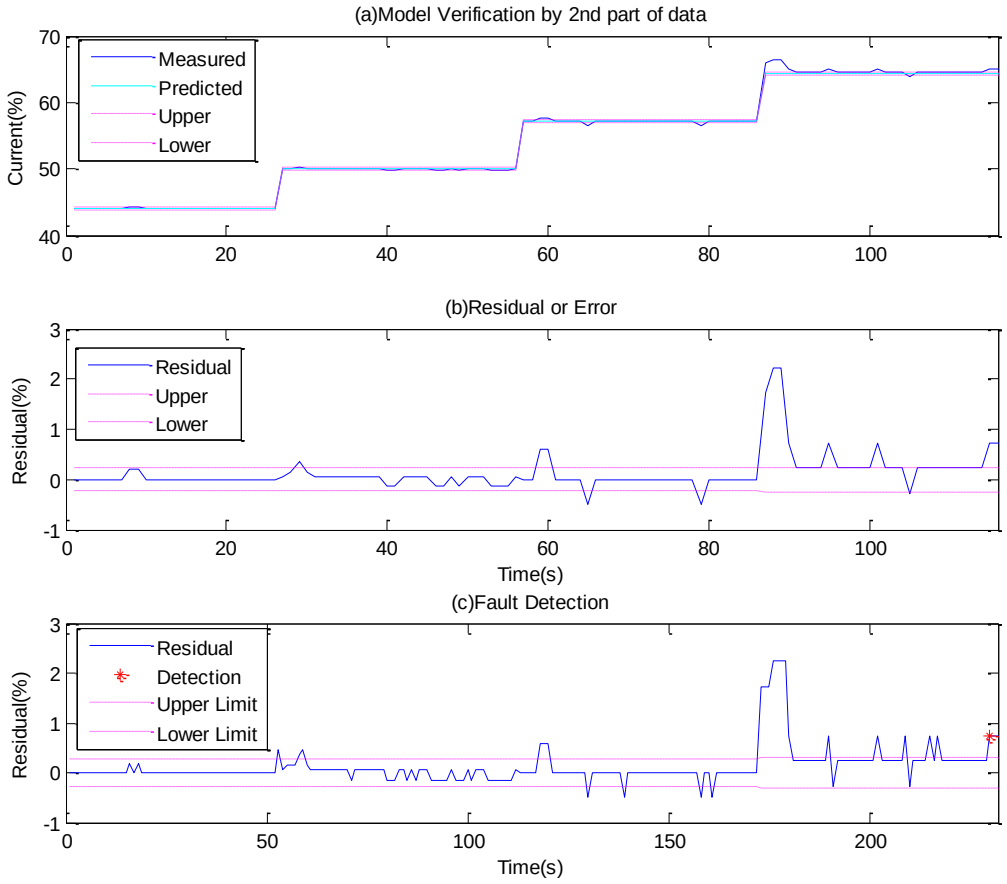

Figure 7-29: (a) Model Verification (b) Residual generation (c) Fault detection

Figure 7-29 (a) shows the model verification using the second half of the data. This figure shows that the model prediction is very close to the measurements. But it is difficult to observe if any data points exceeds the threshold.

By using the model residual on Figure 7-29 (b), this figure gives a clear indication that many data points exceed the threshold, which may indicate there may be abnormalities. However, by careful study it is found that the data spikes are mainly around transient operation stages where speed or load changes occurs and the sensorless vector speed loop PID overshoots in response to the changes. In addition, data values have limited digital accuracy. For robust detection, the transient data is excluded and in the same time the detection of abnormalities is confirmed by checking two continuous data points which exceeds threshold simultaneously. In this way a robust detection results is obtained as illustrated on Figure 7-29 (c) when the baseline data is used for fault detection, this only shows a single fault detection point which can be considered to be noise. The model is now ready to be used to detect real faults.

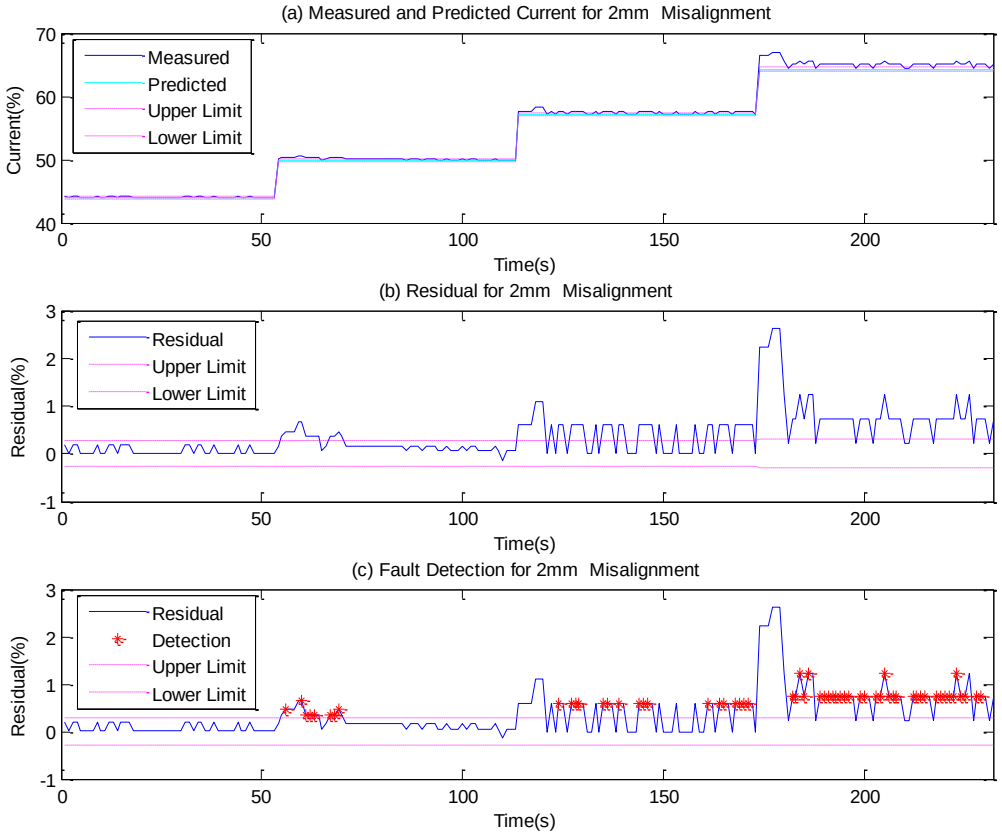

Figure 7-30: 2mm shaft misalignment detection using the designed model

Figure 7-30 illustrates a real fault detection using the designed model. On (a), the predicted results is compared against the measured data; the measured data is above the upper limit of the threshold most of the time which is indicative of a fault. By using the residual on (b) it is clear that a lot more data exceeds the threshold. The principles as used on Figure 7-29 is also applied i.e. ignoring transient operation stages and only looking for two or more simultaneous spikes. The results of the detection illustrated on (c) shows that there are more detection points and the majority of the detection happens when the load setpoint is 30% or above and the speed setpoint 50% or above. This is because at low speed and no load, the motor pulls more current but because the extra current is of a small magnitude it is absorbed within the set threshold. The threshold can of course be lowered so that fault can be detected at low speed and load setpoints but this could lead to false detection due to noise.

7.2 Test data reliability

As mentioned above on section 2.2.5, the rotor resistance will change with temperature. When the machine is offline the rotor resistance is a lot higher and when the machine is started and the temperature slowly rise until it reaches its thermal equilibrium. The gearboxes on the rig will be stiff and have some resistance when cold which means the drive will produce more current hence torque to turn them when cold. When they get warmer and more flexible they will require less torque. The same applies to the coupling; they will be more flexible when they have reached their temperature equilibrium. All these little factors affect the test results and somehow need to be taken into account when gathering the test data.

Drive designs with motor temperature compensation techniques are typically classified as field-oriented control drives as discussed above in section 4.3 above. FOC drives use voltage feedback circuits to calculate changes in motor resistance through voltage drop. These drives adjust the field flux based upon motor operating temperature, providing more accurate operation from a cold condition to normal operating temperature. Speed regulation is more stable too.

Since the drive used in this research paper is sensorless vector drive, there is no way of knowing the motor temperature and for condition monitoring purposes, data collected from the same machine when it is cold will be different from the data collected when the machine has reached its temperature equilibrium. Data consistency is critical to accurate fault diagnosis. To get around the temperature issue two RTD thermocouples are installed, one in each gearbox and the temperature data is continuously monitored until the temperature in both gearboxes stabilise. It is only at this point that data is collected from the machine and each test is done five times to ensure that the results are as identical as possible. Although the thermocouples are not directly connected to the motor windings, heat in the motor will slowly be transfer to the gearbox via the motor shaft. Test results show that the gearbox connected directly to the motor shaft gets a lot warmer that the one connected to the motor via a coupling.

Chapter 8 Conclusions, contribution and future work

8.1 Introduction and objectives review

Accurate means for condition monitoring can improve the reliability and reduce the maintenance costs of induction motors. Much interest has been invested into induction motor condition monitoring but so far it involves installing additional components which usually increase the operating cost of the machine. Research has been carried out on inverter driven motors where the drive feedback parameters are read from the drive terminals but nothing so far has been done using fieldbus to extract raw parameters for analysis.
The aim of this research is to advance the field of remote condition monitoring and fault diagnosis of induction motors under different operating conditions using electrical supply parameters measured by an inverter drive.

It is important at this point to review the project objectives and achievements.

Objective 1

Investigate induction motor condition monitoring techniques with the view to determine whether any research has been conducted in the field of machine remote condition monitoring with emphasis on applying wireless communication techniques to extract the controller parameters for analysis.

Achievement 1

To ensure that this research brings some contribution to the field of machine condition monitoring it is important to ensure that it is not been done already and from extensive literature review. Although M. Lane [64] has conducted research on induction motor condition monitoring using inverter output signals; the inverter used in this research was a closed loop flux vector inverter and the signals were read directly from the drive terminals. This research uses a sensorless flux vector drive and the signals analysed are raw signals extracted from the inverter control loops. Therefore the results of this research will give some contribution in this field.

Objective 2

Analyse the rig's control system and identify the maximum number of signals that can be monitored in its current state because the system is likely to have hardware and/or software limitation, which restrict the amount of data we can read from the inverter.

Achievement 2

After careful analysis, the Parker 650V inverter happens to have some hardware limitation with only one analogue output which means only one parameter can be monitored at the time. In order to fully understand the behaviour of the inverter in a fault condition, it is necessary that as many signals as possible are monitored.

Objective 3

Investigate means of reading more real time control and feedback signals from the drive.

Achievement 3

This was achieved by adding a profibus communication card on the drive to allow the drive to communicate with other automated devices on the same network.

Objective 4

Design and develop a prototype control system based on my research to demonstrate remote condition monitoring, reading control loops signals from a machine and transferring these signals wirelessly to a computer so that they can be analysed.

Achievement 4

This was achieved by using a Siemens S-1200 PLC with build in industrial Ethernet (profinet) and a profibus communication card. The profibus card allows the PLC to extract data from the drive while

the profinet allows data transmission over a wireless network to other devices. Data can be extracted directly from the PLC via wireless network or via VPN using a computer or mobile communication device that supports web browsing. A site PC also connects to the PLC over the wireless network and allows visualisation of parameter while at the same time logging all the data.

Objective 5
Test and commission the prototype.

Achievement 5
After designing and developing the prototype, it was important to ensure that it worked as expected and that all the signals were converted in the correct format for analysis.

Objective 6
Use the modified test rig to run a series of tests on healthy and faulty machine status.

Achievement 6
To ensure that the proposed system will work as expected, series of tests were run on the machine in the healthy and faulty status to ensure that the data collected was reliable and repeatable.

Objective 7
Investigate the signals received from the test rig to establish their usefulness in determining machine faulty or healthy status

Achievement 7
The data collected with the proposed system was analysed using MATHLAB. Model based fault diagnosis technique is used for this purpose where a mathematical model of the system is used to generate estimates of other measurements. The estimated values are then compared to values read from the machine to detect faults.

8.2 Conclusion

Based on the above achievements, it can be concluded that:

- This thesis presents a novel approach for the remote condition monitoring of induction motor by using power supply parameters measured by the drive and transferred over a wireless network for analysis.
- Results from baseline test 1 and 2 shows that the test with systems is reliable and repeatable and when the results deviate it can definitively be said that the deviations are caused by external factors i.e. misaligned shaft.

- From the above tests, when a mechanical fault is introduced the signals gathered by the remote condition monitoring system from the inverter provide sufficient information to differentiate between the test rig healthy status and the presence of a mechanical fault as shown on Figure 7-30.

- The results in the above test were captured and analysed using low sampling frequency i.e. a reading every second; this means that only a time-domain visualisation could be carried out, the difference between healthy and faulty status could still be clearly established. The computer running the SCADA software can be programmed to acquired data at much faster rate and/or on change because computers have more storage capacity that PLC; this means that techniques such as MCSA could be used to analyse the data. If the SCADA system is already part of an automation system, there will be no added cost for implementing this technique but the software for detecting faults will be more complex.

- Although the test rig inverter has many signals that can be monitored and analysed, it is difficult to do this with the single analogue output on the inverter. The used of profibus communication card on the inverter allows more data to be monitored by the system.

- The Siemens S7-200 PLC controlling the inverter was well capable of communicating with the inverter profibus card. This could have been achieved by adding an S7-200 communication card. I decided not to modify the existing code so that the system remains unchanged and the S7-1200 PLC has more flexibility in terms of data acquisition with a faster processor.

- As shown in this research modern automation systems are well suited for remote condition monitoring. The parameters which can be monitored are not limited to vibration alone. Temperature, speed, pressure and airflow can all be monitored in applications where changes would indicate a problem.

- Over the past decades, a lot emphasis have but put on vibration analysis which although over the year have proven to be very effective means of fault detection on induction machines is very expensive as additional sensors have to be mounted on the machine, the signals from the sensors have to be acquired, processed and analysed by specific hardware and software. Adding to the training of user, additional equipment to maintain and the intrusion on the machine. This research shows that induction machine power supply parameter read by an inverter controlling the machine could be used for condition monitoring and that remote condition monitoring could be applied to standard automation equipment.

8.3 Contributions

The main focus of this research is to achieve remote condition monitoring and fault diagnosis of an induction motor by using an intelligent device which forms part of the machine control system to extract parameters from an inverter and transfer the parameters to a SCADA and/or PLC remotely by means of wireless communication and allowing the possibility of the parameters on the Site PC to be access remotely by other devices via a VPN tunnel or an equivalent.
The contributions of this research can be summarised as follows:

- Extensive survey of existing condition monitoring techniques, remote condition monitoring using wireless sensors
- Review of remote communications for condition monitoring and network security
- Understanding of induction motor operation principles
- Using PLC and SCADA system for remote condition monitoring by communication on industrial Ethernet.
- Analysis of inverter feedback parameter using mathlab.
- The use of inverters to control induction motors is rapidly increasing for energy saving reasons and control reasons. Traditional condition monitoring techniques might not be suitable for all applications because of the cost or installation difficulties, the method used in this research is a cost effective alternative for non-intrusive remote condition monitoring and it is hoped that more research will be done in this area in future to make this method more effective and automated.

8.4 Future work

Current and torque production of an induction motor is affected by its temperature and the operating ambient temperature, when run cold a motor has a higher current and torque and this slowly decreases when it reaches its normal operating temperature range. When using current or torque for condition monitoring, it is possible to get false detection if data is monitored when the machine starts up after a long stop so more research should be carried out on how to estimate or measure the temperature of the motor temperature using drive control parameters. A lot of drive manufacturers already use temperature estimation in the drive control loops or overload protection; future researchers could talk to drive manufacturers to see how this information can be extracted from the drive to enhance the reliability of the condition monitoring systems.
Further research will be conducted to fully automated non-intrusive and cost effective condition monitoring such that the control PLC or the SCADA can handle, the model generation, all the decision making, send email and/or text message to alert maintenance. Siemens PLC could be used with the powerful SCL programming to generate a model of the induction motor for condition monitoring purpose, this will allow the PLC to detect faults on the motor and send alarms to a SCADA system. With such system the machine will have two modes of operations all selectable by the user on the HMI:

- A machine learning mode in which parameters are read from the drive and stored in a specific data block in the PLC and are used to generate a model of the system. The model generation can be done at the end of the learning mode by pressing a button on the HMI.

- A normal operation mode in which parameters from the drive are stored in a different data block where an online comparison will be performed by the PLC to detect any abnormalities and inform the operator or maintenance personnel.

References

[1] B. Martin, “Mechanical Signature Analysis,” School of Mechanical Engineering Lecture Notes, University of Adelaide, 2003.

[2] T. NARUKA, “MULTI SENSOR DATA FUSION BASED CONDITION MONITORING OF INDUCTION MOTOR,” Department of Electrical and Instrumentation Engineering Thapar University, Patiala, 147004, Punjab, India, July 2012.

[3] W. T. a. R. Gilmore, “Motor current signature analysis to detect faults in induction motor derives-Fundamentals, data interpretation, and industrial case histories,” Proceedings of 32nd Turbomachinery symposium A&M university, Texas, US, 2003.

[4] R. D. Neelam Mehla, “An Approach of Condition Monitoring of Induction Motor Using MCSA,” *INTERNATIONAL JOURNAL OF SYSTEMS APPLICATIONS, ENGINEERING & DEVELOPMENT,* vol. 1, no. 1, 2007.

[5] T. H. F. K. y. R. B. R. Schoen, “Motor bearing damage detection using stator current monitoring,” *IEEE Trans Industrial. Application,* vol. 31, no. 6, pp. 1274-1279, 1995.

[6] “Wavelet Transforms in MATLAB,” [Online]. Available: http://www.mathworks.co.uk/discovery/wavelet-transforms.html. [Accessed 10 8 2013].

[7] S. B. a. M. S. B. Hocine Bendjama, “Application of Wavelet Transform for Fault Diagnosis in Rotating Machinery,” *International Journal of Machine Learning and Computing,* vol. 2, no. 1, February 2012.

[8] S. L. L. N. S. S. a. P. A. C. Laughman, “Park Transform-Based Method for Condition Monitoring of 3-Phase Electromechanical Systems,” Mitsubishi Electric Research Laboratories , May 2010.

[9] S. L. HARLIŞCA Ciprian, “Wavelet Analysis and Park's Vector Based Condition Monitoring of Induction Machines,” *Journal of Computer Science and Control Systems.*

[10] I. Y. Ö. a. M. E. H. Benbouzid, “Induction Motors Bearing Failures Detection Using a RBF ANN Park Pattern Based Method,” *International Review of Electrical Engineering,* vol. 3, no. 1, pp. 59-165, 2008.

[11] H. R. H. M. B. W. Z. R. Chaari F., “Modelling of AM and FM phenomena in gear pair under non-stationary cyclic load variation,” *CM2009/ MFTP 2009, The Sixth International Conference on Condition Monitoring and Machinery Failure Prevention Technologies DUBLIN, IRLEAND,* June 2009.

[12] W.-J. L. a. C. K. Suratsavadee K. Korkua, “Design and Implementation of ZigBee based Vibration Monitoring and Analysis for Electri-cal Machines,” Energy Systems Research Center, The University of Texas at Arlington, Arlington, TX 76019.

[13] “ IEEE standard test procedure for polyphase induction motors and generators, IEEE Standard 112, November 2004.”.

[14] “ERIKS INDUCTION MOTOR: Energy Efficiency Replacement Charts and Report,” ERIKS UK,

2008.

[15] R. M. A. Drives, “TORQUE PRODUCTION WITH AC DRIVES AND MOTORS:UNDERSTANDING THE TECHNOLOGY,” Marketing Manager Rockwell Automation / Reliance Electric, Euclid, OH 44117.

[16] P. M. a. J. H. Lang, “Monitoring the thermal condition of permanent-magnet,” *EEE Transactions on Aerospace and Electronic Systems,* vol. 32, no. 4, pp. 1421-1429, 1996.

[17] J. S. Hsu, “Monitoring of defects in induction motors through air-gap torque observation,” *IEEE Transactions on Industry Applications,* vol. 31, no. 5, pp. 1016-1021, 1995.

[18] S. J. Y. A. J. Ellison, “Effect of rotor eccentricity on acoustic noise from induction machines,” *Proceedings Electric Power Applications,* vol. 143, no. 3, pp. 202-210, May 1996.

[19] H. D. J. Nelson Baxter, “Remote Machine Monitoring: A Developing Industry,” White Paper , June 2006.

[20] P. W. A. M. S. S. B. S. K. H. S. S. P. Luca Lachello, “System Comparison: The 5 major technologies,” *Industrial Ethernet Facts,* vol. 2, no. 2, pp. 6-7, February 2013.

[21] A. X. Y. S. W. Z. M. L. Y. Zheng, “Industrial wireless deterministic communication based on WLAN: design, implementation and analysis, Communications Technology and Applications,” ISBN: 978-1-4244-4816-6, 2009, p. 274 – 278.

[22] *ZigBee Alliance, “ZigBee specification”, 2007.*

[23] “Wireless Security Setup on WAP4410N Wireless-N Access Points,” [Online]. Available: http://sbkb.cisco.com. [Accessed 24 June 2013].

[24] B. Bowers, “ZigBee Wireless Security: A New Age Penetration Tester's Toolkit,” 9 January 2012. [Online]. Available: http://www.ciscopress.com/articles/article.asp?p=1823368&seqNum=4. [Accessed 23 June 2013].

[25] M. D. J. S. J. A. A. T. S. P. S. C. Pedram Radmand¹, “ZigBee/ZigBee PRO security assessment based on compromised cryptographic keys,” ¹Digital Ecosystem and Business intelligence Institute, Curtin University of Technology, Perth, Australia. ²Estudis d’Inform`atica, Multim`edia i Telecomunicaci´o, UOC, Barcelona, Spain. ³SINTEF ICT, Trondheim, Norway. 4StatoilASA; Trondheim;Norway.

[26] [Online]. Available: http://isc.dcc.ttu.ee/Public/Kuphaldt/AC/AC_13.html. [Accessed 12 March 2012].

[27] “SEW Euro-drive AC Motors DR/DV/DT/DTE/DVE, Asynchronous Servo Motors CT/CV Edition 11/2007 16656938”.

[28] W. S. a. N. E. M.L. Sin, “INDUCTION MACHINE ON-LINE CONDITION MONITORING AND FAULT DIAGNOSIS – A SURVEY,” University of Adelaide .

[29] “Traditional Electromechanical Motor Starters.,” [Online]. Available: http://www.lmphotonics.com/m_start.htm. [Accessed 02 Jully 2013].

[30] R. Parekh, “AN887 AC Induction Motor Fundamentals,” Microchip Technology Inc., 2003.

[31] “Model induction motor powered by ideal AC supply,” Mathworks, [Online]. Available: http://www.mathworks.co.uk/help/physmod/elec/ref/inductionmotor.html. [Accessed 22 June 2013].

[32] T. .. F. C. Y. K. W. a. S. L. .. H. K. L . Shi, “Modeling and simulation of the three-phase induction motor using simulink,” *International Journal of Electrical Engineering Education,* vol. 36, p. 163–172, 1999.

[33] P. S. Jaroslav Lepka, “3-Phase AC Induction Motor Vector Control Using a 56F80x, 56F8100 or 56F8300 Device Rev. 2,” Freescale Semiconductor, 2005.

[34] G. F. a. C. T. F. Filippetti, “AI techniques in induction machines diagnosis including the speed ripple effect,” *IEEE Transactions on Industry Applications,* vol. 34, no. 1, pp. 98-108, 1998.

[35] F. F. G. F. C. T. A. Bellini, “Quantitative evaluation of induction motor broken bars by means of electrical signature analysis,” *IEEE Transactions on Industry Applications,* vol. 37, no. 5, pp. 1248-1255, 2001.

[36] H. T. G. a. T. R. M. Obaid R R, “Detecting load unbalance and shaft misalignment using stator current in inverter-driven induction motors,” *IEEE International Electric Machines & Drives Conference,* pp. 1454-1458, 2003..

[37] “Drives energy efficiency portal,” ABB, [Online]. Available: http://www.abb.com. [Accessed 02 07 2013].

[38] “A REVIEW ON OPTIMIZATION OF ENERGY BY USING PWM INVERTER,” *ISSN: 2278 – 1323 International Journal of Advanced Research in Computer Engineering & Technology (IJARCET),* vol. 2, no. 1, January 2013.

[39] F. W. F. Malte Mohr, “Comparison of Three Phase Current Source Inverters and Voltage Source Inverters Linked with DC to DC Boost Converters for Fuel Cell Generation Systems,” Christian-Albrechts-University of Kiel, Kaiserstr. 2, 24143 Kiel, Germany.

[40] “Allen-Bradley PowerFlex 7000 Frame B Technical Data Guide, 7000-TD2008-EN-P,” 2003.

[41] “www.mathworks.co.uk/help/physmod/powersys/ref/sixstepvsiinductionmotordrive.html,” 22/06/2013.

[42] D. CLENET, “Cahier technique no. 208 Electronic starters and variable speed drives,” Schneider Electric ECT 208 first issue November 2003.

[43] M. L. M. M. O. S. a. M. B. M. Hornkamp, “EconoMAC the first all-in-one IGBT module for matrix converters,” *in Proc. IPEC, Nuremberg,* p. 417–421, Jun 2001.

[44] F. M. I. /. SIMATIC, “Functions SINAMICS G120, SINAMICS G120D, SIMATIC ET 200S FC, SIMATIC ET 200 pro FC,” Edition 06/2007, Software version V3.0.

[45] P. Vas., “ Sensorless Vector and Direct Torque Control,” Oxford University press, Oxford, 1998.

[46] A. K. K. M. K. Rajashekara, “Sensorless Control of AC Motor Drives-Speed and Position

Sensorless Operation," IEEE Press, New York, 1996.

[47] C. Schauder, "Adaptive speed identification for vector control of induction motors without rotational transducers," *IEEE Transactions on Industry Applications,* vol. 28, no. 5, pp. 1054-1061, September/October 1992.

[48] M. T. S. Chen, "A sensorless vector control system of induction motors based on flux observer," *Transactions of China Electrotechnica,* vol. 16, no. 4, pp. 30-33, 2001.

[49] O. T. Samir Moulahoum, "Sensorless Vector Controlled Induction Machine in Field Weakening Region: Comparing MRAS and ANN-Based Speed Estimators," *Journal of Electrical Engineering & Technology,* vol. 2, no. 2, pp. 241-248, 2007.

[50] M. I. D. G. M. I. a. J. F. S. M. I. S. M. Gadoue, "MRAS Sensorless Vector Control of an Induction Motor Using New Sliding Mode and Fuzzy Logic Adaptation Mechanisms".

[51] M. I. D. G. M. I. a. J. F. S. M. I. S. M. Gadoue, "MRAS Sensorless Vector Control of an Induction Motor Using New Sliding Mode and Fuzzy Logic Adaptation Mechanisms".

[52] "Control Technologies Manual PWM AC Drives Revision 1.0".

[53] T. N. Takahashi, "A new quick-response and high-efficiency control strategy of induction motor," *IEEE Trans. On IA,* vol. 22, no. 5, pp. 820-827, September/October 1986.

[54] "ABB Drives Technical guide No. 1 Direct torque control - the world's most advanced AC drive technology".

[55] Drives and servos yearbook 1990-1, Newton: Control Techniques plc, Newton, Powys., 1990.

[56] 650V AC Drive Frame C, D, E & F Installation Product Manual HA467652U002 Issue 7..

[57] "Profibus-DP Communications Interface Technical Manual HA469761U001 Issue 4," Parker Hannifin Ltd, 2010.

[58] SIMATIC S7-1200 Easy Book, Siemens, 04/2012.

[59] "Process Data Acquisition and Monitoring with SIMATIC S7-1200 (Data Logging)," Siemens, [Online]. Available: https://support.automation.siemens.com. [Accessed 02 06 2013].

[60] G. D. D. M. R. S. S. K. VENKATA SIVARAO, "Determination of Misalignment Using Motor Current Signature analysis In Rotating Machine," *International Journal of Engineering Research & Technology (IJERT) ISSN: 2278-0181,* vol. 1, no. 8, Octoober 2012.

[61] M. C. a. D.-I. H. Sammoud, "Sensorless Field Oriented Control (FOC) of an AC Induction Motor (ACIM) Using Field Weakening," Microchip Technology Inc., 2008.

[62] "650V AC Drive Frames 1, 2, 3, C, D, E & F Software Product Manual HA466358U001 Issue 4," SSD Drives Limited, 2005.

[63] M. B. a. I. V. Nikiforov, "Detection of Abrupt Changes: Theory and Application," Information and System Science, Prentice Hall, New York, 1993.

[64] M. Lane, “Using the AC Drive Motor as a Transducer for Detecting Electrical and Electromechanical Faults,” University of Huddersfield, School of Computing and Engineering, Huddersfield, January 2011.

Appendix A. Test Rig AC drive Software

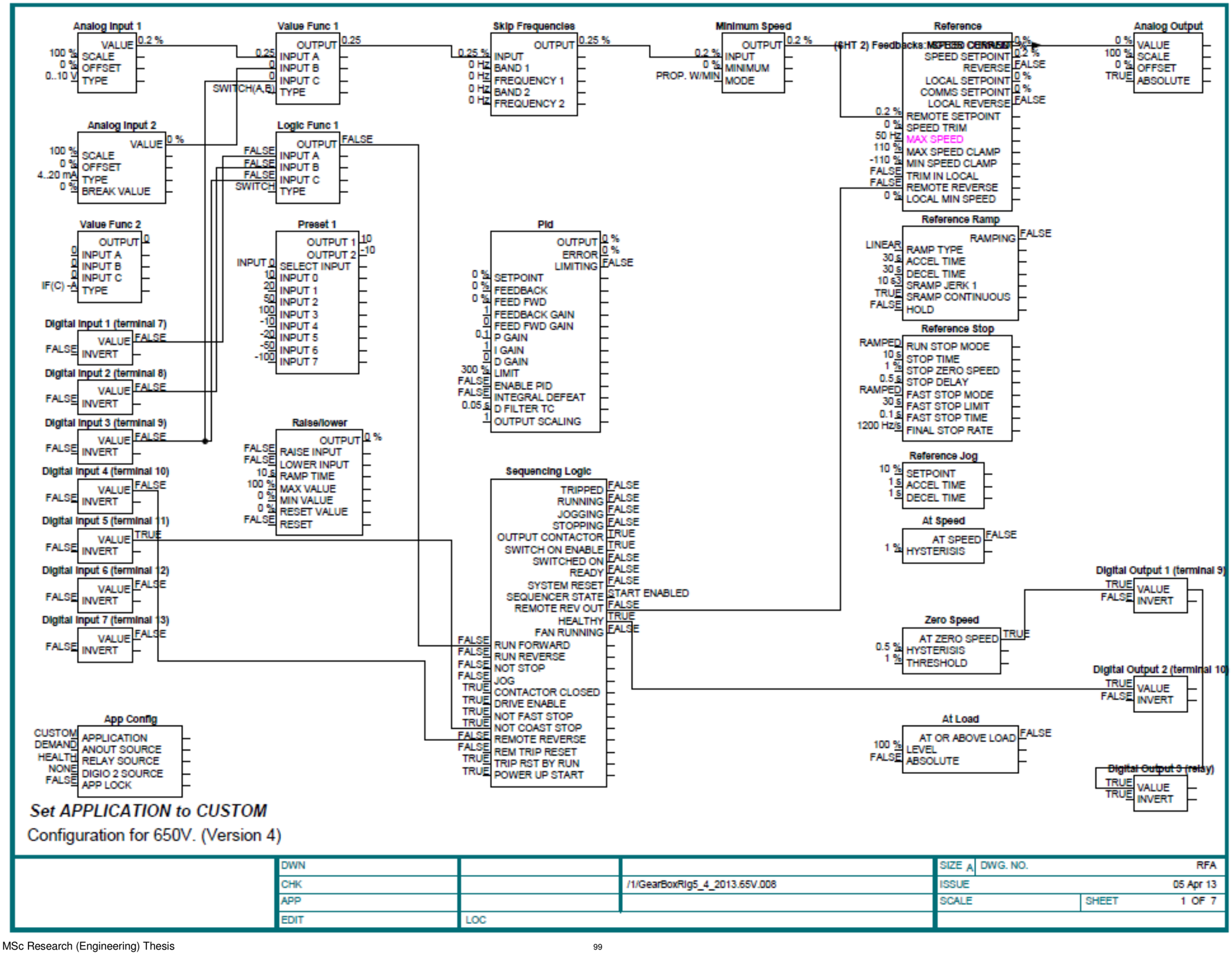
Analog Input 1
VALUE 0.2 %
100 % SCALE
0 % OFFSET
0..10 V TYPE
Value Func 1
OUTPUT 0.25
0.25 INPUT A
0 INPUT B
0 INPUT C
SWITCH(A,B) TYPE
Skip Frequencies
OUTPUT 0.25 %
0.25 % INPUT
0 Hz BAND 1
0 Hz FREQUENCY 1
0 Hz BAND 2
0 Hz FREQUENCY 2
Minimum Speed
OUTPUT 0.2 %
0.2 % INPUT
0 % MINIMUM
PROP. W/MIN MODE
Reference
(SHT 2) Feedbacks: SPEED SETPOINT 0 %
REVERSE 0.2 %
LOCAL SETPOINT FALSE
COMMS SETPOINT 0 %
LOCAL REVERSE FALSE
0.2 % REMOTE SETPOINT
0 % SPEED TRIM
50 Hz MAX SPEED
110 % MAX SPEED CLAMP
-110 % MIN SPEED CLAMP
FALSE TRIM IN LOCAL
FALSE REMOTE REVERSE
0 % LOCAL MIN SPEED
Analog Output
0 % VALUE
100 % SCALE
0 % OFFSET
TRUE ABSOLUTE
Analog Input 2
VALUE 0 %
100 % SCALE
0 % OFFSET
4..20 mA TYPE
0 % BREAK VALUE
Logic Func 1
OUTPUT FALSE
FALSE INPUT A
FALSE INPUT B
FALSE INPUT C
SWITCH TYPE
Value Func 2
OUTPUT 0
0 INPUT A
0 INPUT B
0 INPUT C
IF(C) -A TYPE
Preset 1
OUTPUT 1 10
OUTPUT 2 -10
INPUT 0 SELECT INPUT
10 INPUT 0
20 INPUT 1
50 INPUT 2
100 INPUT 3
-10 INPUT 4
-20 INPUT 5
-50 INPUT 6
-100 INPUT 7
Pid
OUTPUT 0 %
ERROR 0 %
LIMITING FALSE
0 % SETPOINT
0 % FEEDBACK
0 % FEED FWD
1 FEEDBACK GAIN
0 FEED FWD GAIN
0.1 P GAIN
1 I GAIN
0 D GAIN
300 % LIMIT
FALSE ENABLE PID
FALSE INTEGRAL DEFEAT
0.05 s D FILTER TC
1 OUTPUT SCALING
Reference Ramp
RAMPING FALSE
LINEAR RAMP TYPE
30 s ACCEL TIME
30 s DECEL TIME
10 s3 SRAMP JERK 1
TRUE SRAMP CONTINUOUS
FALSE HOLD
Reference Stop
RAMPED RUN STOP MODE
10 s STOP TIME
1 % STOP ZERO SPEED
0.5 s STOP DELAY
RAMPED FAST STOP MODE
30 s FAST STOP LIMIT
0.1 s FAST STOP TIME
1200 Hz/s FINAL STOP RATE
Digital Input 1 (terminal 7)
VALUE FALSE
FALSE INVERT
Digital Input 2 (terminal 8)
VALUE FALSE
FALSE INVERT
Digital Input 3 (terminal 9)
VALUE FALSE
FALSE INVERT
Digital Input 4 (terminal 10)
VALUE FALSE
FALSE INVERT
Digital Input 5 (terminal 11)
VALUE TRUE
FALSE INVERT
Digital Input 6 (terminal 12)
VALUE FALSE
FALSE INVERT
Digital Input 7 (terminal 13)
VALUE FALSE
FALSE INVERT
Raise/lower
OUTPUT 0 %
FALSE RAISE INPUT
FALSE LOWER INPUT
10 s RAMP TIME
100 % MAX VALUE
0 % MIN VALUE
0 % RESET VALUE
FALSE RESET
Sequencing Logic
TRIPPED FALSE
RUNNING FALSE
JOGGING FALSE
STOPPING FALSE
OUTPUT CONTACTOR TRUE
SWITCH ON ENABLE TRUE
SWITCHED ON FALSE
READY FALSE
SYSTEM RESET FALSE
SEQUENCER STATE START ENABLED
REMOTE REV OUT FALSE
HEALTHY TRUE
FAN RUNNING FALSE
FALSE RUN FORWARD
FALSE RUN REVERSE
FALSE NOT STOP
FALSE JOG
TRUE CONTACTOR CLOSED
TRUE DRIVE ENABLE
TRUE NOT FAST STOP
TRUE NOT COAST STOP
FALSE REMOTE REVERSE
FALSE REM TRIP RESET
TRUE TRIP RST BY RUN
TRUE POWER UP START
Reference Jog
10 % SETPOINT
1 s ACCEL TIME
1 s DECEL TIME
At Speed
AT SPEED FALSE
1 % HYSTERISIS
Zero Speed
AT ZERO SPEED TRUE
0.5 % HYSTERISIS
1 % THRESHOLD
At Load
AT OR ABOVE LOAD FALSE
100 % LEVEL
FALSE ABSOLUTE
Digital Output 1 (terminal 9)
TRUE VALUE
FALSE INVERT
Digital Output 2 (terminal 10)
TRUE VALUE
FALSE INVERT
Digital Output 3 (relay)
TRUE VALUE
TRUE INVERT
App Config
CUSTOM APPLICATION
DEMAND ANOUT SOURCE
HEALTH RELAY SOURCE
NONE DIGIO 2 SOURCE
FALSE APP LOCK
Set APPLICATION to CUSTOM
Configuration for 650V. (Version 4)
DWN
CHK
APP
EDIT
LOC
/1/GearBoxRig5_4_2013.65V.008
SIZE A
DWG. NO.
RFA
ISSUE
05 Apr 13
SCALE
SHEET
1 OF 7

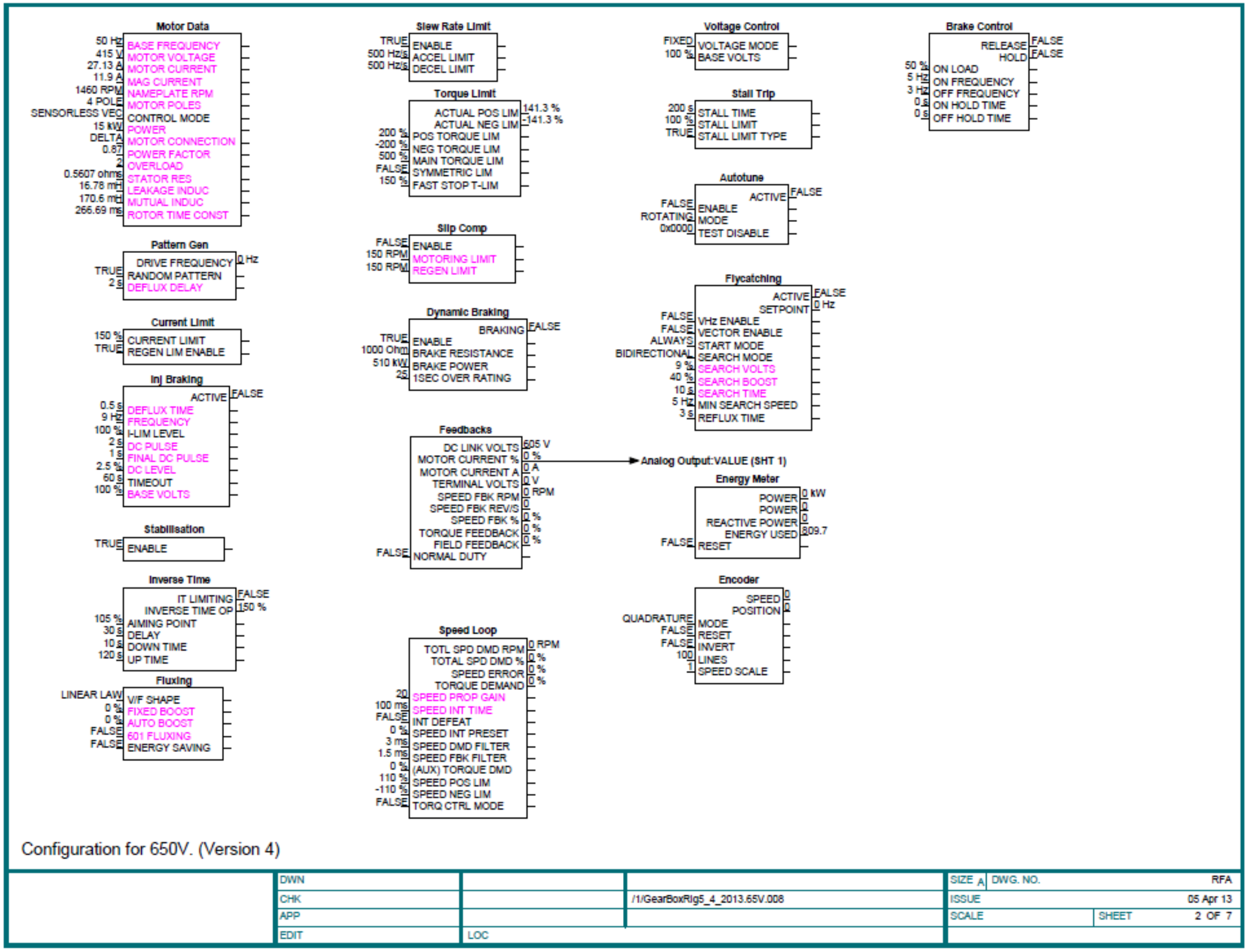

Configuration for 650V. (Version 4)

	DWN			SIZE A	DWG. NO. RFA
	CHK		/1/GearBoxRig5_4_2013.65V.008	ISSUE	05 Apr 13
	APP			SCALE	SHEET 2 OF 7
	EDIT	LOC			

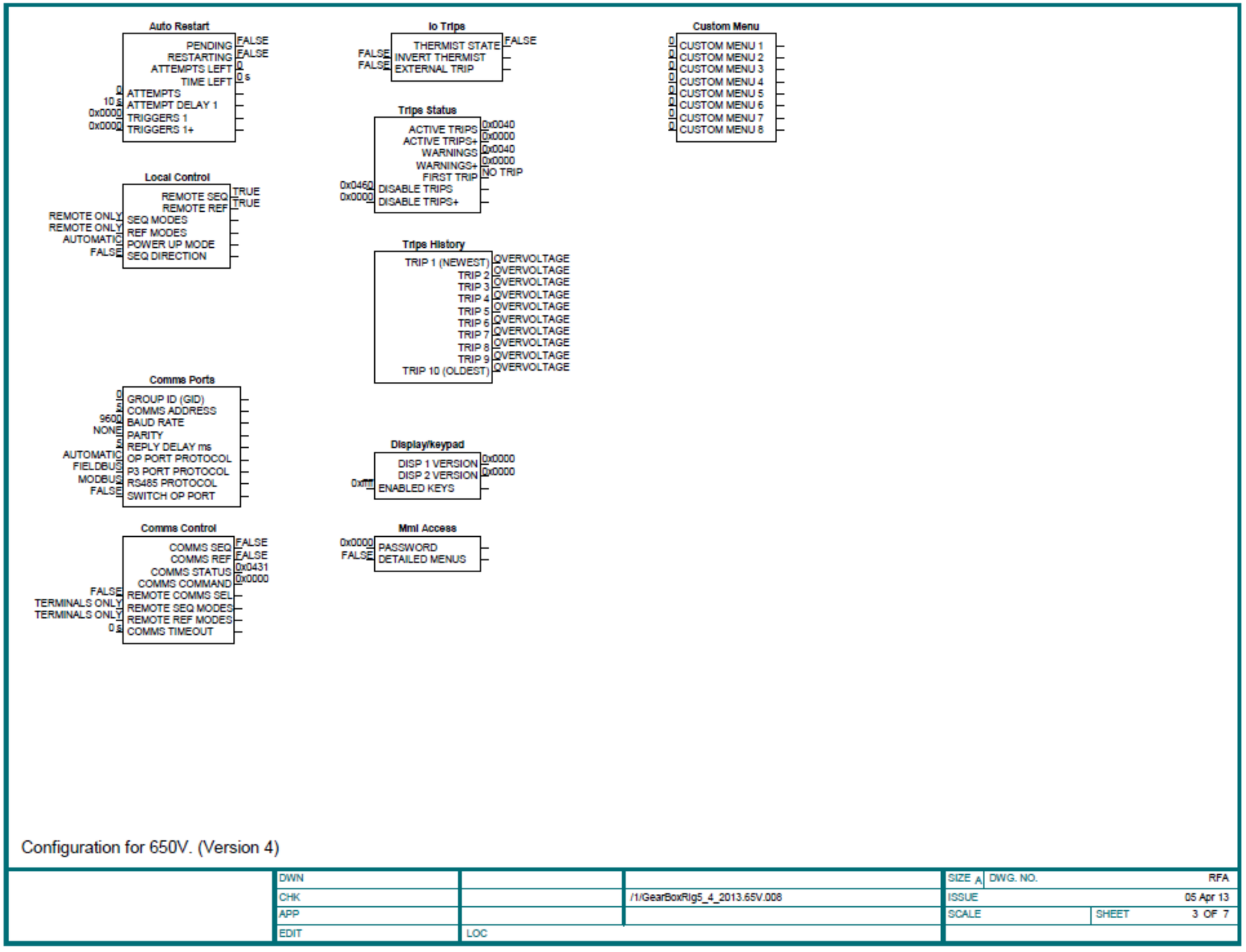

Configuration for 650V. (Version 4)

	DWN			SIZE A	DWG. NO. RFA
	CHK		/1/GearBoxRig5_4_2013.65V.008	ISSUE	05 Apr 13
	APP			SCALE	SHEET 3 OF 7
	EDIT	LOC			

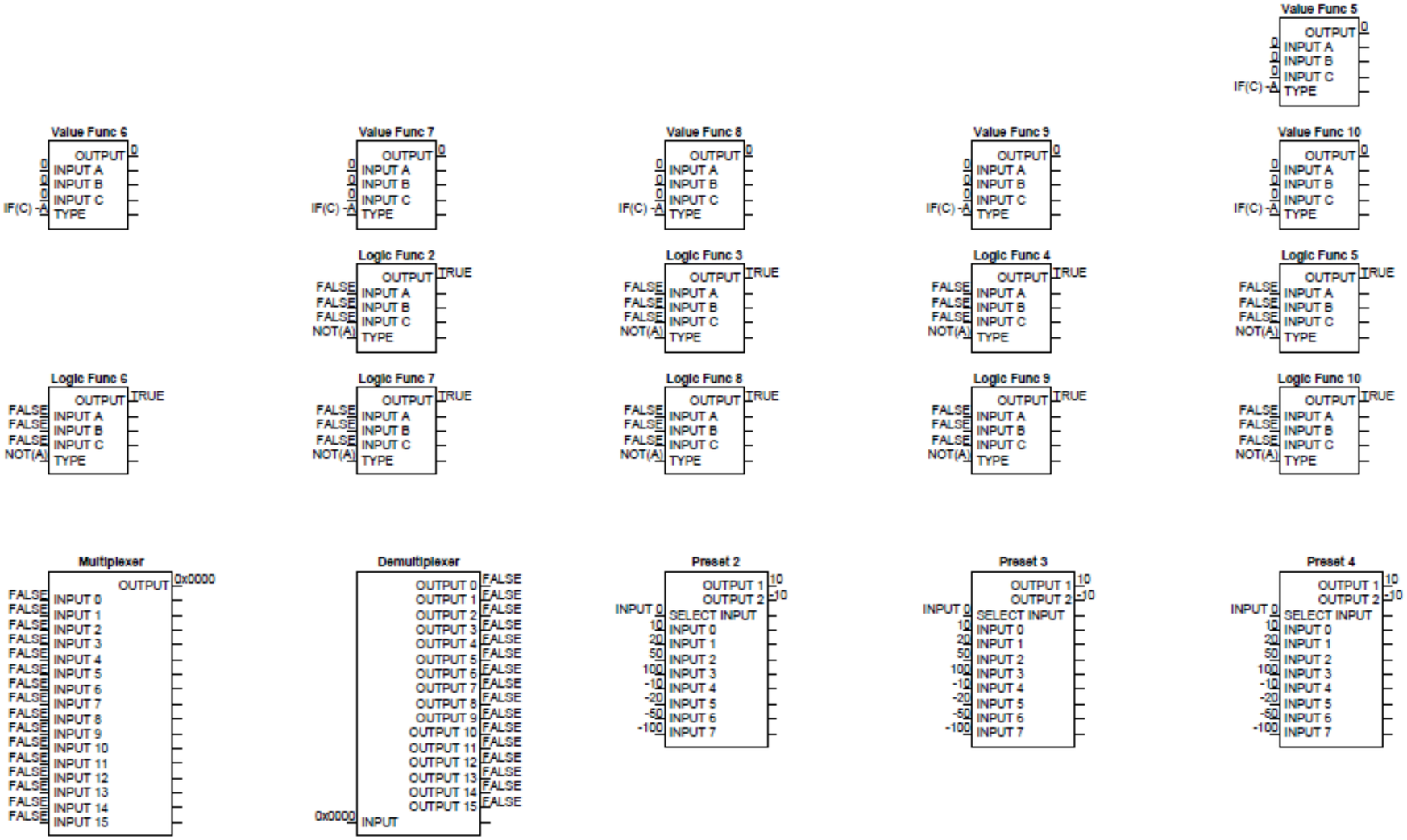

Configuration for 650V. (Version 4)

	DWN			SIZE A	DWG. NO. RFA
	CHK		/1/GearBoxRig5_4_2013.65V.008	ISSUE	05 Apr 13
	APP			SCALE	SHEET 4 OF 7
	EDIT	LOC			

Configuration for 650V. (Version 4)

	DWN			SIZE A	DWG. NO. RFA
	CHK		/1/GearBoxRig5_4_2013.65V.008	ISSUE	05 Apr 13
	APP			SCALE	SHEET 5 OF 7
	EDIT	LOC			

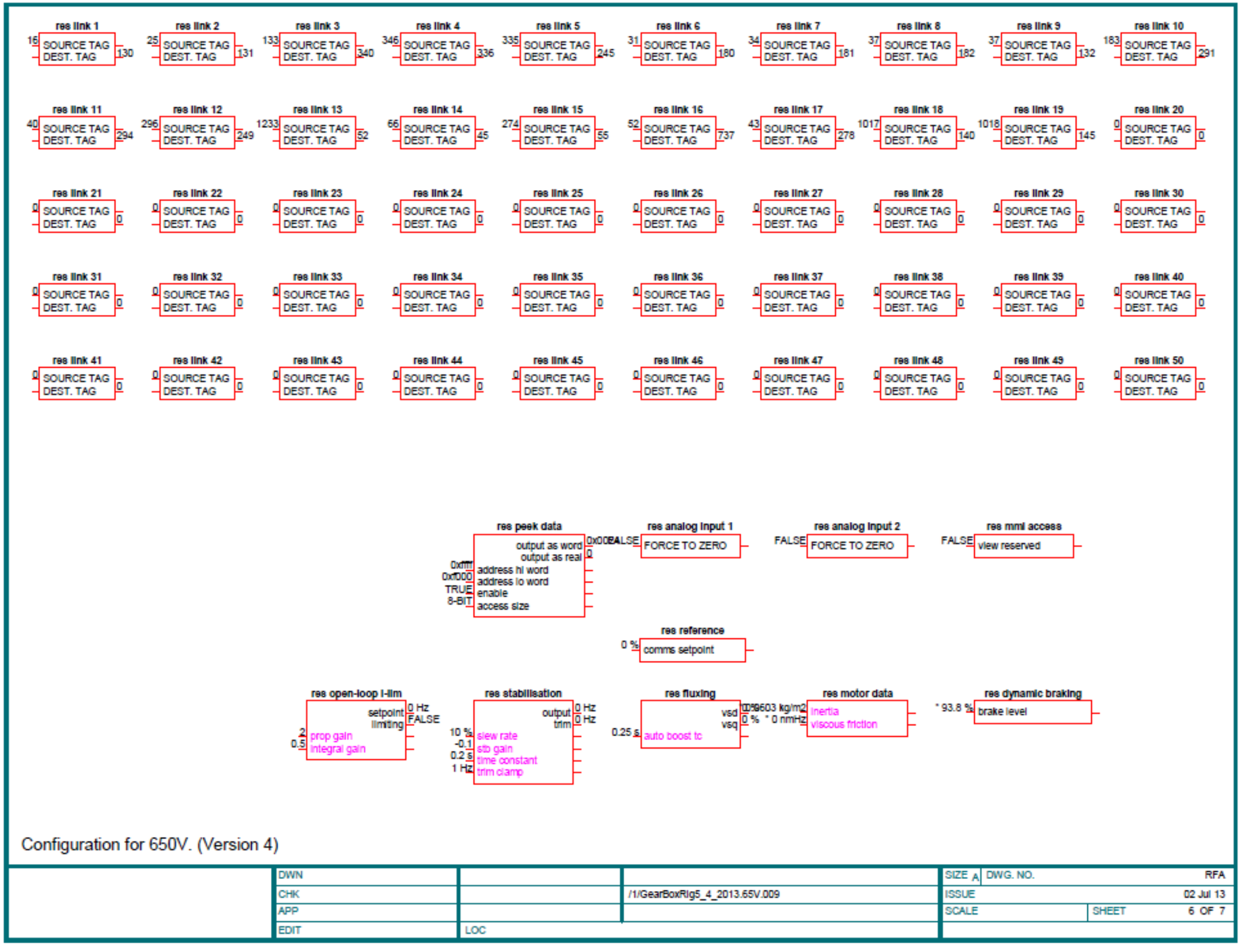

Configuration for 650V. (Version 4)

	DWN			SIZE A	DWG. NO. RFA
	CHK		/1/GearBoxRig5_4_2013.65V.009	ISSUE	02 Jul 13
	APP			SCALE	SHEET 6 OF 7
	EDIT	LOC			

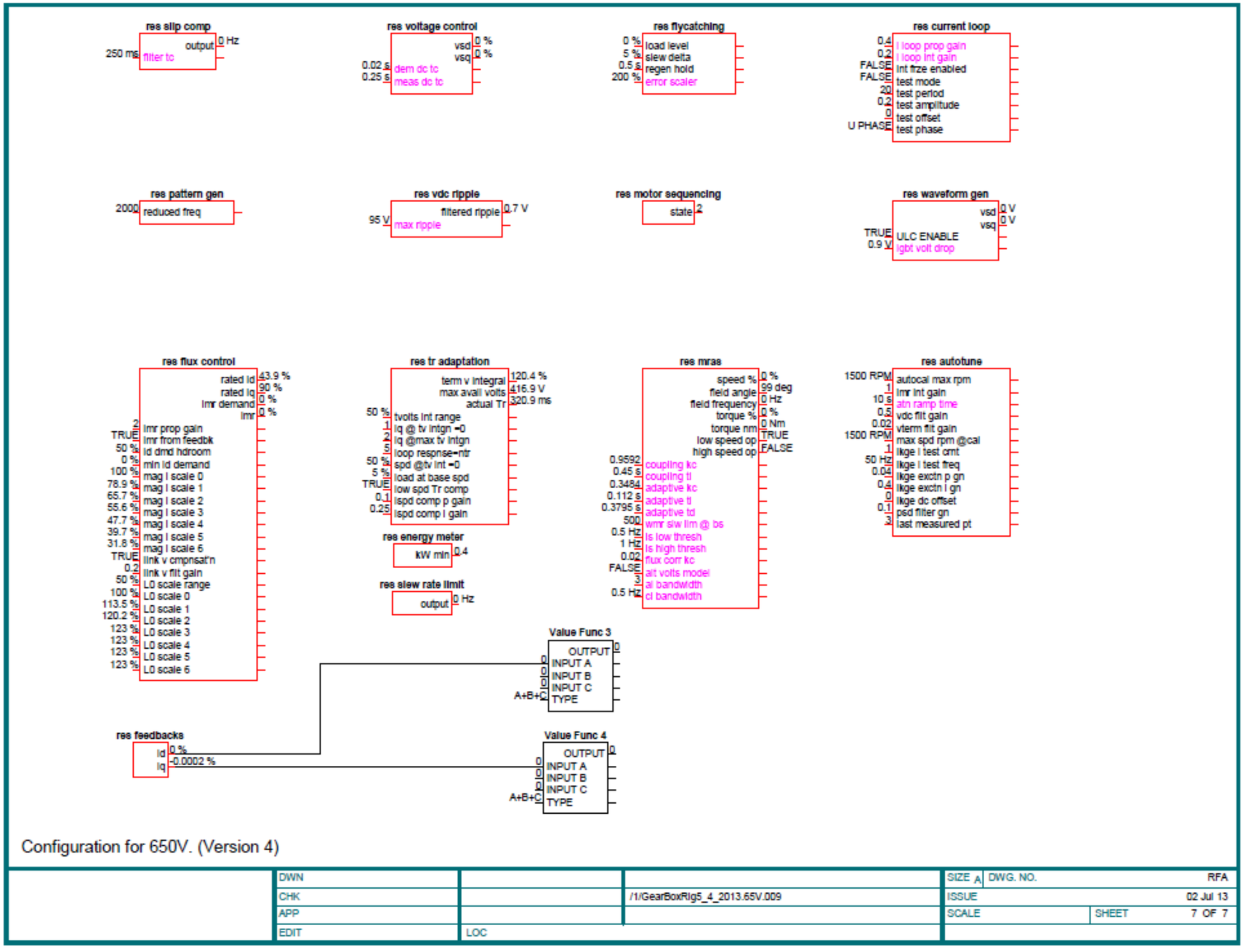

Configuration for 650V. (Version 4)

	DWN			SIZE A	DWG. NO. RFA
	CHK		/1/GearBoxRig5_4_2013.65V.009	ISSUE	02 Jul 13
	APP			SCALE	SHEET 7 OF 7
	EDIT	LOC			

Appendix B. Remote Condition Monitoring PLC Web Server

Remote Condition Monitoring PLC Web Server viewed on a PC

Figure 0-1: Welcome Page

This is the first page of the remote condition monitoring PLC web server, by pressing the **enter** button this will take us to the next page where the user can log into the PLC.

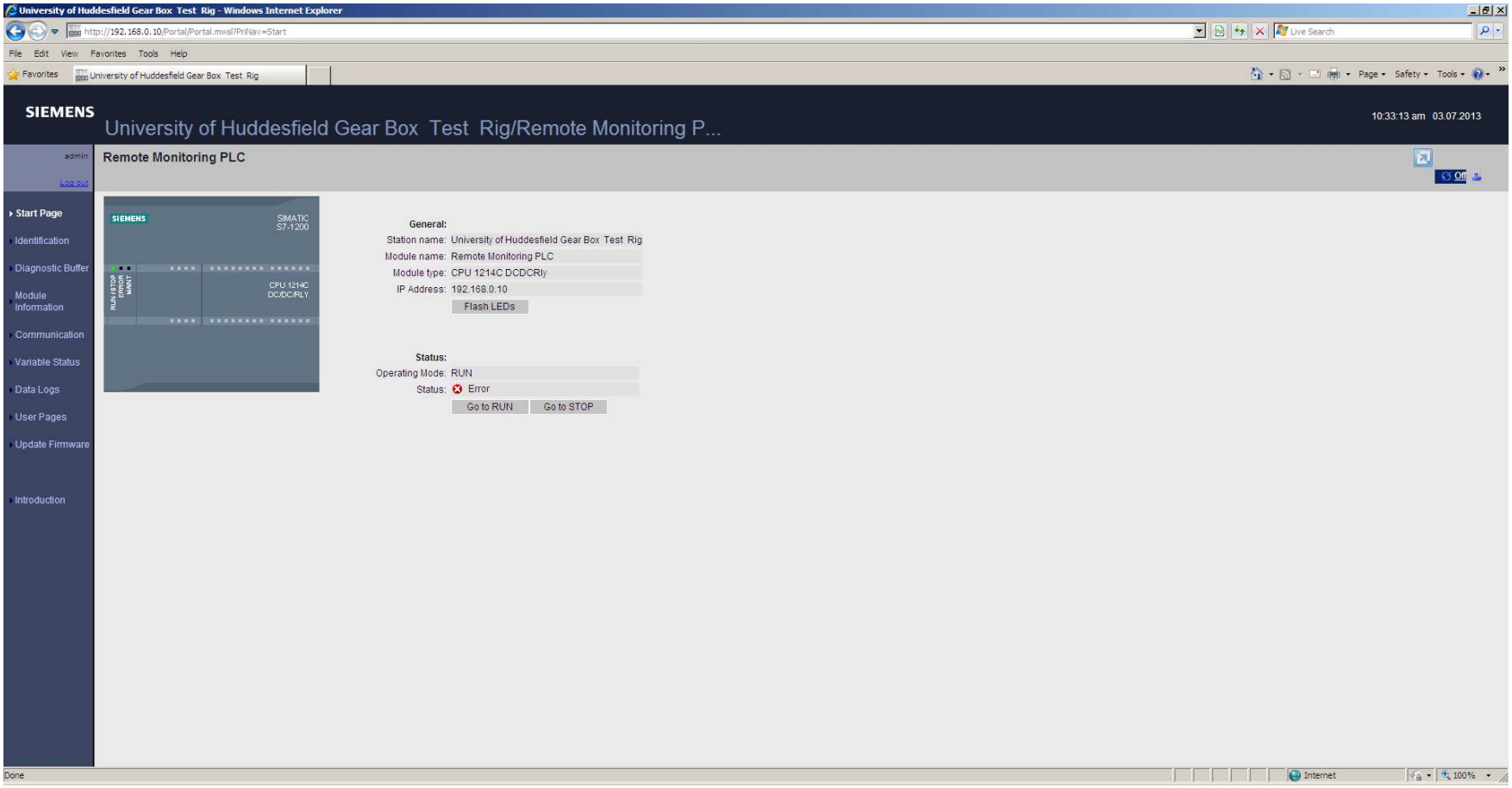

Figure 0-2: Start Page

This is the start page of the web server. Without logging on the user will still be able to navigate but very limited monitoring rights and no control rights. When logged in the user can stop the PLC from this page, put the PLC in run mode or flash the LEDs on the PLC to ensure that the PLC is operating and responding to commands.

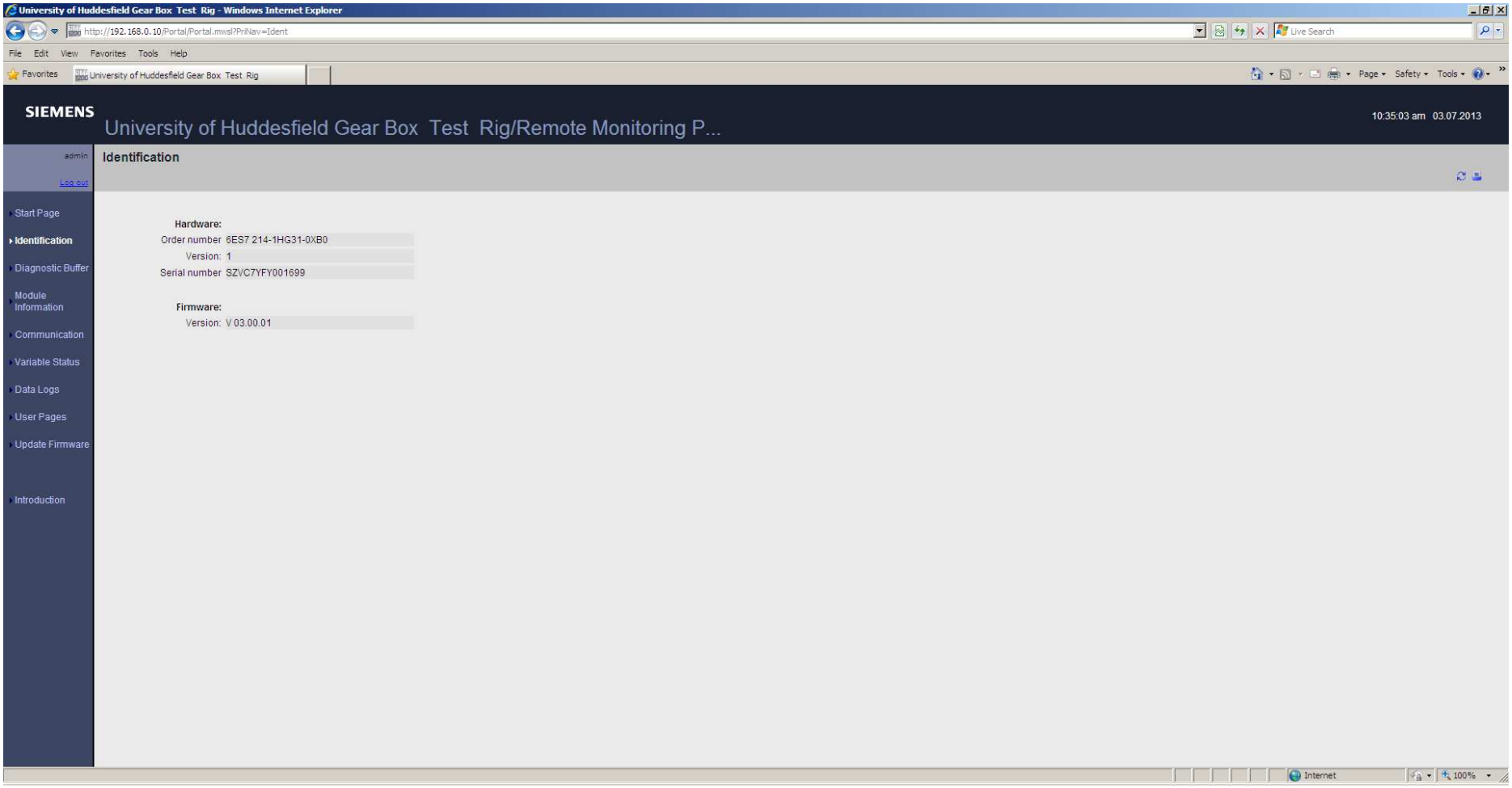

Figure 0-3: PLC Identification

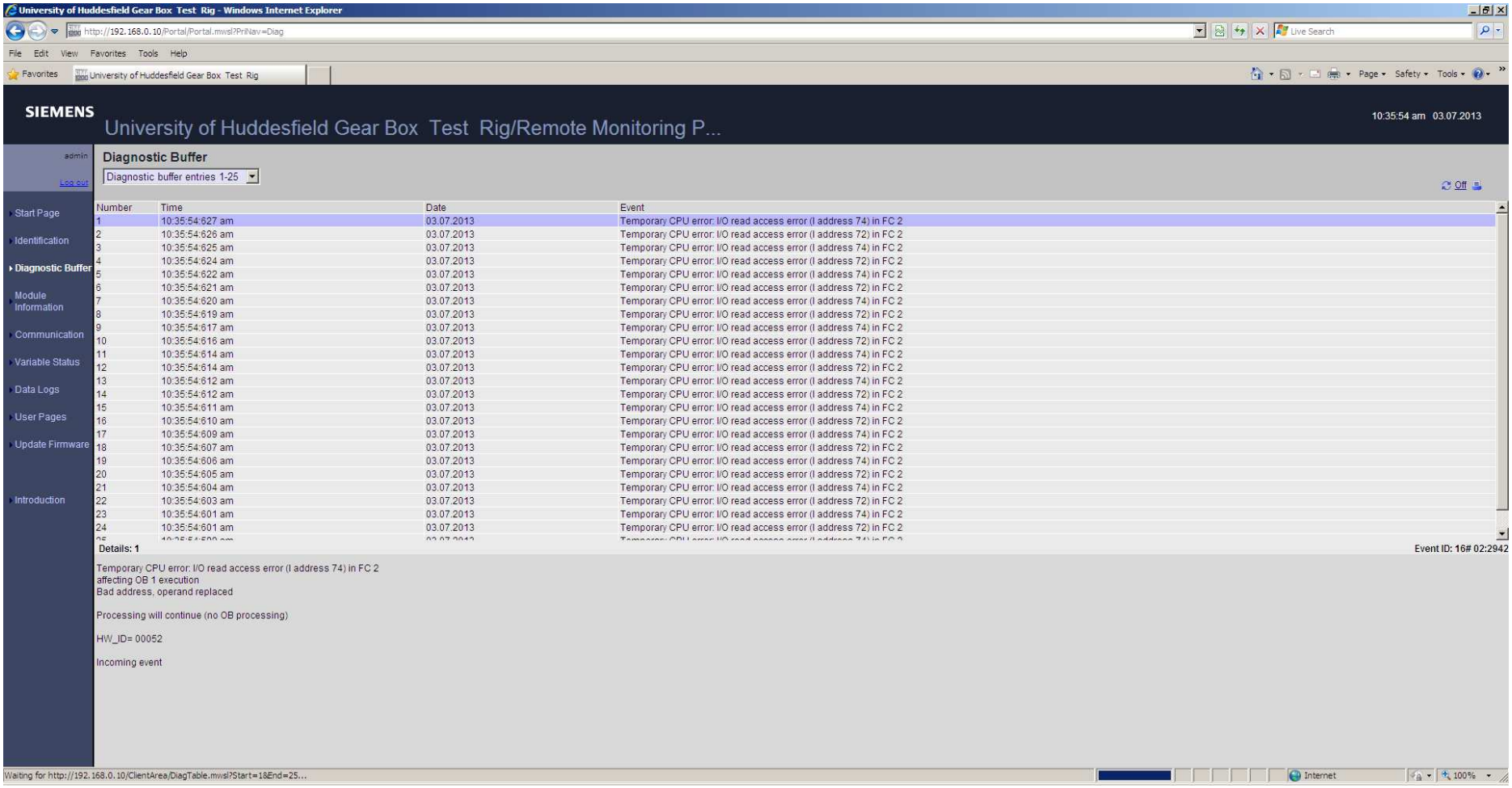

Figure 0-4: Diagnostic Buffer

This page gives a list of all alarms on the PLC.

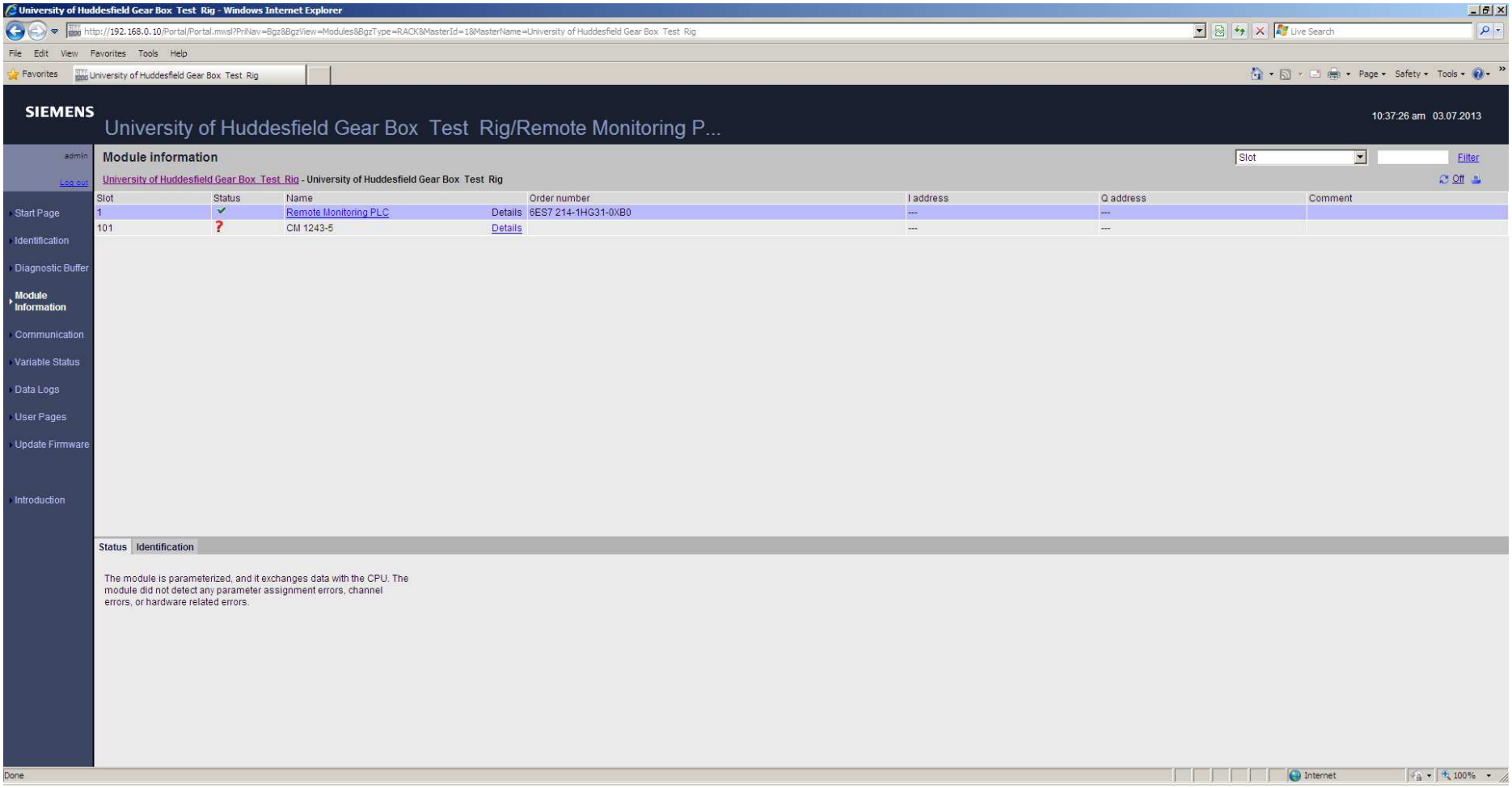

Figure 0-5: Module Information

This page lists all the different modules connected together to form this PLC including slot position on PLC rack, name and their status

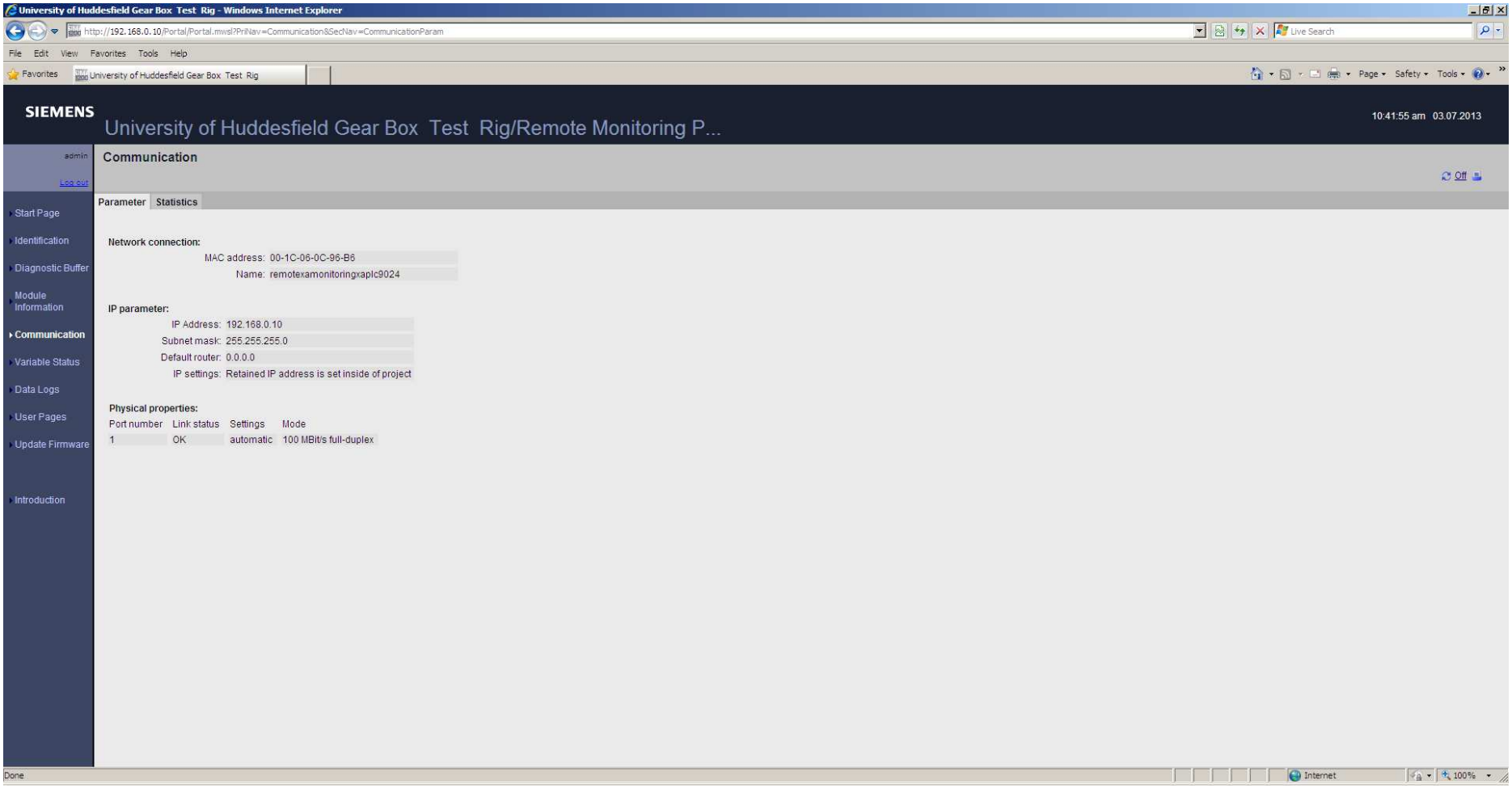

Figure 0-6: PLC Communication

This page contains the network communication details of the PLC.

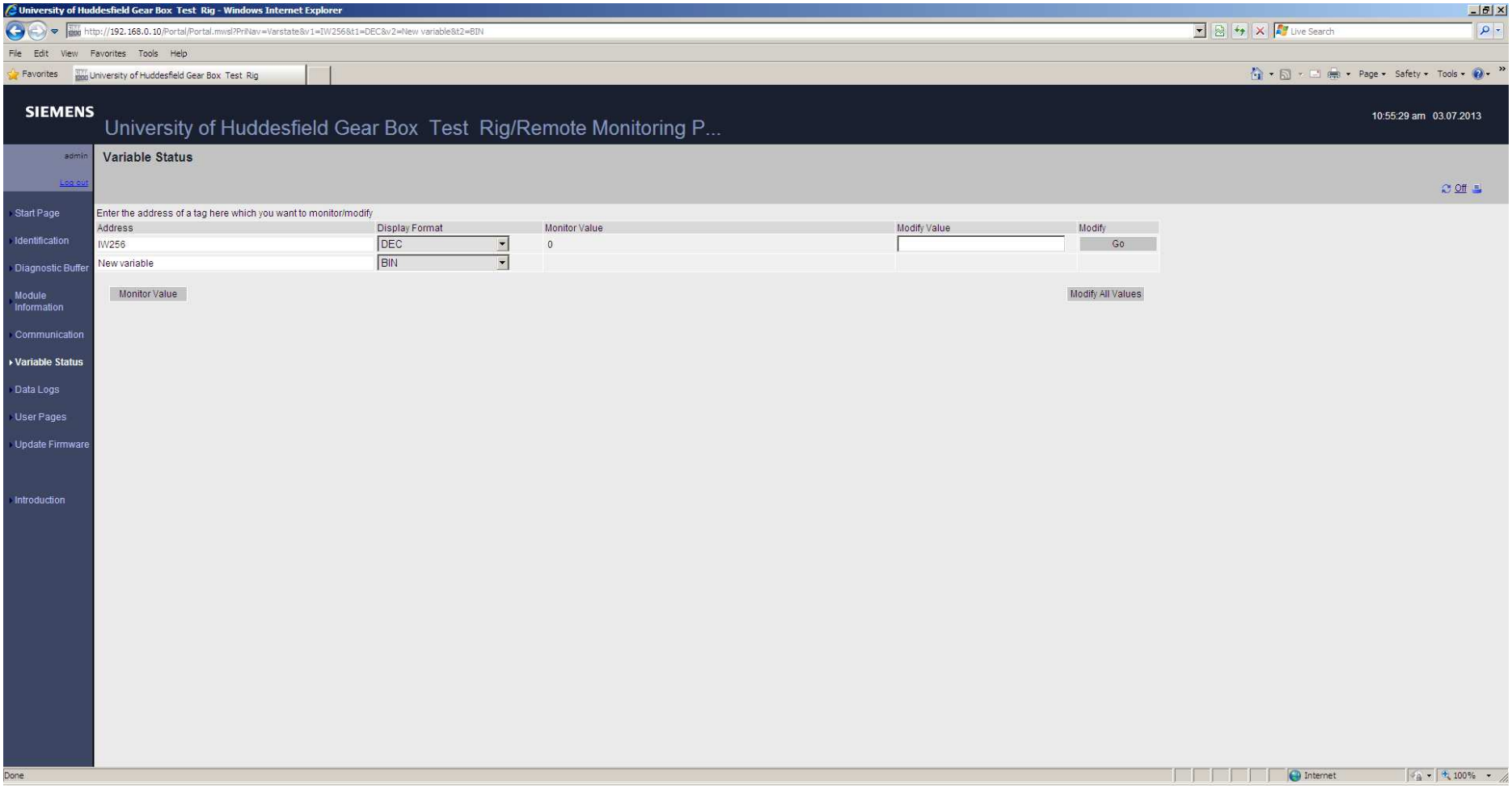

Figure 0-7: Variable Status

This page allows the user to monitor any variable in the PLC provided they have logged on.

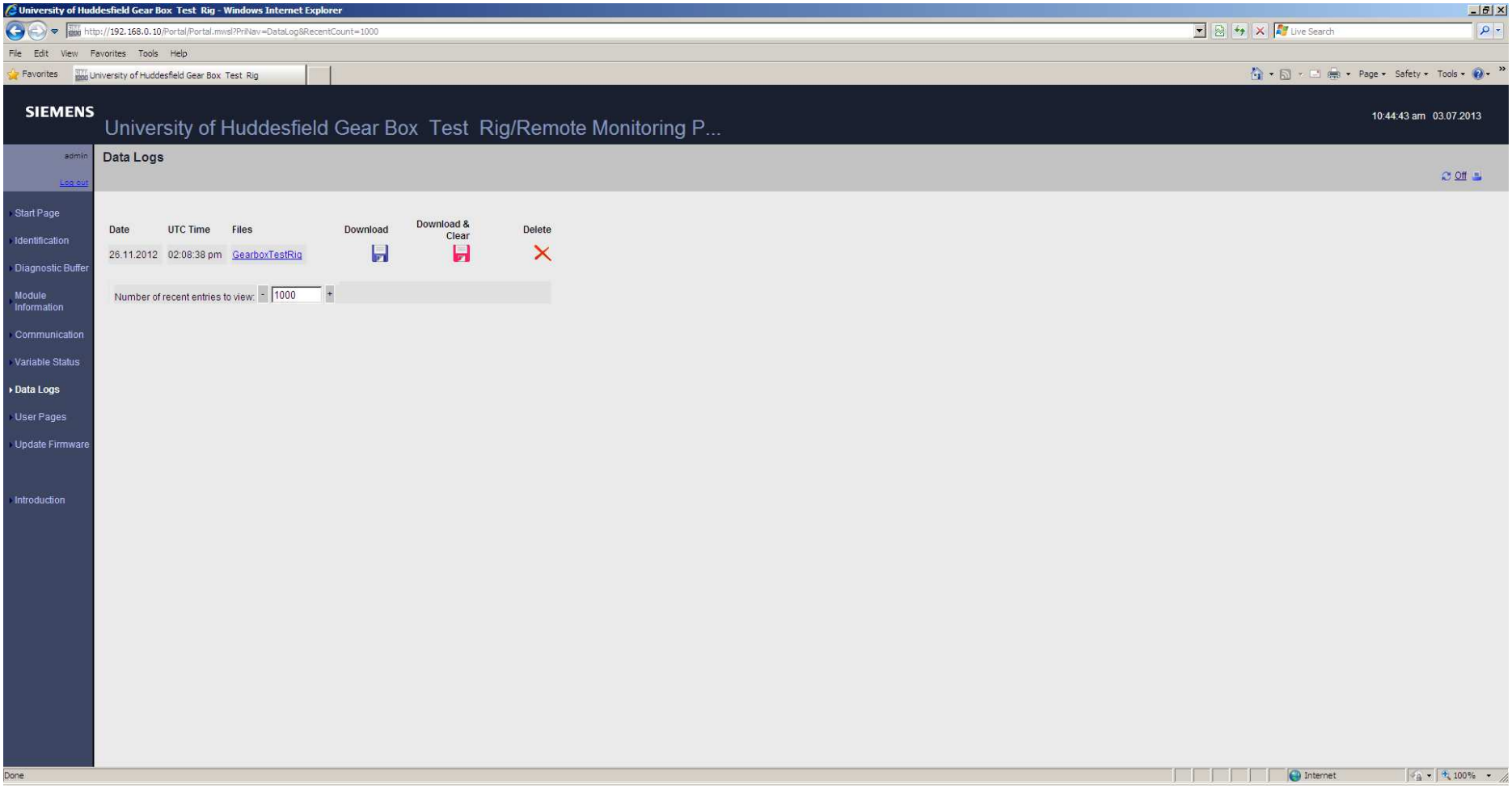

Figure 0-8: Data Logs

All the data logging performed by the PLC are stored in this page, provided the user is logged on, the can download the data logs in the form of CSV files that that can be opened by Microsoft Excel for analysis.

Remote Condition Monitoring PLC Web Server viewed on an iPhone

This screen shots shows that it is also possible to access the remote condition monitoring PLC web server using any smartphone with web browsing capabilities. The user will be able to navigate the pages just as they do if using a personal computer.

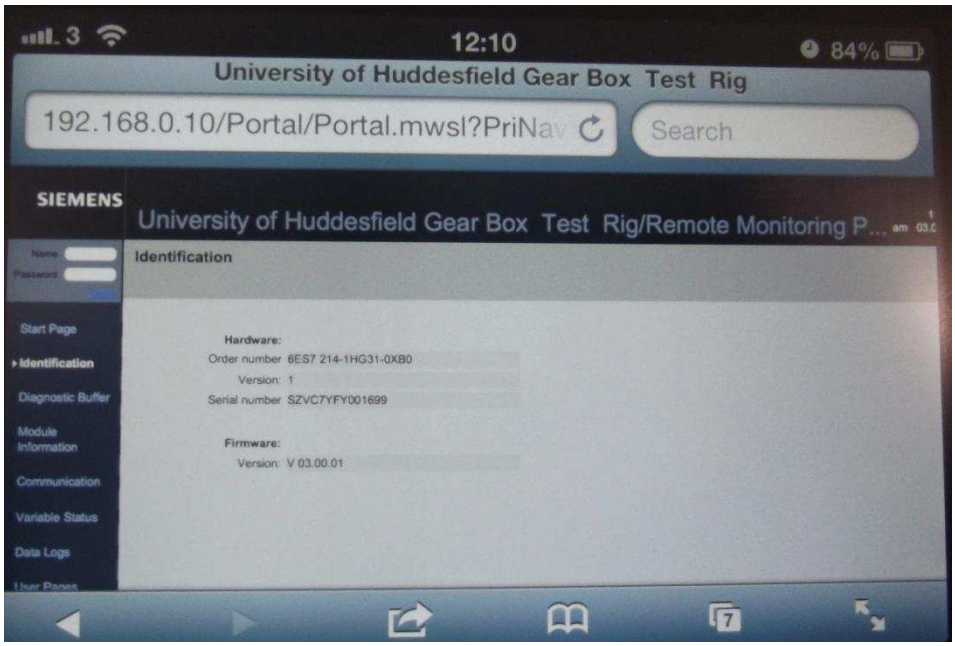

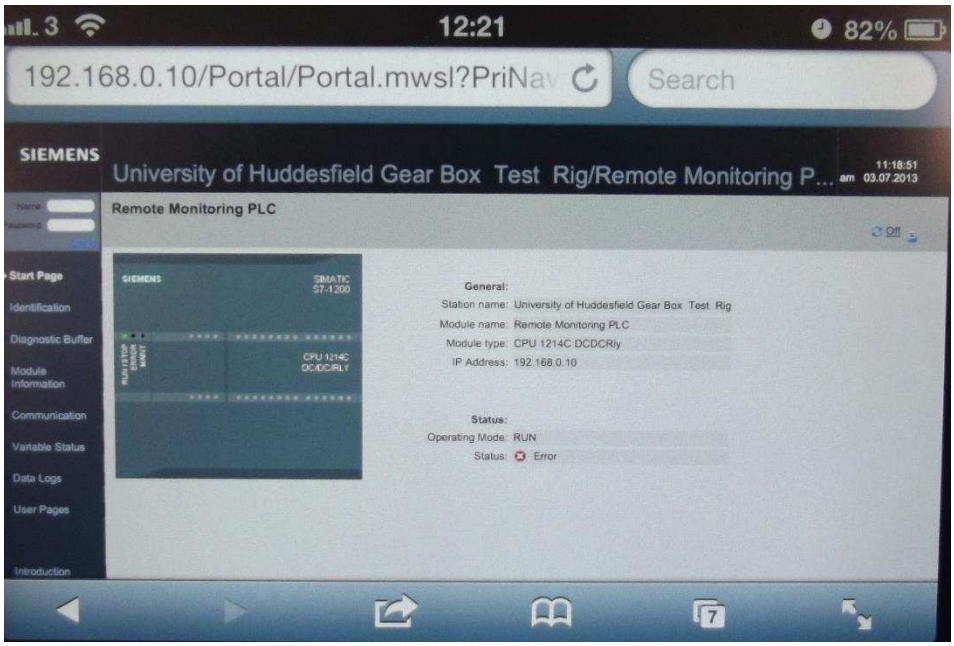

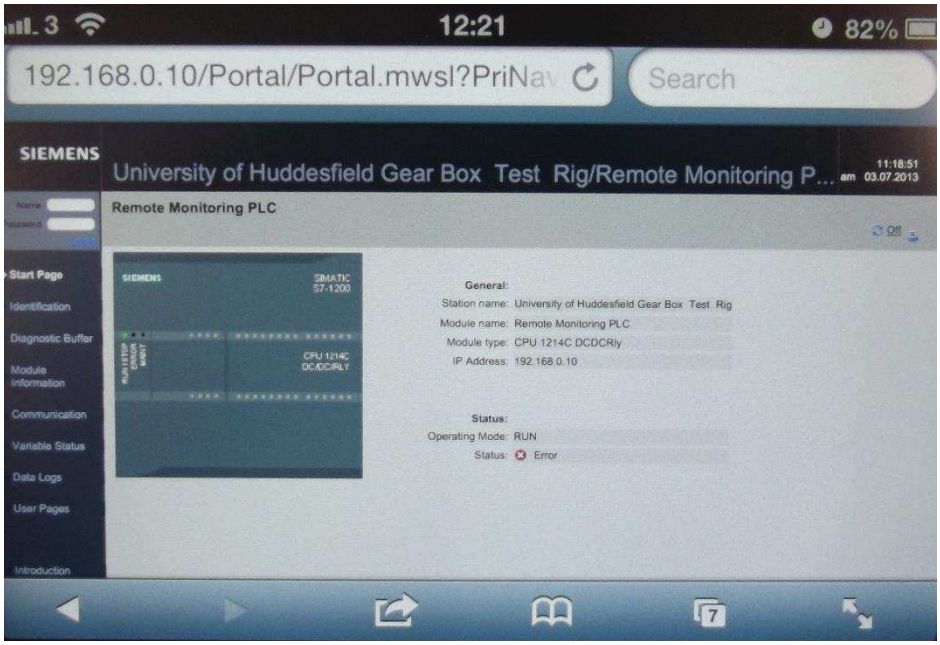
12:21
82%
192.168.0.10/Portal/Portal.mwsl?PriNav
Search
SIEMENS
University of Huddesfield Gear Box Test Rig/Remote Monitoring P...
11:18:51
03.07.2013
Remote Monitoring PLC
Start Page
Identification
Diagnostic Buffer
Module Information
Communication
Variable Status
Data Logs
User Pages
Introduction
SIMATIC S7-1200
CPU 1214C DC/DC/RLY
General:
Station name: University of Huddesfield Gear Box Test Rig
Module name: Remote Monitoring PLC
Module type: CPU 1214C DCDCRly
IP Address: 192.168.0.10
Status:
Operating Mode: RUN
Status: Error

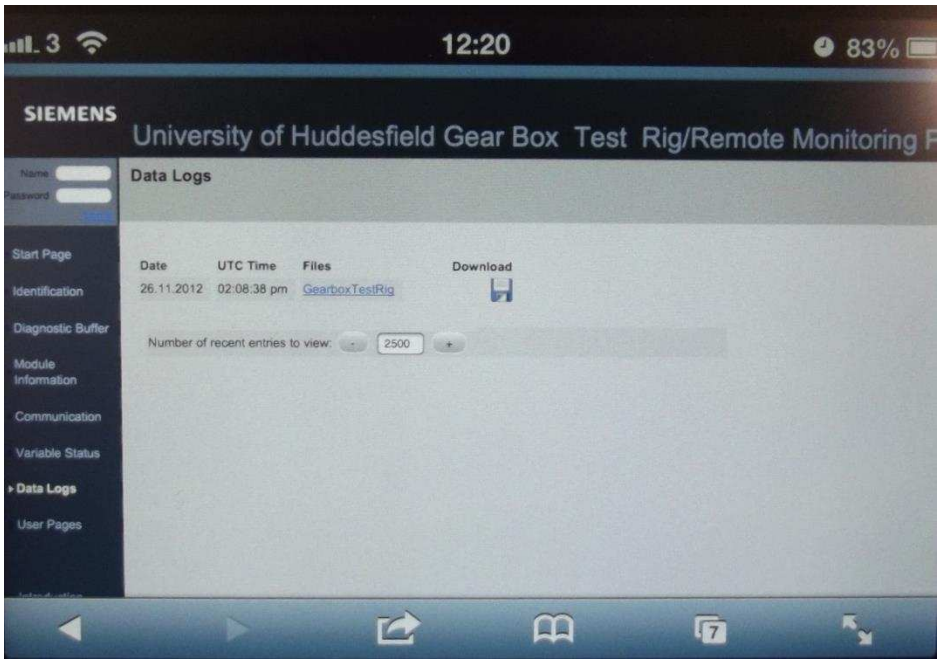
12:20
83%
SIEMENS
University of Huddesfield Gear Box Test Rig/Remote Monitoring
Data Logs
Start Page
Identification
Diagnostic Buffer
Module Information
Communication
Variable Status
Data Logs
User Pages
Date
UTC Time
Files
Download
26.11.2012
02:08:38 pm
GearboxTestRig
Number of recent entries to view:
2500